DOCTORAL THESIS

Grout Development and Methods for Remedial Grouting of Embankment Dams

Johan Lagerlund

Soil Mechanics

LULEÅ UNIVERSITY OF TECHNOLOGY

Doctoral Thesis

Grout Development and Methods for Remedial Grouting of Embankment Dams

Utveckling av injekteringsbruk och metodik vid reparationsinjektering av fyllningsdammar

Johan Lagerlund

Luleå
April 2024

Luleå University of Technology
Department of Civil, Environmental and Natural Resources Engineering
Division of Mining and Geotechnical Engineering

nccnnbunfmfdmb,M,,

Ingrid Helén Louise Lagerlund, 20 months old
2023-09-14

Thesis defence:	Room E632, Luleå University of Technology Thursday, 11 April 2024, 10:00
Faculty opponent:	Professor Dr. **Markus Aufleger** University of Innsbruck Head of the Unit of Hydraulic Engineering Innsbruck, Austria
Examination committee:	Associate Professor Dr. **Annika Gram** Royal Institute of Technology Division of Concrete Structures Stockholm, Sweden
	Associate Professor Dr. **Åsa Fransson** University of Gothenburg Division of Hydrogeology Gothenburg, Sweden
	Professor Dr. **Fjola Gudrun Sigtryggsdottir** Norwegian University of Science and Technology Division of Hydraulic Research Trondheim, Norway
Deputy:	Professor Dr. **Mats Emborg** Luleå University of Technology Division of Fire Engineering Luleå, Sweden
Chairman:	Professor Dr. **Daniel Johansson** Luleå University of Technology Division of Mining and Rock Engineering Luleå, Sweden
Supervisors:	Professor **Jan Laue**, LTU Adjunct Professor **Peter Viklander**, LTU Professor **Anders Sellgren**, LTU Professor **Sven Knutsson**, LTU
Supervisor 2006-2009:	Professor **Håkan Stille**, KTH

PREFACE

The research presented in this thesis was carried out the Division of Mining and Geotechnical Engineering at the Department of Civil, Environmental and Natural Resources Engineering at Luleå University of Technology and at the Vattenfall R&D laboratory in Älvkarleby. The research has been funded by the Swedish Center for Sustainable Hydropower (SVC) and Vattenfall AB.

First, I would like to express my eternal gratitude to my wife, Cecilia. Without your constant encouragement I would never be able to finalize this. My beloved daughters Ingrid and Edith, who taught me how to completely let go of the thesis every day after work. My mother Anne Louise, sisters Åsa and Ulrika, my mother-in-law Helén for taking care of the little ones when I finalized this thesis. Finally, all my thoughts go out to my father, who dreamed of this moment but couldn't be here to experience it.

My supervisors. Jan Laue for all interesting discussions and feedback on experimental designs and paper writing. Peter Viklander for always encouraging me and dealing with my, at times, horrible first drafts. Anders Sellgren who was always available and had to put up with all my own takes on hydraulic related issues. You really had patience and guided me in a world I knew nothing about. I will miss our daily conversations dearly. Sven Knutsson, for your reviewing support and knowledge on how the academic world functions. Håkan Stille, who was my supervisor at KTH during my first half between 2006 – 2009. Without you all, I would be nothing.

My colleagues at the Vattenfall R&D lab. Erik Nordström, always ready to have discussions about concrete and additives. I couldn't have done this without your support. Holger Ecke, my boss, for letting me do this. Per-Erik Thorsell and his team in the concrete lab for putting up with me doing all my laboratory work in their facilities. Anders Sjödin and his team at the workshop. Without you, all my custom-made laboratory equipment would probably be less practical.

My fellow Ph.D.-colleagues at LTU and especially Jasmina Toromanovic for all cooperation, both past and future. I also know you had to put up with a lot of questions of more administrative nature since being a Ph.D.-student far away from the university isn't always very easy. Axel Barrdahl, my master thesis student who helped me out enormously during one of my many laboratory projects.

Per Mårtensson at SKB and Erik Liljeby, Skanska. They had nothing to do with the thesis itself but thanks to all the concrete and grout material development projects

we did together for the nuclear waste repository over the years, I got to learn all the tricks of the trade.

Finally, I must thank my cat, Fnulan. She has been my involuntary editor. The keyboard of the computer is obviously an excellent bed for cats. At times, she took a nap on it and sometimes I forgot to save my documents - things where erased. However, re-writing erased sections always improved it.

And Jindar Espar, I have not forgotten you. Now you must take your bicycle from Stockholm to me in Vattholma so we can have a barbecue together. My treat.

Vattholma, March 2024

Johan Lagerlund

ABSTRACT

An embankment dam can be damaged by internal erosion. During this process, the soil material erodes and is transported out of the dam structure. Some common types of damage due to internal erosion are piping, less dense soil zones, and zones where the fine material has been washed out.

To prevent ongoing internal erosion from developing into a damage or a breach, injection grouting may be performed to replace the eroded soil material. In an embankment dam, injection grouting is usually performed vertically. A pipeline is drilled from the crest of the dam to the damaged zone, to which the grout material is delivered via a pump. The injection grouting methods suitable for embankment dams are compaction and permeation grouting. In compaction grouting, a low-mobility grout material is injected at high pressure, compacting the surrounding soil. In permeation grouting, the injection pressure is lower and the grout material flows more easily, allowing it to permeate the porous structure of the soil into which it is injected.

A grout material for embankment dams should have properties, i.e., particle size distribution, water content, shear strength, and bulk density, similar to those of the original core soil after injection. A grout material with these properties will however be very stiff and difficult to pump, and permeation will be difficult to achieve. Therefore, a new type of non-hardening grout material has been developed and tested in the laboratory. The grout material is a low-mobility grout, but its viscosity and yield strength can be temporarily lowered by replacing the fine aggregates with a limestone filler and by adding a superplasticizer. After injection, the effect of the superplasticizer wears off, leaving a grouted zone with geotechnical characteristics similar to those of the original core soil. The grout material consists of 0–4 mm aggregates, limestone filler, dry bentonite powder, water, superplasticizer, and an air-release agent. The grout material properties and the influence of injection method were tested in three laboratory investigations and the results were presented in four papers.

Development, and fresh and hardened properties of the grout material were investigated in ***Paper I***. The key findings are: (1) The grout material attracted air when homogenized. When homogenized longer than 15 minutes, it was difficult to pump. Air content up to 16.5 % was observed. (2) After 34 days of storage, the water content was ~10 % and the bulk density ~2250 kg/m^3, which are very similar to those of the core soil. The undrained shear strength was ~13 kPa, which was initially lower than that of the core soil but it slowly increased with time.

The factors affecting a grout material's ability to permeate a core soil damaged by internal erosion were investigated in a pilot-scale permeation test series and the

results are presented in ***Paper II***. Three different coarse-grained materials with d_{15} of 35, 75, and 110 mm were grouted. The key findings are: (1) The ratio between limestone filler and aggregates in the grout material greatly influenced the permeation. A grout material with a ratio of 1.7 performed far better than a grout material with a ratio of 1.4. (2) A higher consistency measurement of the grout material (150 mm vs. 100 mm) improved the permeation if low injection pressure was used. At higher pressure, the role of consistency was minor. (3) A higher maximum particle size, D_{max}, of the grout material (4 mm compared to 2 mm) improved the permeation. The difference was most probably caused by higher viscosity and higher yield strength of the grout material with D_{max} = 2 mm compared to that with D_{max} = 4 mm. The lowest ratio between the minimum particle size of the coarse-grained material and the maximum particle size of the grout material was 4, and using higher pressure, the grouting was successful. Ratios below 4 were not tested.

From ***Paper II****,* the most suitable materials for permeation grouting were chosen to be investigated further for their resistance to flow. The results of this investigation were presented in ***Paper III***. Resistance to flow in the pilot-scale permeation test was found to occur within the pipeline and at its exit, where the grout material downflow was redirected 180° to an upward flow. Total frictional losses could be estimated by regarding the grout material flow as Newtonian laminar. Total frictional losses in the 1.3 m length and 0.075 m diameter pipeline during all tests were measured to be 1–67 kPa/m at grout material velocity of 0.01–1.03 m/s. Frictional losses due to the grout material's permeation of the coarse-grained materials could be estimated with the hydraulic conductivity. The mean hydraulic conductivities in the d_{15} = 75 mm coarse-grained material, when permeated by the D_{max} = 2 mm and 4 mm grout materials, were measured to be $1.7x10^{-4}$ and $1.4x10^{-4}$ m/s, respectively; whereas in d_{15} = 110 mm, the values were $2.1x10^{-4}$ and $3.3x10^{-4}$ m/s. These observed values of the hydraulic conductivity were very close to the expected values. With the Newtonian approach, pressure losses may be easily estimated. This will facilitate the estimation of how much of the grouting pressure at the pump is transferred into the core soil during a grouting operation. The possibility to quantify pressure losses during the permeation of the coarse-grained material with hydraulic conductivities can be used when estimating permeation depths vis-à-vis applied injection pressure.

The method, "*Identification – Localization – Characterization – Remediation*", was tested at the abutment of a large-scale test embankment dam with the newly developed grout material and presented in ***Paper IV***. The seepage rate was successfully reduced to 40 % directly after the injection grouting, and up to 70 % after one year. Most of the seepage reduction was caused by the rotary percussion drilling. Remedial grouting should not be regarded as a last resort, but as a part of a maintenance program.

SAMMANFATTNING

En fyllningsdamm kan skadas av inre erosion. Under denna process eroderar framför allt de minsta kornen som transporteras ut ur dammen. Några vanliga skador på grund av inre erosion är piping, löst lagrade zoner och zoner där finmaterial helt saknas.

För att förhindra att pågående inre erosion utvecklas en skada eller haveri kan injektering utföras för att ersätta förlorat material. För en fyllningsdamm utförs vanligtvis injektering vertikalt där injekteringsrör borras på plats från dammkrönet rakt ner till den skadade zonen. Ett injekteringsbruk pumpas därefter ner genom injekteringsröret till skadan. Lämpliga injekteringsmetoder för fyllningsdammar är kompakterings- och permeationsinjektering. Vid kompaktinjektering injekteras ett styvt injekteringsbruk under höga tryck vilket kompakterar den omgivande jorden. Vid permeationsinjektering är injekteringstrycken lägre och injekteringsbruket mer lättflytande så att det kan tränga in i porerna i det jordmaterial som injekteras.

Ett injekteringsbruk för fyllningsdammar bör efter injektering ha liknande egenskaper som dammens tätjord, med avseende på exempelvis liknande kornstorleksfördelning, vattenkvot, skjuvhållfasthet och densitet. Ett injekteringsbruk med dessa egenskaper blir dock styvt och svårpumpat. Av denna anledning har en ny typ av icke härdande injekteringsbruk utvecklats och testats i laboratoriemiljö. Injekteringsbruket är i grunden ett kompaktinjekteringsbruk där viskositet och flytgräns temporärt sänks genom att ersätta injekteringsbrukets finmaterial med kalkstensfiller samt tillsätta en superplasticiserare. Efter injektering avtar effekten av superplasticiseraren, varför injekteringsbruket återfår liknande egenskaper som tätjorden. Injekteringsbruket består av 0 – 4 mm ballast, kalkstensfiller, bentonitpulver, vatten, superplasticiserare och luftreducerare. Provning av injekteringsbrukets egenskaper och injekteringsmetod utfördes genom fyra delprojekt vars resultat presenteras i fyra papers.

Ett konceptuellt injekteringsbruk utvecklades vars färska och hårdnande egenskaper testades i ***Paper I***. Huvudslutsatser var: (1) Injekteringsbruket absorberar luft när det blandas. Om det blandas längre tid än 15-minuter blir det svårpumpat. Lufthalter på upp till 16,5 % uppmättes. (2) Efter 34 dagars lagring var vattenkvoten (~10 %) och densiteten (~2250 kg/m^3) i injekteringsbruket snarlik en tätjords. Odränerad skjuvhållfasthet (~13 kPa) var lägre än vad som kan förväntas i en tätjord men ökade långsamt med tiden.

Faktorer som påverkar ett injekteringsmaterials permeationsförmåga i en tätjord skadad av inre erosion undersöktes genom injekteringsförsök i pilotskala i ***Paper II***. Tre olika typer av grovkorniga material (fiktiva skador) med d_{15}-mått på antingen 35, 75 or 110 mm injekterades med olika bruksmaterial. Huvudslutsatser var: (1)

Relationen mellan kalkstenfiller och ballast påverkade kraftigt injekteringsbrukets permeationsförmåga. Ett bruksmaterial med en relation på 1,7 presterade mycket bättre än ett bruksmaterial med relationen 1,4. (2) Ett högre konsistensmått på injekteringsbruket (150 mm jämfört med 100 mm) förbättrade dess permeationsförmåga om låga injekteringstryck användes. Vid högre injekteringstryck hade konsistensmåttet mindre betydelse. (3) En högre maximal partikelstorlek på injekteringsbruket (4 mm jämfört med 2 mm) förbättrade dess permeationsförmåga. Skillnaden berodde med största sannolikhet på den något högre flytgränsen och viskositeten i injekteringsbruket med maximal partikelstorlek på 2 mm. Den lägsta kvoten mellan den minsta partikelstorleken i det grovkorniga materialet och den största partikelstorleken i injekteringsbruket var 4. Lägre kvoter testades aldrig.

Från ***Paper II*** valdes de mest lämpliga injekteringsbruken för permeationsinjektering ut för att undersöka friktionsförluster. Resultat från denna undersökning presenteras i ***Paper III***. Friktionsförluster uppstår i injekteringsröret samt vid dess utlopp, där injekteringsbruket nedåtgående flöde ändras 180° till ett uppåtgående flöde. Friktionsförluster kunde uppskattas genom att betrakta injekteringsbrukets flöde som laminärt Newtonskt. Friktionsförluster i det 1,3 m långa injekteringsröret med 0,075 m diameter varierade i testerna mellan 1 – 67 kPa/m vid hastigheter på 0,01 – 1,03 m/s. Friktionsförluster som uppstår då injekteringsbruket injekteras i de grovkorniga materialen kunde uppskattas genom dess hydrauliska konduktivitet. Den hydrauliska konduktiviteten för det grovkorniga materialet med d_{15} = 75 mm var $1,7x10^{-4}$ och $1,4x10^{-4}$ m/s då det injekterades med 2- respektive 4 mm injekteringsbruket. Hydraulisk konduktivitet för det grovkorniga materialet med d_{15} = 110 mm var $2,1x10^{-4}$ och $3,3x10^{-4}$ m/s då det injekterades med 2- respektive 4 mm injekteringsbruket. Dessa hydrauliska konduktiviteter låg mycket nära förväntade värden. Genom att betrakta injekteringsbrukets flöde som Newtonskt kan friktionsförluster enkelt uppskattas, vilket kommer att förenkla uppskattningar av hur mycket av injekteringstrycken vid pump som överförs in i dammens tätjord under en reparationsinjektering. Möjligheten att kvantifiera friktionsförluster under injekteringsförloppet av de grovkorniga materialen med dess hydrauliska konduktivitet kan användas för att uppskatta ett injekteringsbruks inträngningsdjup visavi använda injekteringstryck.

Reparationsmetodiken, *identifiera – lokalisera – karaktärisera – reparera* presenterades i ***Paper IV***. Metodiken testades därefter på en damm. Ett fullskaligt injekteringstest genomfördes vid dammens anslutning, mellan betongkonstruktion och tätjord, med det utvecklade injekteringsbruket. Vattenläckage vid anslutningen minskade direkt med 40 % och ett år efter injekteringen låg läckagereduceringen på 70 %. Största anledningen till läckagereduceringen berodde på borrningen med topphammare. Injektering av en damm bör inte ses som en sista utväg utan som en del i ett underhållsprogram.

TABLE OF CONTENTS

SYMBOLS AND NOTATIONS

Roman Letters

C/A	Cement to aggregate ratio
C_u	Uniformity coefficient (D_{10}/D_{60})
d_{15}	Particle size for the coarse-grained material at which 15 % of the material is finer [mm]
d_{max}	Maximum particle size of the coarse-grained material [mm]
d_{min}	Minimum particle size of the coarse-grained material [mm]
D	Pipeline diameter [m]
D_{max}	Maximum particle size of the grout material [mm]
g	Gravitational constant [9.81 m/s^2]
h_1	Upper grout material surface [m]
h_2	Lower grout material surface [m]
h_f	Pipeline frictional loss [m]
h_{fl}	Total friction head loss [m]
h_l	Local loss at the exit of the pipeline [m]
h_{perm}	Frictional loss during the permeation of the coarse-grained material [m]
h_{pump}	Pump pressure [m]
h_{tot}	Total friction losses [m]
j	Frictional loss gradient
k	Permeability [m^2]
K	Hydraulic conductivity [m/s]
$K_{expected}$	Expected hydraulic conductivity [m/s]
K_l	Constant for h_l [-]
L	Length of pipeline [m]
L/A	Limestone filler to aggregate ratio
L_{active}	Active length of pipeline [m]
N	Porosity [%]
n_a	Air content [%]
$P_{1,\,2}$	Atmospheric pressure [Pa]
P_{pump}	Pumping pressure [Pa]
Q	Grout material flow [l/s]
Re_{pipe}	Reynolds number in a pipeline
rpm	Rounds per minute
UCS	Unconfined compression tests
V_1	Pipeline velocity [m/s]
V_2	Pore velocity [m/s]
w	Water content [%]

w/c	Water to cement ratio

Greek Letters

μ	Dynamic viscosity [Pas]
ρ_{grout}	Grout material density [kg/m^3]
τ_0	Yield strength [Pa]

APPENDED PAPERS

Paper I

Lagerlund, J., Viklander, P., Laue, J. and Knutsson, S. (2023). Design and strength development of a low-mobility grout for repair of embankment dams. Submitted to *Ground Improvement (October 2023)*. Under review.

Paper II

Lagerlund, J., Laue, J., Viklander, P. and Nordström, E. (2023). Testing of a low-mobility grout material for permeation grouting in embankment dams. *Geotechnical Research, 10(4): 154 - 164.* https://doi.org/10.1680/jgere.22.00066.

Paper III

Lagerlund, J., Sellgren, A., Viklander, P., Laue, J. and Knutsson, S. (2024). Permeation grouting laboratory testing for embankment dams – a note on flow resistance. Submitted to *Geotechnical Engineering (March 2024)*

Paper IV

Lagerlund, J., Viklander, P., Laue, J. and Toromanovic, J. (2023). Methodology for remediation grouting in embankment dams – grouting with a new type of non-hardening grout. 91st ICOLD annual meeting 2023, Gothenburg, 1788 – 1797.

Publications not appended

Lagerlund, J. (2015). Utveckling av injekteringsbruk för 2 BMA [Development of grout material for 2 BMA]. Vattenfall Report VRD-R01:2015 (in Swedish).

Lagerlund, J. (2015). Injektering av sprickor med injekteringsbruk för 1 BMA [Injection grouting of cracks with grout material for 1 BMA]. Vattenfall Report VRD-R03:2015 (in Swedish).

Lagerlund, J. (2015). Utveckling av konstruktionsbetong för gjutning av kassuner i 2 BMA [Development of construction concrete for casting of caissons in 2 BMA]. Vattenfall Report VRD-R51:2015 (in Swedish).

Lagerlund. J., Vazquez, A., Svensson, M., Billstein, M. and Viklander, P. (2016). Breach Formation in a Fuse Plug – Evaluation of Field and Laboratory Tests. 2a-117. In proceedings from ICOLD 2016, Johannesburg, South Africa

Lagerlund, J and Thorsell, P-E. (2017). Undersökning angående störthöjdens inverkan på struktur och egenskaper hos kringgjutningsbruket till silon [Investigation of the influence of free fall height on the structure and properties of the silo grout material]. Vattenfall Report VRD-R47:2017 (in Swedish).

Lagerlund, J. (2018). Fuse plug breach tests. Energiforsk Report 2018:465.

Toromanovic, J., Lagerlund, J., Viklander, P. and Laue, J. (2020). Geotechnical instrumentation of an experimental embankment dam. ECPMG 2020, 4th European conference on physical modelling in geotechnics, 171 – 176.

Lagerlund, J. (2020). Rivning av en fyllningsdammsanslutning [Dismantling of an embankment dam abutment]. Energiforsk Report 2020-641 (in Swedish).

Lagerlund, J and Nilsson, Å. (2020). Anslutningar i fyllningsdammar [Abutments in Embankment Dams]. Energiforsk Report 2020:643 (In Swedish).

Bernstone, C., Lagerlund, J., Toromanovic, J. and Juhlin, C. (2021). Deformationer och portryck i en experimentell fyllningsdamm [Deformations and pore pressures in an experimental embankment dam]. Energiforsk Report 2021:772 (In Swedish).

Lagerlund, J. (2022). Hydraulisk konduktivitet i grovkorniga jordar [Hydraulic conductivity in coarse-grained soils]. Energiforsk Report 2022:849.

Viklander, P., Lagerlund, J., Riaz, S. and Nordström, E. (2023). Non-destructive test methods for detecting defects in an experimental embankment dam. *International journal on Hydropower and dams 30(3): 74 – 79.*

1 INTRODUCTION

1.1 Background

An embankment dam is a man-made structure, designed to keep a reservoir on its upstream side. There are two main types of embankment dams: earth-fill and rock-fill. An embankment dam can be founded both on rock and soil. It is built in several zones, e.g., core, filters, structural fill, erosion protection and dam toe, (Fell et al., 2005). To keep water in the reservoir, the embankment dam has an impervious core. In Sweden, the core is typically made from moraine. On either side of the core, filter zones are placed. The filter zones will prevent core soil particles from being eroded by the seepage. Outside the filter zones, the structural fill is located. The structural fill prevents erosion of the filter materials and provides structural stability. Erosion protection zones are placed on the slopes and crest. Finally, a dam toe berm is normally built on the downstream side of the embankment dam to increase slope stability (RIDAS, 2020).

With time, the likelihood of damages forming inside, under and on the surface of the embankment dam will rise. A study from Rice and Duncan (2010) showed that ageing embankment dams commonly have increased seepage rates. International statistics on embankment dam breaches presented in ICOLD (2017) revealed that 1 of 80 embankment dams has experienced either an accident or a breach during its lifetime. Accidents, i.e., an event that unattended will lead to a breach, are much more common than breaches. From 1800 – 1986, 94 % of all recorded breaches in large embankment dams, i.e., height >15 m, were caused by erosion, *Table 1* and 36 % of all breaches occurred during the first filling.

Table 1. Statistics for embankment dam breaches between 1800 - 1986 (ICOLD, 2017).

Erosion		Slope stability	
Overtopping	Internal erosion	Static instability	Seismic instability
48%	46%	4%	2%

In a study by Nilsson (1993), Swedish embankment dams were investigated with regards to anomalies. 171 anomalies were detected and divided into 13 different types on a total of 84 embankment dams, *Table 2*. If the same type of anomaly were found in different places on the same embankment dam, it was only recorded once in the statistics.

Table 2. Anomalies in 84 Swedish embankment dams (Nilsson, 1993).

Type of anomaly	Amount	% of total
Leakage underground	16	9
Leakage through dam body	19	12
Slope damages	45	26[1]
Abnormal movements (settlements or lateral movements)	16	9[1]
Internal erosion in underground	5	3[2]
Internal erosion in dam body	13	8[2]
Slope movements	5	3[1]
Changes in abutment dam-concrete	16	9[2]
Changes in drainage system or filter	1	0.5[2]
Pore pressure changes	4	2[1]
Grout curtain deterioration	1	0.5
Sink holes on crest or slopes	27	16[2]
Other changes	3	2

[1]May be caused by internal erosion. [2]Caused by internal erosion.

An anomaly can lead to an accident or a breach. The anomaly should be identified, localized, characterized and, if necessary, remediated. Remedial measures can either be long-term, short-term, or acute (Bradley et al., 2007). Long-term measures may involve new filters, drains, cut-offs, dam toe berms, grouting or relief wells. Short-term measures may include modified dam operation strategies as reservoir drawdown, reservoir restrictions, but also measures as grouting and relief wells. Acute measures may include emergency drawdown of reservoir, evacuation of downstream residents, grouting and filling of sinkholes.

According to Bradley et al. (2007), grouting is often chosen as remedial measure. A grouting operation can be undertaken when soil material has been found to be washed out from the embankment dam. The grouting operation requires the instalment of one or more pipelines by drilling from the embankment dam surface to the location of the anomaly. A grout material is then injected, ideally replacing the lost soil material.

Internationally, case histories on remedial grouting of embankment dams are rare and no empirical standards for applying the method have been identified (Park and Oh, 2018). The restoration of damaged embankment dams is often kept out of public view. The know-how of grouting is considered as secrets of the trade and at many times rules of thumb are applied.

To develop a concept on how to perform remedial grouting in embankment dams, the following issues are studied:

a) The embankment dam structure and its materials.
b) How an anomaly inside the embankment dam is developed and its appearance.
c) Available grouting methods and suitable grout material that can be used to remediate the anomaly.

With these issues covered, the research questions are defined, outlining needed physical laboratory investigations. These investigations will allow direct observations and may therefore be instrumental in understanding of grout material behaviour and its efficiency before, during and after a grouting operation.

1.2 Structure of the thesis

The thesis consists of seven chapters, where **Chapter 1** states the background, how the thesis is structured and its limitations.

Chapter 2 gives the current state-of-the-art of embankment dams, internal erosion and remedial grouting methods used in embankment dams. To this date, most of the research has been focused on grouting within rock formations. Therefore, understanding the embankment dam is important when designing both grout material and grouting methods. The damaging processes in embankment dams are described to understand what appearances of damages most likely to be grouted. The historical use of remedial grouting methods is described and their suitability for use in embankment dams. This is important when deciding the best suited grouting methods. In the end, the research questions are defined.

Chapter 3 describes what an ideal grout material for embankment dams should contain. Material and methods for all laboratory investigations are presented.

Chapter 4 presents the results from the laboratory investigations.

Chapter 5 discusses the presented results and how the results can be related to works of other researchers.

Chapter 6 presents the main conclusions.

Chapter 7 proposes future work.

1.3 Limitations

Remedial grouting of embankment dams should be approached by first *identifying*, *localize* and *characterize* the damage. After this, the most suitable grouting method and grout material is chosen and finally *remediated* by drilling and grouting. Neither *identification* nor *localization* of damages inside an embankment dam is investigated within this thesis. Damage detection requires the use of:

a) Geophysical methods, e.g., seismic, acoustics, resistivity and temperature measurements.
b) Geotechnical investigations and measurements, e.g., settlement or movement detection, pore pressure, seepage measurements, sounding, drilling, sampling and testing.

Research and development on this topic in Sweden is covered by several authors, e.g., Salas Romero et al. (2020), Johansson et al. (2020), Johansson et al. (2021), Bernstone et al. (2021), Nooroz et al. (2021) and Lagerlund (2022).

Drilling in embankment dams is not covered within the thesis and only embankment dams with a central core of moraine are studied. Rockfill dams with other types of hydraulic barriers, e.g., face slabs of bitumen or concrete, are not considered.

1.4 Licentiate thesis

A research project was performed at the Royal Institute of Technology (KTH) between 2006 – 2008. This part was presented as a licentiate thesis in the form of a monography (Lagerlund, 2009).

The licentiate thesis was performed as both a literature study and two laboratory investigations. In the literature study, the embankment dam, internal erosion and remedial methods were covered. It was concluded that non-hardening grout materials should be used. Two laboratory investigations were therefore launched. In the first laboratory investigation, the influence of particle size distribution of non-hardening grout materials was tested in a 50 mm diameter rigid wall permeameter. The testing was done to examine if a non-hardening grout material can remain durable if grouted in a dam. An injected grout material will be exposed to the same erosive forces as the original core soil of the dam. The non-hardening grout material must therefore be tested in an environment where it can be permeated. Evaluations were done by comparing the particle size distribution of the non-hardening grout material before and after permeation. The results from the tests show that the particle size distribution curve of the non-hardening grout material had a large influence on its long-term resistance to erosion.

In the second laboratory investigation, the cooperation between a core soil and an injected grout material was studied. Both hardening and non-hardening grout materials were tested. In the laboratory investigation, a cylinder with a diameter of 120 mm was filled with a moraine. Centrally in the moraine, a grout material "plug" with a diameter of ~50 mm was placed. The cylinder was then closed off, placed horizontally, and permeated with water up to two weeks. After testing, the cylinder was dismantled and investigated. It was discovered that small cracks formed at the interface between grout material and core soil. Cracks did not develop when a non-hardening grout material was used.

In 2021, Ph.D.-studies were restarted at Luleå University of Technology.

2 STATE OF THE ART

2.1 Embankment dams with moraine core soil

An earthfill embankment dam is built in zones where each zone contains different soil materials. A principal layout of an embankment dam can be seen in *Figure 1*.

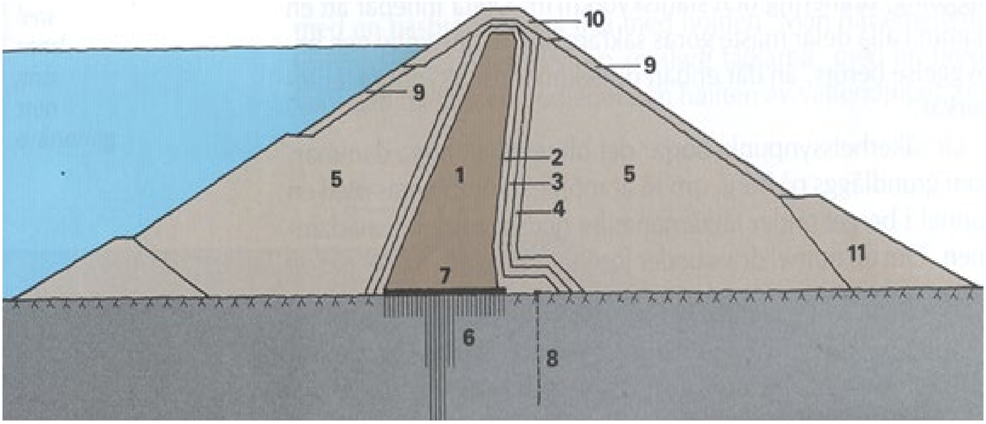

Figure 1. Example of an earthfill embankment dam founded on rock (Vattenfall, 1988).

The zones are: (1) core soil, (2 – 4) fine-, medium-, and coarse filters, (5) structural fill, (6) grout curtain, (7) concrete plate and sealing, (8) filter well, (9) riprap, (10) crest protection and (11) toe berm.

The *core soil* of an earthfill embankment dam in Sweden is normally made of moraine (RIDAS, 2020). The core soil should have the following properties:

- Water content 2 – 3 % above its optimum (RIDAS, 2020).
- Content of fines (<0.063 mm) > 20 weight-% and D_{max} ≤ 63 mm (Rönnqvist, 2020).
- D_{85} > 2 mm and D_{70} < 20 mm to lower the risk of separation during construction.
- Hydraulic conductivity < $3x10^{-7}$ m/s.
- Optimal thickness of each layer during construction depends on the moraine and should be decided with test compaction before the embankment dam is built.

The main objective of the *filter* zones is to protect the core soil from erosion and to drain excessive pore water. The first filter criterion was presented by Karl Terzaghi in 1926 and has continuously been developed over the years (Fannin, 2008). The filter criterions are guidelines on how to design the particle size distribution of a filter material with respect to the particle size distribution of the soil it protects. If the filters are not functioning properly, i.e., separated or segregated, internal erosion is more likely to occur (Rönnqvist, 2015).

If several filters are built, the outer, i.e., coarser-graded, filter will protect the inner, i.e., finer, filter from erosion. The ideal filter should have the following properties (Nilsson et al., 1999 and Fell et al., 2005):

- Not separate during construction.
- Not change its particle size distribution during construction or usage.
- Neither be cohesive, nor consolidate to prevent cracks.
- Internally stable.
- Have a suitable permeability to allow drainage.
- Able to seal an eventual leak in the core soil (upstream filter).

A filter material must not change properties due to excavation, transportation, compaction, weathering or erosion (RIDAS, 2020; ICOLD, 1993; ICOLD, 2008 and USBR 2012). Filter materials may be sand, gravel or crushed rock. In Sweden, artificial materials like geotextiles may not be used in vital parts of dams due to their tendency of becoming clogged (RIDAS, 2020). The particle size distribution of a filter should neither be gap nor broadly graded. Content of fines in the fine filter must not exceed 5 %, i.e., $D_5 \geq 0.063$ mm.

The design of new filters in Sweden is governed by RIDAS (2020). The particle size distributions of the different filter materials are derived from the particle size distribution of the core soil. Specified envelops for the filter materials can then be designed and the particle size distribution of the actual filter material must fit into these envelops, *Figure 2*.

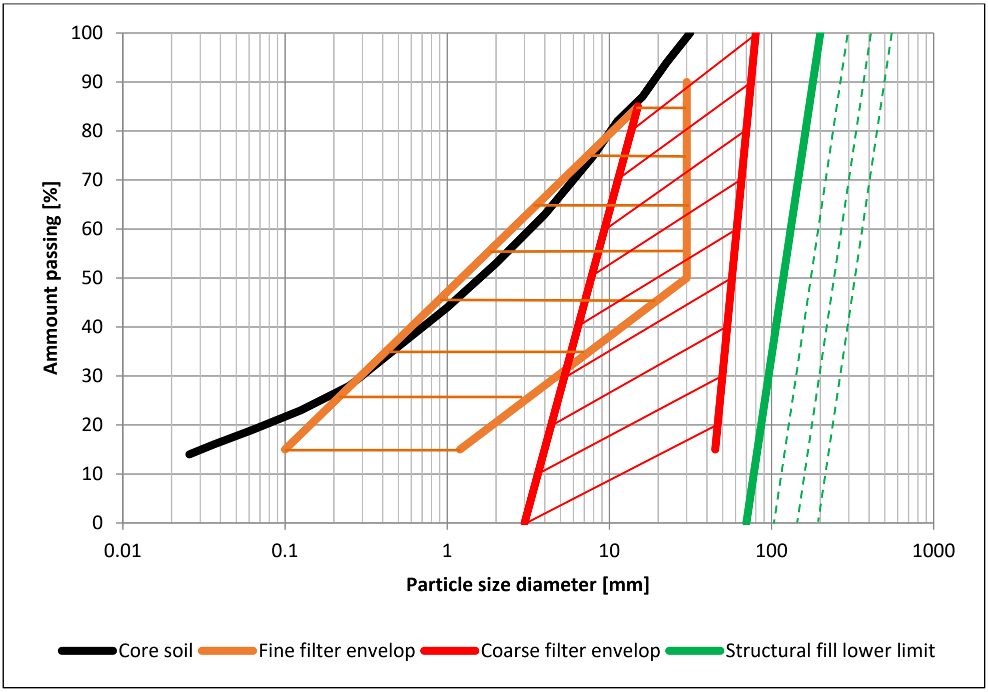

Figure 2. Particle size distribution envelops for fine- and coarse filters and lower limit for structural fill, used in a large-scale test embankment test dam, (Lagerlund et al., 2022).

Outside the filter zone is the *structural fill*. The structural fill constitutes the main bulk material of the embankment dam. The structural fill must also fulfil the filter criterion towards the filter zones.

Riprap and *crest protection* protects the embankment dam from external erosion, e.g., waves, ice formation, heavy rain falls and snow melting. The *dam toe support* protects the dam toe from erosion and improves the slope stability.

2.2 Damages in embankment dams

Damaging processes in embankment dams are frequently caused by internal erosion. During internal erosion, soil material from the dam is eroded and transported out of the structure with the seepage. For internal erosion to occur, three conditions must exist (Fell et al., 2005):

1. A seepage flow and a source of water.
2. Erodible material within the flow path and this material must be carried by the seepage flow.
3. An unprotected exit, e.g., open or unfiltered, through which the eroded material may escape.

According to ICOLD (2017), Internal erosion can go through four stages:

1. Initiation – An event occurs in the embankment dam that leads to the initiation of erosion.
2. Continuation – After initiation, the erosion continues. Filter functions are not working and hydraulic loads are too high.
3. Progression – The internal erosion progresses even further. A pipe may form, fine material is being washed out, sinkholes may develop on the crest and slopes of the embankment dam.
4. Breach or failure – The structural stability of the dam may no longer be sustained.

From a physical point of view, three main factors cause internal erosion: material susceptibility, hydraulic load and stress conditions, see *Figure 3*.

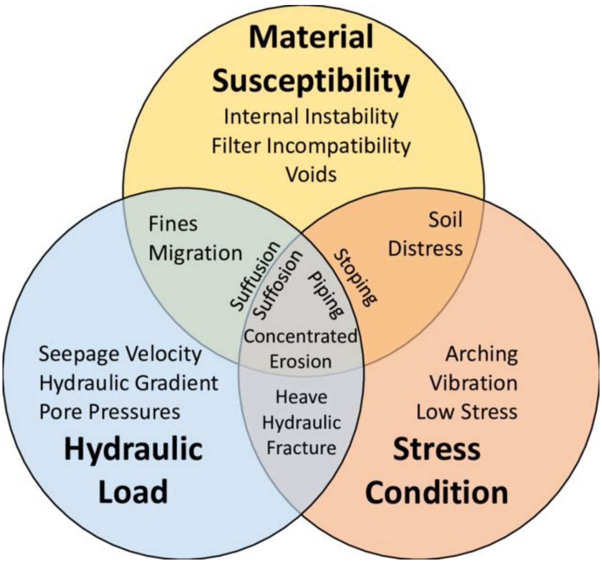

Figure 3. Factors affecting internal erosion in embankment dams (Garner and Fannin, 2010). Note that "concentrated erosion" = Concentrated leaks and contact erosion.

According to ICOLD (2017), there are four types of internal erosion:

1. Concentrated leak erosion.
2. Backward erosion.
3. Contact erosion.
4. Suffusion.

2.2.1 Concentrated leak erosion

The initiation of a concentrated leak requires an opening, e.g., crack, through the soil where seepage may pass at accelerated velocities. Why cracks develop in an embankment dam is seldom investigated since they are repaired as soon as they are discovered (Sherard et al., 1963). Cracks may develop due to differential settlements, arching and drilling works (Sherard, 1986). According to Ekström and Pusch (2001) cracks may also develop due to:

- Settlements in a dry compacted core during the first filling.
- Settlements in a low-permeable, wet compacted core. When the core soil drains, settlements are induced.
- Suspension of core soil material towards abutments.
- Creation of arches between differentials on the surface and underground.

Fell et al. (2007) states that the requirement for a crack to develop is that the shear strength of the soil is exceeded. Cracks in embankment dams are more likely to develop near the surface or close to the abutments than deeper inside it (Terzaghi et al., 1996). Cracks may furthermore develop in freezing conditions due to creation of ice lenses (Vuola et al., 2007), due to repeated freeze and thaw cycles (Viklander, 1997) or drying.

2.2.2 Backward erosion

According to Rönnqvist (2015) there are three types of backward erosion:

- Backward erosion piping – occurs mainly in foundations of non-cohesive soils.
- Global backward erosion – Occurs in the dam and is assisted by gravity leading to vertical or near vertical pipes in the core soil.
- Suffusion – the smaller particles in a gap graded soil is eroded and the volume of the eroded soil decrease.

During backward erosion, a pipe is formed inside the soil. Sherard (1953) labelled it "water veins". The core soils ability to resist it depends on its (1) plasticity or cohesiveness, (2) uniformity or gradation and (3) degree of compaction. For backward erosion to occur, the soil must have the ability to form and support a roof. The process originates from an unfiltered or incompatible filter exit on the downstream side of the embankment dam and propagates towards the upstream source of water, forming a pipe. Usually, the process takes a long time, e.g., years, to develop (Garner and Fannin, 2010). The process may be accelerated if combined with a concentrated leak. In this case, an accident or breach may occur within hours to days (Fell et al., 2003). Plastic soils exhibit higher resistance to backward erosion than non-plastic cohesionless fine-grained materials (Rönnqvist, 2015). Backward erosion may not only occur inside an embankment dam but also in the ground underneath it (Koenders and Sellmeijer, 1992 and Van Beek et al., 2014).

2.2.3 Contact erosion

Contact erosion may be initiated at the interface between two soils with different grain sizes (Guidoux et al., 2010). Contact erosion may then be initiated when the velocity induced frictional force of the seepage in the high-permeable soil exceeds a critical shear stress value in the low-permeable soil (Partheniades, 1965). The soil from the low-permeable soil is thus eroded and transported through the high-permeable soil. According to Terzaghi et al., 1996 and Beguin et al., 2013, contact erosion is less likely to occur if the filter criteria $D_{15F}/d_{15b} < 40$ is fulfilled.

In an embankment dam, the interfaces where contact erosion may occur are most likely found at the abutments, foundation, interface between core soil and filter and around drainage zones. During the event of an overtopping, contact erosion may occur at the core crest given the critical water velocities are exceeded (Lagerlund et al., 2016).

2.2.4 Suffusion

Suffusion may occur in a gap graded soil during seepage and may be initiated when the hydraulic load is increased (Garner and Fannin, 2010). In a gap graded soil, the mid-sized soil particles are missing (Yerro et al., 2017), thus, smaller particles may be eroded through the pores formed by the larger grains (ICOLD, 2017). During suffusion, the bulk volume of the soil remains unchanged (Fannin and Slangen, 2014). Because of suffusion, the amount of fines in the soil is decreased. Consequently, the void ratio and permeability of the soil will gradually increase. Soffosion is similar to suffusion, but the bulk volume of the eroded soil is lowered.

2.2.5 Other factors leading to internal erosion

Different events in an embankment dam may be harmful but can ultimately lead to the initiation of internal erosion. Examples on such events are according to Lagerlund and Nilsson, (2020):

- Drying – Cracks may form if the water content in a soil gets lower than its plastic limit. Soils with low content of fines will be less prone to cracking. In an embankment dam, this may occur in the core or a clogged filter. Furthermore, if a dried soil, e.g., clay or core soil, is rehydrated it may become very loose (Cernica, 1995).
- Hydraulic fracturing – If the hydraulic load, i.e., pore-water pressure, in a soil exceeds the vertical stress of the soil, effective stresses will become very low. The shear forces between the soil particles will then diminish, leading to hydraulic fracturing or uplift. If a high hydraulic load affects a soil under drained conditions, hydraulic fracturing is less likely to occur (Mitchell et al., 2005). Consequently, hydraulic fracturing is more likely to occur in the core than in other parts of the dam. High pore-water pressures may enter the core through cracks, high-permeable zones or through the foundation.
- Arching – During settlements, the loading of the soil particles may be reformed so an arch is formed. The vertical stress on the soil particles directly underneath the arch will therefore be very low, making the soil vulnerable to hydraulic loads. Fell et al. (2008) describes that arching may occur in narrow, high embankment dams where the width of the core is wider (abutment-to-abutment) than 1/4 of its height and the abutments steeper than 60°. If the abutments are 45° or less, arching is less likely to occur.

2.3 Remedial grouting methods

When an embankment dam is exposed to internal erosion, there will be a loss of soil material inside it. Remedial grouting is a method where lost soil material can be replaced via the injection of a grout material. Grouting methods that may be of interest for embankment dams are according to Lagerlund (2009):

- Permeation grouting.
- Fracture grouting.
- Jet grouting.
- Compaction grouting.

A grouting operation requires that the damage inside the embankment dam has been identified, localized and characterized. To transfer the grout material to the damage, a pipeline is drilled in place from the surface of the dam, through which a grout material can be injected. The four grouting methods are shown in *Figure 4*:

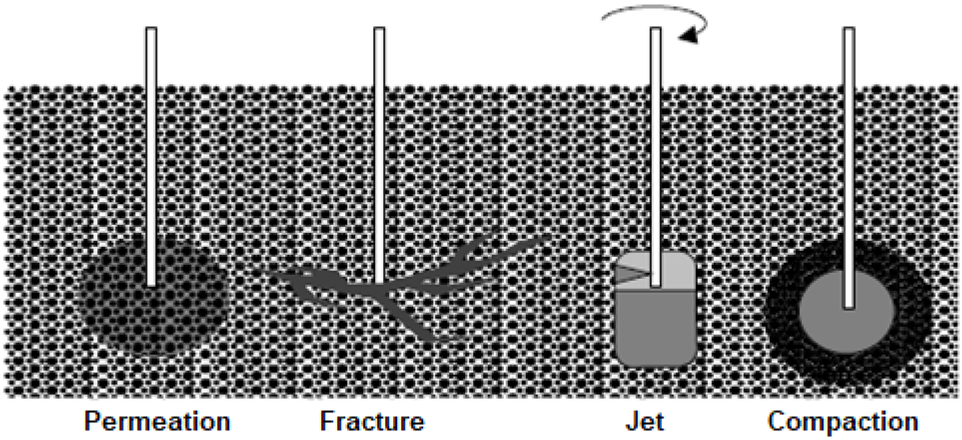

Figure 4. Four different types of grouting methods (Hansson, 1999).

During a grouting operation in an embankment dam, a surveillance program of the injection process should be set up as not to damage the dam. Creating further damages when grouting must always be avoided (Warner, 2004). The most common surveillance method during the injection is the pressure and flow curve of the grout material (Sjöström, 1999). During injection, the pressure and flow changes in real-time is correlated to the properties of the damage.

Before injection, maximum allowed grout material pressure should be determined to avoid unintentional fracturing or heaving of the surrounding soil (Shuttle and Jefferies, 2000). If the grout pressure suddenly lowers during injection, the grouted damage has probably become enlarged, e.g., fracturing or heave in the surrounding soil. A low, uniform flow of the grout material is desired to allow pore water in the surrounding soil to be drained off. To avoid fracturing, the flow rate of grout material should therefore be adapted according to the hydraulic conductivity of the surrounding soil. The build-up of pressure in grout material and surrounding soil is related to the pumping pressure and flow rate of the grout material. Pore-water pressure in the surrounding soil may be monitored with piezometers (Warner et al., 2003).

The effectiveness of grouting in either soil or rock depends on several factors. According to Brantberger (2000), these are:

- For a grout curtain – distance between drilled holes, depth of drill work, drilling equipment and circulation flush.
- For the grout material – penetration or permeation ability, hardening, filling of the voids and durability.
- For the equipment – blender, mixer, pumps, dosage- and recording equipment.
- For the injection method – grout pressure- and stopping criteria for the grout material, order of injection, multiple holes injected simultaneously and intervals of injection.

2.3.1 Permeation grouting

Permeation grouting is a type of method where the grout material has very easy-flowing properties, i.e., low viscosity and yield strength. Viscosity in a grout material is defined as its resistance to flow wile yield strength is defined by the amount of shear strength that needs to be applied before it starts to flow. The low viscosity grout material should ideally penetrate the porous system of the soil and strengthen it through adhesion of the soil particles (Warner, 2004). The method is suitable for soils with hydraulic conductivity > 10^{-6} m/s. If the hydraulic conductivity is lower, there is an elevated risk of fracturing the soil since the grout material can't enter its pores (Widing, 1987). The largest use of permeation grouting in soils is in short-term strengthening and sealing of soils during construction (Warner, 2004). Permeation grout material consist of either fine graded cements and water or sodium silicate, i.e., water glass.

Smaller particle sizes in *cement-based* permeation grout materials are desired. As a rule of thumb, D_{max} of the cement particles should not be larger than 1/3 of the pore size it intends to permeate or penetrate (Bergman et al., 1970). If the cement particles are too large vis-à-vis pore width of the soil, plug formation is likely to occur. Apart from D_{max} of the grout material, its yield strength is also important to consider. According to Eriksson (2002) and Hässler (1991), yield strength of the grout material is the most important rheological property for predicting grout material penetration depth. Yield strength of a grout material containing cement and water may be controlled by the water-to-cement-ratio, i.e., w/c- ratio. For smaller cracks or voids, a w/c-ratio of 1 – 3 is often used while a w/c-ratio of 0.5 – 1 is used for larger voids or cracks. (Ekström and Pusch, 2001).

Sodium silicate is a liquid type of grout material for permeation grouting. Water glass grout materials can permeate very fine graded soils but tends to shrink during hardening (Yongmin et al., 2021). It is furthermore easily washed away if grouted into seepage zones (Hansson, 2005). Time dependant degradation of sodium silicate grouts has been studied by Krizek and Madden (1985) and Karol (2003). Both shrinkage and erosion were the main causes behind the degradation of the grout material.

2.3.2 Fracture grouting

Fracture grouting is well suited for cohesive soils since this type of soil can be intentionally fractured. The grout material has a higher yield strength and viscosity compared to permeation grout material. It is injected under high pressure, creating cracks in the soil which are sealed by the grout material itself (Li and Deng, 2023). After the grouting procedure, the grout material is left to harden. This will enhance the strength of the soil through a network of interconnected grout lenses. It will also lower the overall hydraulic conductivity of the soil since the seepage has to take longer routes through the soil.

The grout material for fracture grouting usually consists of cement and water, or fine soil materials and water. The resulting grout lenses will have a low tensile strength and easily break. Polymer fibres are therefore often mixed with the grout material (Warner, 2004). Control of the direction of the fractures is difficult. Fracture grouting has been used in several embankment dams (Chen, 1982).

2.3.3 Jet grouting

With jet grouting, the fines in a soil are replaced with hardening particles under high pressure. The coarser part of the soil forms a new, harder structure together with the injected grout material (Windelhed, 2001). A hole is drilled, and a nozzle is placed into the hole. The nozzle rotates and is slowly raised throughout the procedure. During the raise, the upper part of the nozzle washes out the fines from the surrounding soil with the use of water or air. Meanwhile, the lower part of the nozzle injects a hardening grout material into the soil. The process is manageable by using one nozzle only and creates vertical, hard, low hydraulic conductivity pillars in the soil. The method is most suitable for sand and gravel.

2.3.4 Compaction grouting

Compaction grouting is the most common soil grouting method (Warner, 2004). The function of the method is to compact the soil around the injected grout material. Compaction grouting is versatile and is applicable in any kind of soil. The grout material is called low-mobility grout material and is very stiff, i.e., high viscosity and yield strength, compared to permeation grout materials. During injection, the grout material ideally expands radially. The expansion can however cause problems in the surrounding soil since shear forces may evolve at the interface of the expanding grout material and the soil (Shrivastava and Ken, 2018). The grout material is not intended to enter the pores of the soil into which it is injected.

Since the grout material expands and densifies the surrounding soil, the injection should be done at low flow rates. This will allow the pore water in the surrounding soil to be drained, lowering the risk of hydraulic fracturing (Warner 2004). Maximal grout pressures should be pre-determined to prevent damaging, e.g., heave, of the surrounding soil. The grout material is usually made from cement, sand, gravel and bentonite.

2.3.5 Evaluation of remedial grouting methods for use in embankment dams

To evaluate the applicability of described grouting methods in embankment dams, advantages and disadvantages of respective method are listed:

Permeation grouting

- *Advantages* – Does not damage the original structure of the soil into which it is injected. Well suited to use in soils that have low amounts of fines.
- *Disadvantages* – Durability is questionable, especially when using sodium silicate grout material or when grouting in high seepage zones. Shrinkage of the grout material is likely to occur.

Fracture grouting

- *Advantages* – Lowers the hydraulic conductivity of the soil and is suitable for cohesive soils.
- *Disadvantages* – Difficult to control the orientation of the fractures. Fractures are not desired in a core soil.

Jet grouting

- *Advantages* – Attained hydraulic conductivity will be low and the method is suitable for sand and gravel.
- *Disadvantages* – The method is "damaging" and does not allow safe drainage of fine material. Shear strength is very high.

Compaction grouting

- *Advantages* – Compacts the soil and is suitable for any type of loosely compacted soil and to fill cavities. Flexible method with great possibilities in designing a grout material.
- *Disadvantages* – Requires a skilled operator as it may damage the surrounding soil.

From a technical point of view, neither fracture grouting nor jet grouting should be considered as a remedial grouting method for embankment dams since both these methods will damage the core soil. Compaction grouting and permeation grouting should however be considered.

There are several case studies describing remedial work on Swedish embankment dams from 1976 to 2006, see e.g., Sjöström (1999), Ekström and Pusch (2001), Lagerlund (2007), Johansson and Edeskär (2012), Ekström et al. (2016) and Lagerlund and Nilsson (2020). These studies revealed that compaction grouting with grout materials made from sand, cement and bentonite was used in almost all cases. Sometimes, complemented with permeation grouting with either cement and water or sodium silicate grout materials. Internationally, permeation grouting, see e.g., (Littlejohn, 2003; Granata et al., 2012; Kociánová et al., 2015; and Park and Oh, 2018), has been used extensively as a remedial grouting method as well as compaction grouting, see e.g., (Brown and Warner, 1973; El-Kelesh et al., 2012; Yea et al., 2013 and Shrivastava and Ken, 2018).

Compaction or permeation grouting is therefore recommended as suitable grouting methods in embankment dams.

2.4 Research questions

If grouting is chosen as a measure to repair an embankment dam, the procedure should be approached with great consideration. A successful injection grouting requires an adequate description of the environment to be grouted to determine both grouting method and grout material (Fransson et al., 2016). Used grouting method should be related to the type of damage. Grouting should preferably be performed without interfering with the normal operation of the dam. Most usual damage types found in embankment dams caused by internal erosion are cavities (pipes), high permeable zones (suffusion) and loose soil zones (sinkholes), see *Figure 5*.


(A) Piping


(B) Suffusion


(C) Sinkhole on crest


(D) Sinkhole at abutment

Figure 5. (A) and (B) Piping and suffusion found in the Lövö embankment dam during its demolition (Ericsson and Jender, 1998), (C) sinkhole on crest of Bennett Dam (Garner, 2006) and (D) sinkhole at abutment on a Swedish embankment dam (Lagerlund and Nilsson, 2020).

The purpose when grouting an embankment dam is to lower the seepage rate by lowering the permeability of the core (Foster et al., 2000). Grouting must be done carefully as not to provoke any excessive pore-water pressures but at the same time minimizing the presence of interconnected voids, (Fell et al., 2005 and Park and Oh, 2018). Stiffer, cement reinforced soil zones should be avoided due to the large contrast of geotechnical properties between the surrounding embankment dam and the grouted zone, i.e., increased risk of cracking and arching due to differential settlements or grout material shrinkage, (Lim et al., 2004 and Lagerlund, 2009).

Grouting methods vis-à-vis common damage types are:

- Cavity damage, *Figure 5* (A), compaction grouting must be used.
- Suffusion of core soil, *Figure 5* (B), compaction grouting will not be suitable since the compaction of larger particle sizes will not diminish the hydraulic conductivity of the soil. Permeation grouting must be used.
- Sinkhole damages, i.e., *Figure 5* (C) and (D), compaction grouting must be used.

Grouting is still regarded as an empirical technology (Pan et al., 2023). Available case histories from grouting projects in embankment dams exist, but apart from how it was repaired and how the result was, further information is difficult to find. Among the case histories, there is a consensus on what grouting methods to use, i.e., compaction or permeation grouting. It is very rare to find detailed information regarding grout material composition. Most case studies have described the use of cementitious grout materials, especially with compaction and permeation grouting. However, hardening grout materials are unwanted in the core of an embankment dam. Therefore, research must be undertaken to develop a non-hardening grout material that with time, will become a part of core. It is hypothesised that by using this approach, the damaged core soil will not only be repaired but restored.

The following research questions are addressed:

1. Is it possible to compose a non-cementitious grout material for use within embankment dams suitable for both compaction- and permeation grouting?
2. How does particle size, viscosity and yield strength of the grout material affect its penetrability?
3. How does the appearance of a suffusion damage type affect the penetrability of a grout material?
4. How can frictional losses due to the grout materials resistance to flow be estimated, i.e., how much of the grouting pressure as measured at the pump end up inside the embankment dam?
5. Can an injection approach with low grout pressures be utilized in the field to minimize the risk of fracturing or heave?

To answer the research questions, three different laboratory investigations were undertaken:

a) Grout material development, fresh and hardening properties.
b) Permeation tests.
c) Large-scale grouting test.

The planning, execution and results of each study is presented in four appended papers.

2.5 Outline of the papers

All appended papers were based on the laboratory investigations performed between the licentiate thesis and the doctoral thesis. Since the licentiate thesis was written as a monography, no papers were appended to it. The general outline of each of the four papers are as follows.

Paper I *"Design and strength development of a low-mobility grout for repair of embankment dams."*

Research question 1 and *laboratory investigation a).* In this paper, the constituents for an ideal grout material for embankment dams and how to perform the pre-testing to determine their proportioning (recipe) is explained. Furthermore, the grout materials behaviour during homogenization and shear strength development in samples stored up to 34 days was investigated.

Paper II *"Testing of a modified low-mobility grout material for permeation grouting in embankment dams."*

Research question 2, 3 and 5 and *laboratory investigation b).* In this paper, the influence of the following properties on the penetrability of a modified low-mobility grout material into a core soil, damaged by suffusion, were investigated:

- Grout material - D_{max}, consistency and amount of limestone filler.
- Damage – d_{min}, d_{15} and porosity.
- Method – Slow or fast injection.

Paper III *"Permeation grouting laboratory testing for embankment dams – a note on flow resistance."*

Research question 4 and *laboratory investigation b).* The resistance to flow of the two most suitable grout materials for permeation grouting presented in ***Paper II*** were studied. Influence of the pipeline loss, local loss at the pipeline exit and the permeation of the coarse-grained material could be quantified.

Paper IV *"Methodology for remediation grouting in embankment dams - grouting with a new type of non-hardening grout."*

Research question 5 and *laboratory investigation c).* In this paper, a grouting method was proposed and executed on a large-scale test embankment dam at full reservoir level. The grouting was done with low pressure at the abutment with the modified low-mobility grout material. The efficiency of the grouting was evaluated by measuring the seepage before, during and after the grouting operation.

3 LABORATORY INVESTIGATIONS

Developing an ideal non-hardening grout material for embankment dams requires a grout material without cement. Therefore, grout material constituents and their properties must be determined before the laboratory investigations.

3.1 Grout material constituents

Constituents for a non-hardening grout material for use in embankment dams were investigated in ***Paper I***. The grout material was then used in the three subsequent laboratory investigations presented in ***Paper II – Paper IV***, however slightly adjusted. The grout materials were made from sand and gravel aggregates, limestone filler, water and additives.

3.1.1 Aggregates

The main constituents of a grout material for embankment dams are the aggregates. Aggregates may range in particle size from clay to gravel. The particle size distribution of a grout material for embankment dams should be similar to the particle size distribution of the intact core soil into which it is injected. Particle size distribution of the aggregates is important to prevent internal erosion of the non-hardening grout material when percolated (Lagerlund, 2009), segregation and bleeding (Peng and Jacobsen, 2013). Segregation will cause the grout material to be unevenly dispersed, leaving un-grouted zones (Baltazar et al., 2012). Bleeding occurs when the aggregates of the grout material sediments after injection, increasing the water content in the uppermost part of the grouted zone (Warner, 2004).

Large particle sizes will lower the grout materials ability to penetrate or permeate cracks or pores when injected (Eklund and Stille, 2008). According to RIDAS (2020), the amount of fines in a core soil should be at least 20 weight-% to assure a sufficiently low hydraulic conductivity. Therefore, the lower limit of fines in a grout material for embankment dams is suggested to be similar.

Particle shapes of the aggregates is an important property from a pumpability point of view (Adiguzel and Bascetin, 2019). A grout material consisting of rounded aggregates is easier to pump compared to a grout material with more flake-shaped aggregates (Lagerblad et al., 2008). For this reason, rounded aggregates were chosen for the grout material.

3.1.2 Limestone filler

In fresh concrete, the cement particles and aggregates smaller than 0.125 mm, i.e., filler materials, constitutes the paste. The paste material is the lubricant, allowing the larger aggregates to roll or slide with less friction. Limestone filler can replace the cement as a paste material (Benjeddou et al., 2017). Incorporating a limestone filler will reduce the porosity of the grout material due to improved particle packing (Vogt, 2010). Too little paste-material in a grout material will increase the friction between the aggregates while too much will make it difficult to pump. According to Thorsén (2017), finding the optimal ratio of total surface area of the paste material and aggregates (C/A-ratio) is a key factor in developing pumpable concrete. Finally, a grout material where all cement is exchanged with a limestone filler will not harden.

3.1.3 Water and Additives

High water- and air content will lower the density of a grout material by increasing its void ratio. Since a grout material for embankment dams must have a very low hydraulic gradient after injection ($<10^{-7}$ m/s), it is important that both water and air content is low, i.e., high particle concentration in the grout material. It is therefore proposed that the water content in the grout material will be similar to water contents in a moraine core soil, e.g., 8 – 10 %. Air content in the grout material is proposed to be <5 % since higher air contents make the grout material difficult to pump (Betonghandboken, 1997).

A grout material at these proposed water and air contents will be very stiff and lumpy. Therefore, modification of the grout material must be undertaken to facilitate pumping. properties affecting pumpability, i.e., viscosity and yield strength, was investigated by Wallevik and Wallevik (2011). They tested how the addition of either water, air, superplasticizer or silica fume affected viscosity and yield strength of a reference concrete. Their findings are shown in *Figure 6.* The blue dot in the centre of the figure represents the yield strength and viscosity of a concrete. The arrows from the reference point, marks how the yield strength and viscosity is affected by the extra addition of either water, air, superplasticizer or silica fume.

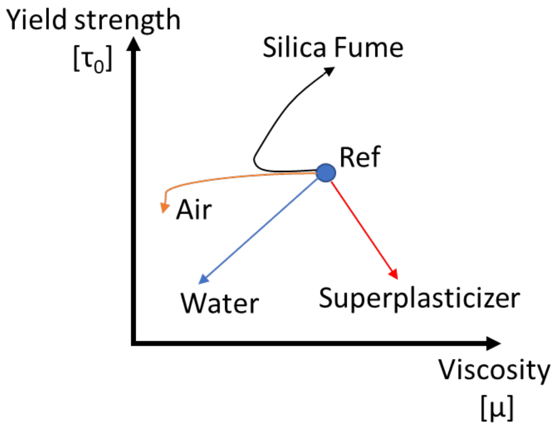

Figure 6. Influence of additional water (blue arrow), air (yellow arrow), superplasticizer (red arrow) and silica fume (black arrow) on the rheology of a reference concrete. Adapted from Wallevik and Wallevik (2011).

Addition of water will decrease both viscosity and yield strength. Addition of air will decrease yield strength. Addition of silica fume will lower the yield strength at low concentrations but ultimately increase its yield strength. Addition of superplasticizer will lower the yield strength but increase the viscosity. Since more water and air is unwanted and silica fume will increase both viscosity and yield strength in the grout material, the addition of a superplasticizer is the only viable alternative. When adding a superplasticizer to a grout material, it is adsorbed and interferes with the interparticle attractive forces causing the particles not to bond to each other. For a grout material for embankment dams, where water contents will be ~10 %, polynaphtalene- and sulfonate-based superplasticizers will have difficulties to fully function while polycarboxylic superplasticizers are more efficient (Lu, et al., 2019). Using polycarboxylic-based superplasticizers, Danzinger et al. (2003) produced pumpable concretes at w/c-ratios below 0.2.

The addition of a polycarboxylate superplasticizer will cause steric repulsion between the particles, reducing the magnitude of attractive forces (Flatt and Schober, 2012). For this reason, it is likely that a grout material containing it and water content as low as ~10 % will absorb air when homogenized (Lange and Plank, 2012). Consequently, an air-release agent must be added. An air-release agent is a polysiloxane based polymer and will facilitate the evacuation of air in the grout material, lowering its air content (Betonghandboken 1997). Finally, dry bentonite powder may be used as an additive in the grout material to reduce the risk of bleeding and provide it with a slight swelling capability after its injection (Ekström and Pusch, 2001).

3.1.4 Non hardening grout material constituents

The following important properties for an ideal grout material for embankment dam cores consisting of fine-grained moraine, should be considered:

- Similar particle size distribution as the original core soil (fines, sand, gravel). Aggregates must be rounded or sub-rounded (natural aggregates) to facilitate pumping.
- At least 20 weight- % of fines. The main source of fines will be a limestone filler material, which will also function as a paste material, facilitating pumping and lowering the permeability of the grout material.
- Water content ~10 % to have a high particle concentration in the grout material.
- Superplasticizer to improve pumpability.
- Air release agent to prevent excessive air content during homogenization.
- Dry bentonite to reduce bleed and allow the grout material to swell slightly after injection.

Development of the grout material was done in laboratory investigation a) and was presented in ***Paper I***. For the remaining two laboratory investigations, the grout materials were slightly adjusted.

3.2 Laboratory equipment

3.2.1 Grout material development, fresh and hardened properties

For the development of the grout material, testing of its fresh and hardened properties, a Hobart mixer was used, see *Figure 7.*

Figure 7. Hobart mixer, 139 rpm.

3.2.2 Permeation tests

Permeation tests were performed and presented in ***Paper II*** and ***Paper III***. The equipment used is shown in *Figure 8*.

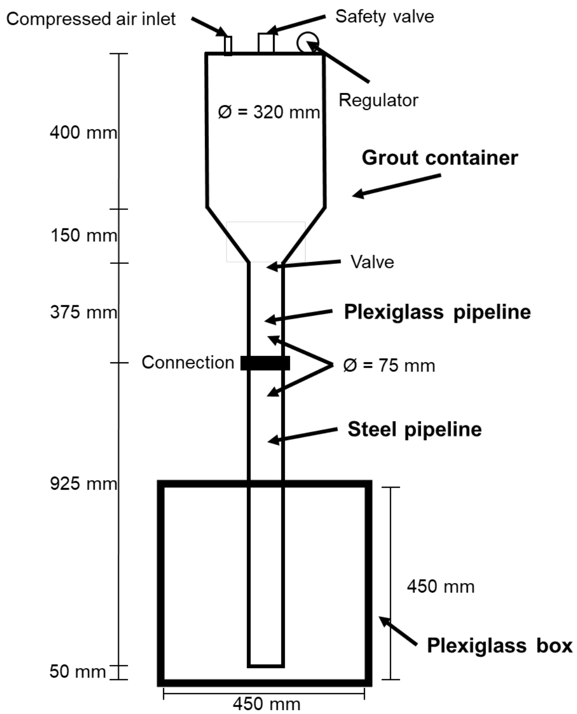

Figure 8. Grouting equipment used in all permeation tests.

The pilot-scale grouting equipment was designed to mimic a vertical injection procedure in an embankment dam with a suffusion damage. Exit of the pipeline was 50 mm above the bottom of the Plexiglass box. Grout material flow was down going in the pipeline but the flow in the Plexiglas box was bottom-up. The grouting equipment consisted of three parts:

1. A **grout container** of steel, i.e., the pump. The top of the grout container had a lid that could be bolted shut, a compressed air inlet, pressure gauge and a safety valve enabling both pressurized and own weight driven injection. The bottom of the grout container had a cone shaped ending, narrowing the 320 mm diameter grout container to 75 mm over a length of 150 mm. The total height of the grout container was 550 mm. A valve was installed at the bottom of the cone.

2. A **pipeline** of Plexiglass and steel. Internal diameter of the pipeline was 75 mm and total length was 1300 mm. The Plexiglass pipeline was 375 mm long and enabled visual observations of the down going grout material. The bottom steel pipeline was 975 mm long. The two pipelines were coupled with a screw connection.
3. **Plexiglass box**, which was the boundaries of the damage. The inside measurements of the box were 450 mm and wall thickness was 25 mm. The Plexiglass box was filled with a coarse-grained material, e.g., gravel and stone, similar to the material found in soils damaged by suffusion.

The Plexiglass box was placed on a scale with an accuracy of 50 g to measure grout material uptake during the permeation tests. The grout container and pipeline were lifted with an overhead crane and hung independently over the Plexiglass box. Neither the pipeline nor the grout container added any weight to the scale during any of the permeation tests.

3.2.3 Large-scale grouting test

Injection grouting was performed at the left abutment on a large-scale test embankment dam, primarily built for a non-destructive study of geophysical methods to detect built in faults. The results from the grouting test are presented in ***Paper IV.*** A description of the embankment dam has been presented by Toromanovic et al. (2020), Bernstone et al. (2021) and Viklander et al. (2023). The embankment dam has a central core of moraine, fine and coarse filters and a structural fill of rockfill material. It is 4 m heigh, 20 m long and 15 m wide, i.e., upstream to downstream, at the base, see *Figure 9.*

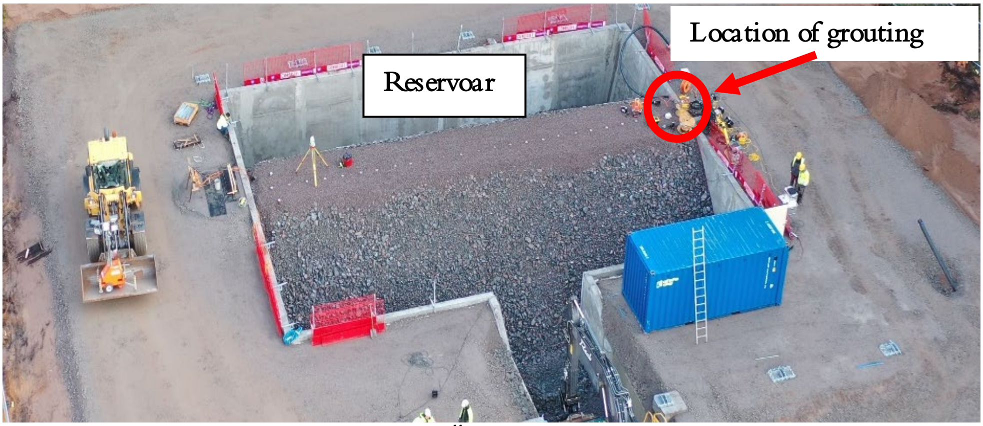

Figure 9. Embankment dam at the Älvkarleby laboratory. Red arrow and circle mark the location of the grouting test, at the left abutment. Original photo: Anders Lindström, Vattenfall R&D

The embankment dam was built inside a watertight concrete structure, allowing for a 3.3 m high water reservoir on its upstream side. The abutments has an outward angle of 1:8 and the bottom plate has a 1° drop toward the downstream side. Six rubber fenders (5 cm high with D-profile) were installed in the bottom plate to divide the seepage through the embankment dam into seven separate sections. Each section ends up in a Thomson weir where the seepage rate was continuously logged, *Figure 10*.

Figure 10. Close up view of the Thomson weirs nearest the left abutment at the downstream dam toe.

3.3 Performing the laboratory investigations

3.3.1 Grout material development, fresh and hardened properties

A laboratory investigation to find the optimal proportions of all constituents, defined in *subchapter 3.1.4,* was performed and its results are presented in ***Paper I***. Aggregate proportioning and limestone filler, i.e., particle size distribution curve, plus water content was determined before the testing was started. The particle size distribution of the aggregates was designed to be similar to the particle size distribution of the core soil used in the test embankment dam. Thereafter, the necessary amounts of superplasticizer, air-release agent and bentonite were investigated in an iterative process.

The following testing procedure was adapted:

1. The water content of each type of aggregate was measured. A dry weight of 2000 g of aggregate and limestone filler was used for each batch.
2. If bentonite powder was used in the batch, it was weighed and added dry to the aggregate and limestone filler.
3. Tap water at 8°C was weighed so the desired water content in the batch was obtained when the water was added.
4. If a superplasticizer or a superplasticizer + air release agent was used in the batch, it was weighed and mixed with the tap water.
5. Aggregates and bentonite powder (if any) were homogenized for 5 minutes in a Hobart mixer with a flat stainless-steel beater at 139 rpm.
6. The water with additives was slowly added, and the grout material was homogenized for another 10 minutes.
7. The grout material was characterized according to bulk density, bleeding, settlements, and consistency. Adjustments of the grout material had to be done if results fell below or over pre-determined limit values.

Pre-determined limit values were:

- Bulk density> 2150 kg/m^3 (SS-EN ISO 17892-2:2014). If the bulk density of the batch fell below 2150 kg/m^3, the air content was too high (> 5 %).
- Bleeding < 1.0 % after 24 hours (SS-EN 480-4:2005).
- Settlements < 1.0 % after 24 hours (measured during the bleeding test). The limiting values for bleed and settlements were derived from previous experiences by the authors when developing similar grout materials, e.g., Lagerlund and Holmberg (2021).
- Consistency = 100 mm and measured with a mini-slump-flow test. This limit was chosen since the grout material was estimated to be difficult to use for permeation grouting at lower consistencies. Consistency is an indirect measurement of both viscosity and yield strength of a grout material. A higher consistency measurement means the grout material is more easy flowing.

To study the influence of homogenization on the **fresh properties** of the grout material, testing was done with either *ceased homogenization* or *continuous homogenization.*

- *Ceased homogenization* – After 15 minutes of homogenization, the full batch of ca 1 litre of grout material was tested for undrained shear strength (SS-EN ISO 17892-6:2017), water content (SS-EN ISO 17892-1:2014), and bulk density. Thereafter, the grout material was evenly distributed in nine paper cups. The insides of the cups were coated with a thin polymer lining to prevent water suction. The top of each cup covered with a thin plastic film to prevent evaporation. Testing was done on the grout material in one new cup every 10 minutes. The total time from start of homogenization to the test of the grout material in the last cup was 125 minutes.
- *Continuous homogenization* – After 15 minutes of homogenization, the mixer was stopped so the grout material in the mixing bowl could be tested for undrained shear strength, water content, and bulk density. The grout material was kept in the mixing bowl and was continuously homogenized. Every 10 minutes, the homogenization was stopped so the undrained shear strength could be measured. The total time of the test was 125 minutes. After the last measurement of the undrained shear strength, water content and bulk density were measured.

To study the **hardened properties**, samples of grout materials were made and stored up to 34 days in fibre glass tubes. Undrained shear strength was tested on the stored samples with both fall cone tests and unconfined compressive strength (UCS) tests (ISO 17892-7:2017). Water content, bulk density and settlements of the grout material inside the fibre glass tubes during storage were also tested. Each sample had a 50 mm diameter and a height of 170 mm, sealed in the top with a rubber cap and a filter stone in the bottom. The grout material was not compacted inside the fibre glass tubes when prepared. Instead, the grout material was put inside the fibre glass tube with an ordinary spoon. The fibre glass tubes were placed in a bucket filled with a layer of gravel to allow drainage, *Figure 11*.

Figure 11. Sample preparation and storage of grout material.

All samples were stored in a fridge at a constant temperature of 8°C until testing. A new sample was tested each testing day after 2, 4, 7, 15 and 34 days of storage with fall cone and three samples each testing day after 7, 15 and 34 days of storage with UCS-testing.

3.3.2 Permeation tests

The permeation tests presented in ***Paper II*** were performed to investigate how the following properties affected a grout materials permeation of a coarse-grained material:

- *Grout material* – D_{max} = 2 or 4 mm and a ratio of limestone filler/aggregates (L/A) = 1.4 or 1.7. Consistency of the grout material was either low (100 mm) or high (150 mm)
- *Damage* – A coarse-grained material to be grouted with d_{15} = 35, 75, or 110 mm and porosity = 0.45, 0.46 or 0.48 respectively.
- *Injection method* – Slow or fast injection.

To study how the presented properties affected the permeation of the grout material, a test matrix was made, consisting of 48 different test combinations divided into 8 test series, see *Table 3*. Determination of how well the injected grout material permeated the coarse-grained material was made by measuring grout uptake, i.e., weight of injected grout material during and after each test.

Table 3. Test matrix. All grouting tests done in three different coarse-grained materials with d_{15} = 35, 75 or 110 mm. Consistency = 100 mm was high yield strength while Consistency = 150 mm was low yield strength.

	Grout material			Injection method	Coarse-grained material
Series	L/A ratio	D_{max} [mm]	Consistency [mm]	1 = Slow 2 = Fast	d_{15} [mm]
1	1.4	4	100/150	1	35/75/110
2	1.4	4	100/150	2	35/75/110
3	1.4	2	100/150	1	35/75/110
4	1.4	2	100/150	2	35/75/110
5	1.7	4	100/150	1	35/75/110
6	1.7	4	100/150	2	35/75/110
7	1.7	2	100/150	1	35/75/110
8	1.7	2	100/150	2	35/75/110

Before, during and after each test, the following characterization was done on the involved materials, *Table 4*.

Table 4. Tested properties before, during and after a permeation test.

Grout material	Coarse-grained material	Injection procedure
Bulk density [kg/m^3][1]	Particle size distribution[1]	Grout uptake [s/5 kg][2]
Air content [%][1]	Bulk density [kg/m^3][1]	Total grout uptake [kg][3]
Bleed and settlement [%][3]	Porosity [-][1]	
Mini-slump flow [mm][1]		

[1]Before the test, [2]During the test, [3]After the test.

The laboratory execution of each permeation test is described:

1. The empty Plexiglass box was placed on a scale. The coarse-grained material was put inside the Plexiglass box with the pipeline placed centrally. The weight was measured before and after filling the Plexiglass box with the coarse-grained material. The weight of the pipeline was deducted. After this, the Plexiglass box was filled with water and weighed again. The water was then drained from the Plexiglass box. Porosity could be calculated. Injection always took place in wet coarse-grained material.
2. The weight of the aggregates and limestone filler according to the grout material recipes was measured. The dry weight of aggregates and limestone filler was 60 kg for each batch, giving roughly 27 litres of grout material. The bentonite powder was added dry without pre-swelling.
3. The tap water was run for 2 minutes in all batches to achieve similar temperature. Water was weighed and the superplasticizer and air release agent were added to the water.
4. All aggregates and limestone filler were put in a pan mixer and homogenized for 5 minutes. Water and additives where then added and homogenized for another 5 minutes. After 10 minutes of homogenization, the grout material was poured into a wheelbarrow.
5. The grout material was kept in the wheelbarrow until the desired consistency of either 150 or 100 mm was reached.
6. The properties of the grout material according to *Table 4* was measured. A small portion of the grout material was set aside for the 24 h measurement of bleed and settlement.
7. The grout material was poured into the grout container, the lid was bolted shut, and the hose for compressed air was connected.
8. The grout container was connected to the overhead crane, lifted in position, and connected to the pipeline in the Plexiglass box. The grout container and pipeline were elevated so the pipeline exit was 50 mm above the bottom of the Plexiglass box.

9. Injection was done in either two ways:
    a. Slow injection. The flow of grout material was governed only by its own weight. When the flow stopped, 40 kPa of compressed air was added on top of the grout material inside the grout container to restart the injection. If the flow stopped once again, the compressed air was evacuated from the grout container so it would not affect the weighing of the Plexiglass box. 80 kPa of pressure was thereafter added in a second pressure increase. 40 kPa extra pressure was thus added in each pressure increase. Maximum pressure was 280 kPa. Pressure was always set to zero between each pressure increase.
    b. Fast injection. An extra amount of compressed air of 80 kPa was added before the permeation test started. Pipeline velocity was governed by the own weight of the grout material plus the additional compressed air. No extra pressure was added at any time.
10. For each 5 kg of grout material injected, the time interval from the start of the test was logged.
11. Each permeation test was ended when the grout container was either empty or no more weight increase was achieved.
12. 24 hours after each permeation test, the bleeding and settlement of the grout material was measured.

Viscosity and yield strength was tested for the grout materials with an L/A ratio = 1.7 after all 48 test combinations according to *Table 3* had been tested. The choice of only testing the grout materials with an L/A ratio = 1.7 was taken since they permeated the coarse-grained material far better than the grout material with an L/A ratio = 1.4. Testing of viscosity and yield strength was done at the CBI, laboratory in Stockholm. Equipment used was a coaxial cylinder ConTec BML viscometer, developed for concretes with a $D_{max} \leq 16$ mm, see *Figure 12*. The measurements were done by shearing a certain volume of grout material in the annulus between two ribbed concentric cylinders to prevent slipping of the grout material along the side walls. Shearing was done at varying rotational velocities of the inner cylinder, i.e., shear rates. At each rotational velocity, the angular velocity and torque was measured. Measurements were done when the inner cylinder rotates between 0.09 – 0.43 rounds per second, i.e., steady laminar flow. Viscosity and yield strength was then calculated under the assumption that the grout material was a Bingham fluid, i.e., a fluid that requires a certain amount of yield stress before it starts to flow.

Figure 12. ConTec BML viscometer. A similar device was used for the testing of viscosity and yield strength of the grout materials with an L/A ratio = 1.7 (Zerbino et al., 2009).

3.3.3 Tests without permeation

To measure frictional losses occurring in the vertical grouting system before the grout material enters the coarse-grained materials, tests without any coarse-grained materials in the Plexiglass box was performed. These "blank" tests were performed as the permeation tests but there was no coarse-grained material in the Plexiglass box. One test was performed for each of the two grout materials used in ***Paper III***, and one test per injection method, four tests in total. For these blank tests, side elements of Plexiglass were added inside the Plexiglass box. This would enable a similar elevation velocity of the grout material surface as in the permeation test.

3.3.4 Hydraulic characterization

To evaluate the resistance to flow in the tests, a hydraulic characterisation was used. Upper grout material surface, h_1, lower grout material surface in the Plexiglass box, h_2, and pipeline velocity, V_1, (*Figure 13*) were measured at each cumulative injected 5 kg of grout material. The mechanical energy balance in a vertical grouting system can be expressed with the Bernoulli equation, Eq. 1. The result from the hydraulic characterization is presented in ***Paper III***.

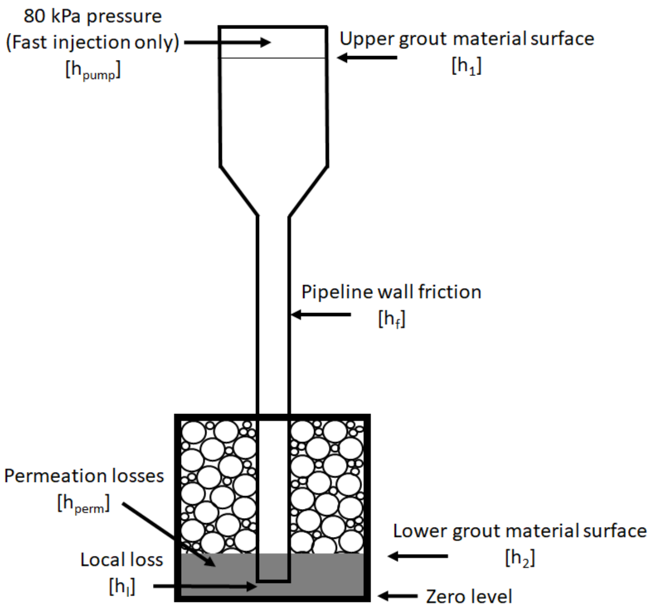

Figure 13. The vertical grouting system.

$$P_1 + h_{pump} + h_1 + \frac{V_1^2}{2g} = P_2 + h_2 + \frac{V_2^2}{2g} + h_{tot} \quad \text{Eq. 1.}$$

Where $P_{1,\,2}$ = atmospheric pressure [m], h_{pump} = pump pressure [m], h_1 = upper grout material surface [m], h_2 = lower grout material surface [m], V_1 = pipeline velocity [m/s], V_2 = pore velocity [m/s], g = 9.81 m/s^2 and h_{tot} = total friction losses [m]. P_1 = P_2 and low grout material velocities (V_{1max} ~ 1 m/s and V_2 = V_1/~20) are expected. P_1 and P_2 are therefore excluded and V_2 will be neglected during the evaluations. The h_{pump} is expressed in [m] according to Eq. 2.

$$h_{pump} = \frac{P_{pump}}{g\rho_{grout}} \quad \text{Eq. 2.}$$

Where P_{pump} = pumping pressure [Pa], g = 9.81 m/s^2 and ρ_{grout} = grout material density [kg/m^3]. Frictional losses in grout container are neglected, hence, the total frictional losses, h_{tot}, is expressed according to Eq. 3.

$$h_{tot} = h_f + h_l + h_{perm} \quad \text{Eq. 3.}$$

Where h_f = pipeline frictional loss [m], h_l =local loss at the exit of the pipeline [m] and h_{perm} = frictional loss during the permeation of the coarse-grained material [m].

During the laboratory investigation presented in ***Paper II***, viscometrical results of the grout material indicated a viscosity of the order of 10 Pas, which is about 10^4 times the viscosity of water. Yield strength values of the order of 100 Pa seen here are common for highly thickened tailings, i.e., paste, in the mining industry. Corresponding viscosities for these pastes are usually in the order of 10 – 100 times the water value with average particle sizes of 20 to 60 µm and a D_{max} ≤ of 0.5 mm (Wennberg, 2010). Therefore, the grout material pipeline flow can be considered as laminar Newtonian. The Darcy-Weisbach formula, h_f, for friction loss in laminar Newtonian pipeline is defined as Eq. 4.:

$$h_f = \left(\frac{64}{Re_{pipe}}\right)\frac{LV_1^2}{2gD} \qquad \text{Eq. 4.}$$

Where L = length of pipeline [m], V_1 = pipeline velocity [m/s], g = 9.81 m/s^2 and D = pipeline diameter [m]. Re_{pipe} is the Reynolds number and is defined in Eq. 5.

$$Re_{pipe} = \frac{\rho_{grout}DV_1}{\mu} \qquad \text{Eq. 5.}$$

Where ρ_{grout} = grout material density [kg/m^3], D = pipeline diameter [m], V_1 = pipeline velocity [m/s] and μ = dynamic viscosity [Pas].

Local loss, occurring at the end of the pipeline where the direction of the grout material flow is redirected 180° was estimated with Eq. 6. Generally, a coefficient K_l is related to the pipeline velocity head $V_1^2/2g$ giving the extra losses in addition to pipeline friction as a local loss.

$$h_l = K_l\frac{V_1^2}{2g} \qquad \text{Eq. 6.}$$

Where V_1 = pipeline velocity [m/s] and g = 9.81 m/s^2. The K_l value for laminar liquid flow is normally estimated based on an inverse proportionality to the Re_{pipe} number multiplied with the K_l -value in Eq. 6., giving the start of turbulent flow at about 1000 for the abrupt change in flow direction at the exit of the pipeline, Eq. 7. (Miller, 1990).

$$h_l = \left(\frac{1000}{Re_{pipe}}\right)K_l\frac{V_1^2}{2g} \qquad \text{Eq. 7.}$$

Where Re_{pipe} was given in Eq. 5., $K_l = 1$, V_1 = pipeline velocity [m/s] and g = 9.81 m/s^2. The flow of grout material from the vertical pipeline into the coarse-grained material can be considered as an annular bend for which K_l in Eq. 7. may be taken as 1 for liquid flow (Miller, 1990). If the grout material flow remains attached to the bottom, not turning immediately into the annulus, this may change the loss by a factor of two corresponding to a Re of 2000 in Eq. 7. (Miller, 1990). h_f is measured and defined on straight pipelines only. Therefore, h_l must be regarded as a part of h_f, i.e., $h_f = (h_f + h_l)$, during the measurements in the tests, see *Figure 14.*

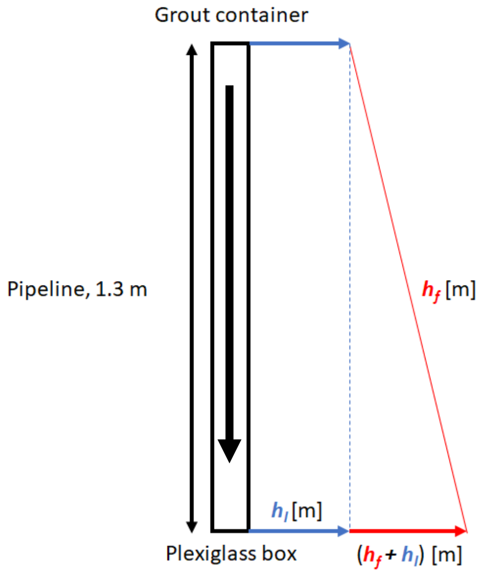

Figure 14. Schematic development of friction head loss over the pipeline for (h_f + h_l). Flow direction of grout material vertically down.

Each injection procedure of a limited batch size of grout material will be transient, meaning h_1, will decrease while h_2 and h_{perm} will increase. Available heads, $h_{available}$, during each test procedure at any time will therefore lower throughout the injection procedure. $h_{available}$ is derived from Eq. 1. into Eq. 8. for slow injection and Eq. 9. for fast injection.

Slow injection: $h_{available,\ slow} = (h_1 - h_2) + \frac{V_1^2}{2g}$ Eq. 8.

Fast injection: $h_{available,\ fast} = \frac{80000}{g\rho_{grout}} + (h_1 - h_2) + \frac{V_1^2}{2g}$ Eq. 9.

Where h_1 = upper grout material surface [m], h_2 = lower grout material surface [m], V_1 = pipeline velocity [m/s], g = 9.81 m/s^2 and ρ_{grout} = grout material density [kg/m^3]. For fast injection, when h_1 > 1.3m, the velocity term $V_1^2/2g$ is replaced with -(1000/Re_{pipe}) $K_1V_1^2/2g$ with K_1 = 0.2 for the conical shaped bottom of the grout container, based in an assumed viscosity of 10 Pas (Miller, 1990).

3.3.4.1 Evaluation procedures

From all the permeation tests performed and presented in ***Paper II***, the permeation tests where an even grout material surface was formed and possible to measure inside the Plexiglas box was evaluated further. According to the permeation test results, results from test series 5 – 8 were used (*Table 3*). Only used results was with grout material with an L/A ratio = 1.7, a consistency of 150 mm and when the d_{15} = 75 and 110 mm coarse-grained materials were permeated. From these permeation tests, evaluation of the grout materials resistance to flow was done. The results are presented in ***Paper III***. A description of the evaluation procedure for these tests follows.

The following description is supported by *Figure 15* and *Figure 16*. Zero level = bottom of plexiglass box.

1. Before the start of a test, h_1 is at the grout material surface in the grout container and h_2 at the bottom of the grout container, just above the valve.
2. Right after the opening of the valve, grout material will fall into the pipeline, partially filling it (not a uniform grout material front moving down the pipeline). As soon as the first portion of the grout material reaches the bottom of the Plexiglass box, both h_1 and h_2 are relocated to the bottom of the Plexiglass box.
3. A grout material surface begins to form inside the pipeline, h_1, moving up through the pipeline at an unknown rate. Simultaneously, the grout material will start to permeate the coarse-grained material, forming a grout material surface inside the Plexiglass box, h_2.
4. h_1 continues to rise through the pipeline until it reaches the bottom of the grout container. At this moment, h_1 is immediately relocated to the top of the grout material inside the grout container. Until h_1 reaches grout material in the grout container, the pipeline above h_1 and below the grout container will always be partially filled.
5. After h_1 has been established at the grout material surface inside the grout container, grout material flow will begin to slow down until all available grout material is either injected or the resistance to flow is higher than the available head, stopping the grout material flow.

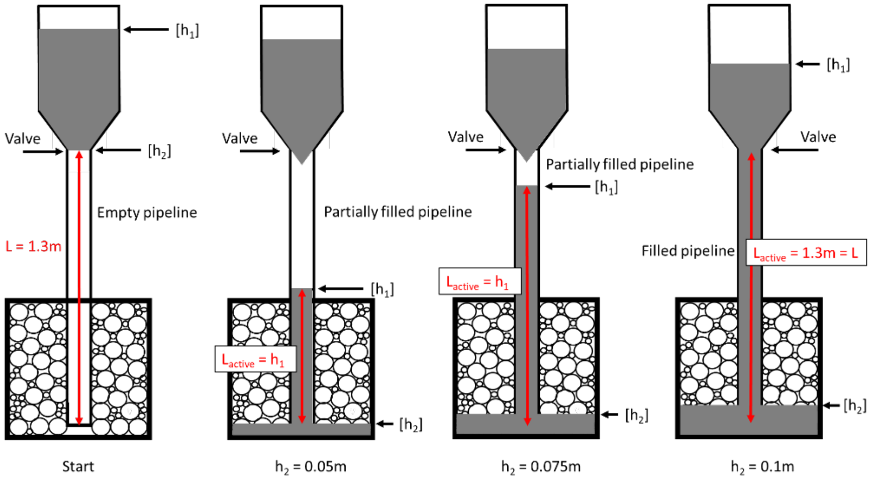

Figure 15. Evolution of h_1, h_2 and L_{active} during the filling of pipeline with grout material when grout material surface in the pipeline reached the bottom of the grout container at h_2 = 0.1 m. Zero level = bottom of Plexiglass box.

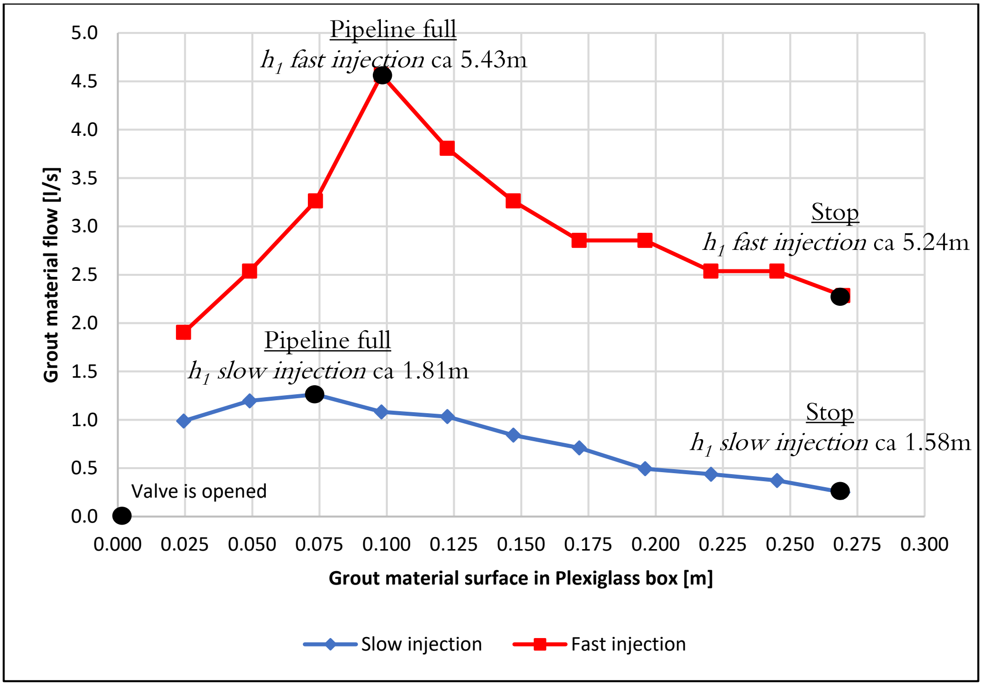

Figure 16. Example plot of grout material flow rate vs. height of grout material surface, h_2, in the Plexiglass box during a full test. Slow and fast injection compared.

The grout material surface in the Plexiglass box, h_2, will be measured directly by observing it through the Plexiglass side wall. h_1 is estimated by measuring the initial height of the grout material in the grout container. Thereafter, a mass balance is used to calculate the position of h_1. Pipeline velocity, V_1, is calculated by dividing the grout material flow with the area of the 0.075 m diameter pipeline. The moment the pipeline has been filled is important since this is when h_1 will be known for the first time during the permeation test, h_{perm} according to Eq. 3. is at its lowest and $L_{active} = L$. Verification of when pipeline is full can be done in two ways:

1. Visual observation of the grout material surface, h_1, inside the pipeline when it connects with the grout material inside the grout container. Can be observed through the Plexiglass part of the pipeline, just beneath the grout container, see *Figure 8*.
2. Through the grout material flow rate vs. height of grout material surface plot, see *Figure 16*. Maximum grout material flow is achieved when $h_{available}$ is at its maximum, i.e., when h_1 is relocated to the top of the grout material surface inside the grout container.

At this moment, h_1 will be ca 1.8 m during slow injection and 5.4 m during fast injection, see *Figure 16*. Corresponding h_2 will be between 0.05 – 0.1 m. The gradient, j, can then be written as $(h_1 - h_2)/L$ which is equal to $(h_f + h_l)/m$. The gradient is then plotted against the measured pipeline velocity. It follows from *Figure 16* how the chaotic situation at the pipeline exit introduces additional losses through the start of permeation. Therefore, the permeation resistance to flow, h_{perm}, will be coupled to the grout material surface elevation span 0.075 or 0.1 – 0.27 m.

The combined pipeline and local frictional loss ($h_f + h_l$) can be written as a total friction head loss, h_{fl}. h_{fl} can then expressed in terms of a gradient $j = h_{fl}/L$ where L is the considered pipeline length, are expressed through j together with Eq. 4. as:

$$j = \frac{h_{fl}}{L} = \left(\frac{64}{Re_{pipe}}\right)\frac{V_1^2}{2gD}$$

Where the viscosity for the grout material during the measurements can be directly extracted from Reynolds number $Re_{pipe} = \rho_{grout}VD/\mu$, Eq. 10.

$$\mu = \frac{\rho_{grout}D^2\frac{h_{fl}}{L}2g}{64V_1} \qquad \text{Eq. 10.}$$

Where ρ_{grout} = grout material density [kg/m^3], V_1 = pipeline velocity [m/s], D = pipeline diameter [m], h_{fl} = total friction head loss [m], L = length of pipeline [m] and g = 9.81 m/s^2. The active length, L_{active}, of the filled pipeline where resistance to pipeline flow is generated is equal to h_1 during the filling of the pipeline. When viscosity is determined from the permeation tests, the viscosity will be labelled as fictitious viscosity. h_{perm} from the coarse-grained material will cause the pipeline velocity to lower but without being included in Eq. 10. Viscosities calculated from the blank tests will be considered as "true". The calculated viscosities with Eq. 10. is valid for the used test setup. In longer pipelines, see subsequent *subchapter 5.4.3.1., section Longer pipelines.*

3.3.4.2 Hydraulic conductivity

With the h_{fl}/m measured in the blank tests, the results were utilized to evaluate the remaining h_{perm} factor from the permeation tests. At each cumulative injected 5 kg of grout material in the permeation test, h_1, h_2 and V_1 was known. $h_{available}$ was then calculated with Eq. 8. or Eq. 9. From the blank test results, the h_{fl}/m vs. pipeline velocity plot could be used to calculate the h_{fl} occurring over the 1.3 m pipeline and local loss. h_{perm} could then be extracted from Eq. 11. Calculations were done from the moment pipeline was full until the grout material in the grout container reached the cone shaped ending, i.e., h_2 = ~0.075 – 0.27 m. Thus, pipeline was always full during all calculations.

$$h_{perm} = h_{available} - \left(\frac{h_{fl}}{m} L\right) \qquad \text{Eq. 11.}$$

Where $h_{available}$ = available head (Eq. 8. or Eq. 9.) [m], h_{fl} = total frictional head loss [m] and L = pipeline length [m]. With the h_{perm} known, hydraulic conductivity was calculated with Darcy's law, Eq. 12.

$$K_{min,max} = \frac{Q \Delta L_{min,max}}{(h_{perm})An} \qquad \text{Eq. 12.}$$

Where Q = grout material flow [l/s], $\Delta L_{min,max}$ = min or max length over which the frictional loss occurs [m], h_{perm} = frictional loss over coarse-grained material [m], A = area of Plexiglass box [m^2] and n = porosity of the coarse-grained material [-].

Calculating the hydraulic conductivity at each cumulative injected 5 kg grout material during each permeation test required an approximation of the flow path length, ΔL. Flow paths for a grout material, especially in squared geometries, e.g., a slot or a box, was observed by Lagerlund et al. (2014) to occur in a small portion of a large, squared geometry. Flow paths were always observed at the shortest route between an entrance and exit point during injection, see *Figure 17*. Outside the flow path, the grout material was at stand-still.

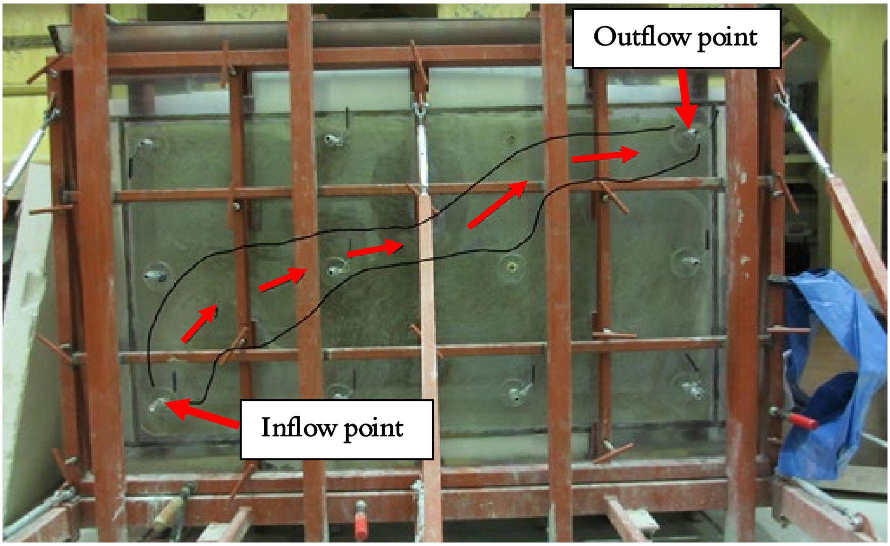

Figure 17. Flow path during an injection grouting test of a 1.7x0.9 m wide slot with 1 mm thickness. Example of a grout material flow path marked in figure, Lagerlund et al. (2014).

An estimation of the shortest and longest flow paths, i.e., ΔL_{min} and ΔL_{max} was therefore required, see *Figure 18*.

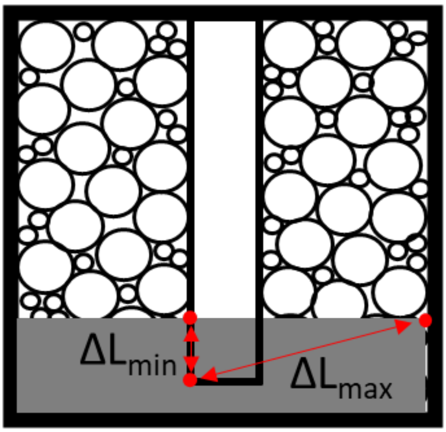

Figure 18. Shortest (ΔL_{min}) and longest (ΔL_{max}) routes for the grout material between the pipeline exit and the grout material surface.

Results from hydraulic conductivity are therefore presented as K_{min} or K_{max}. Verification of the calculated hydraulic conductivity was done by comparing the result as given by Eq. 12. with the expected hydraulic conductivity, calculated with Eq. 13.

$$K_{expected} = \frac{k\rho_{grout}g}{\mu} \qquad \text{Eq. 13.}$$

Where k = permeability of the coarse-grained material [m^2], ρ_{grout} = grout material density [kg/m^3], g = 9.81 [m/s^2] and μ = dynamic viscosity [Pas].

3.3.5 Large-scale grouting test

The large-scale grouting test is presented in ***Paper IV***. To remediate an embankment dam, the following steps should be applied:

Identification – Localization – Characterization – Remediation

Where:

- *Identification* - Something happens in the embankment dam, i.e., higher seepages rates, increased turbidity, settlements, sinkholes etc. This may indicate that internal erosion is ongoing inside the embankment dam. Acuteness of the situation should be evaluated immediately, and suitable remedial method chosen.
- *Localization* – The actual position where the damage is happening must be determined. Geophysical methods and geotechnical methods may be used.
- *Characterization* - The identified and localized damage should be characterised. This can be done by drilling and sampling. If grouting is chosen as a remedial method, the grout material should be designed according to the damage. The amount of grout material needed should be evaluated and maximal allowed grouting pressures vis-à-vis injection depth determined.
- *Remediation* – The grouting should be performed as careful as possible and the whole process should be under real-time surveillance. Measurement of grout material pressures and flow as well as pore water pressures inside the embankment dam is very important (Warner, 2004).

A large-scale grouting test, i.e., *remediation*, was performed at the left abutment of a test embankment dam at low grouting pressures (only compensating for frictional losses within the pipeline). The grout material had an addition of magnetite powder to facilitate its localization after injection. Localization of the grout material was investigated by another research team and the results hereof will not be presented. The steps in executing the large-scale grouting test follows:

1. Rotary percussion drilling of the core soil at the left abutment. Firstly, a steel casing (88 mm internal diameter, 100 mm outer diameter) was drilled to a depth of 3.6 m, *Figure 19 left*. Thereafter, a solid stem auger was used to remove the core soil to a depth of 3.7 m. The water content of the removed core soil was measured.
2. A pipeline with an internal diameter of 65 mm and length of 3.4 m was inserted into the casing. The top of the pipeline was locked in place ~20 cm above the top of the casing and attached to the grout container used in ***Paper II***. After this, the pipeline and grout container were lowered, resting on the top of the casing, *Figure 19 centre*. At the bottom of the pipeline, a steel packer with a diameter of 88 mm was installed. The steel packer was to prevent the grout material from moving up between the pipeline and casing, while allow water and air to be evacuated.
3. The grout material was made with a pan mixer. Aggregates, limestone filler, magnetite powder and dry bentonite powder, was first homogenized for 5 minutes after which the water and additives were added. The additives were first mixed with the water in a bucket and then added to the aggregates in the pan mixer. The grout material was homogenized for another 5 minutes. After homogenization, the grout material was characterized, e.g., bulk density and consistency.
4. The grout container was filled with 30 litres of grout-material and bolted shut. Via a vent on the top of the lid, compressed air was applied between into the grout container. The pressure during the grouting was calculated to be the height of the grout material inside the pipeline plus an additional 50 kPa. The extra pressure was calculated to compensate for the grout materials resistance to flow in the pipeline.
5. The valve on the bottom of the grout container was opened and the grout material was injected until a stand-still in the pipeline.
6. The grout container, casing and pipeline were raised in one single movement by using a pulley system, *Figure 19 right*. The grout material column inside the pipeline were at the same position because of the extra pressure of 50 kPa while the equipment was raised. When the casing and pipeline was above the crest, all grout material had refilled the drilled hole. Seepage from the dam was measured during and after the procedure.

Figure 19. (left) Installation of casing, (centre) pipeline inserted into casing and grout container attached to pipeline, (right) simultaneously raising of the grout container, casing and pipeline.

4 RESULTS

4.1 Proportioning of the grout material

Particle size distribution for aggregates and limestone filler used in all developed grout materials is shown in *Figure 20.*

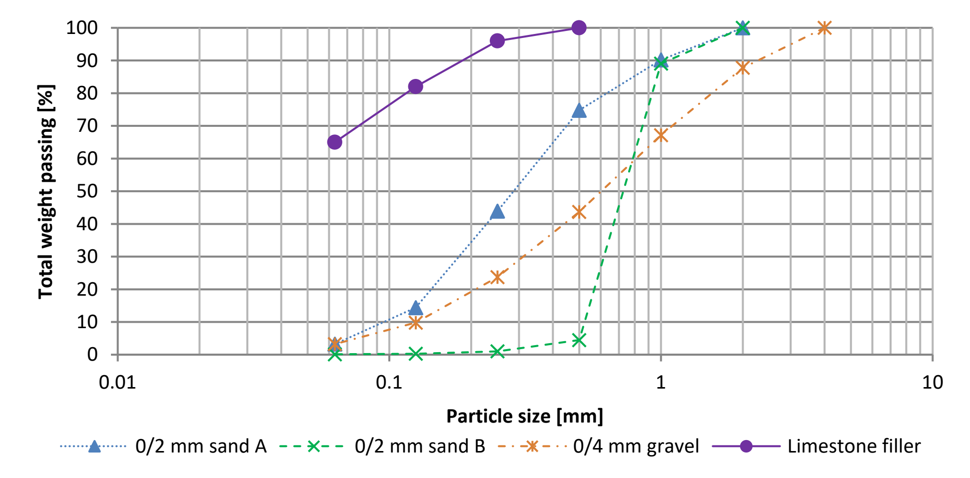

Figure 20. Particle size distribution for all involved aggregates and limestone filler.

Two grout materials with a D_{max} of either 2 or 4 mm was developed and characterized for their fresh and hardened properties in ***Paper I***. Recipes for the two grout materials are shown in *Table 5.* Fine content of aggregates was 20.0 % and 19.9 % and water content 13.1 % and 12.0 % in the 2 mm and 4 mm grout material respectively.

*Table 5. Grout materials used in **Paper I**. All amounts in weight-%.*

D_{max}	2 mm	4 mm
L/A ratio[1]	1.1	1.1
0/2 mm sand A	29.8	
0/2 mm sand B	32.4	18.6
0/4 mm gravel		45.1
Limestone filler	25.4	24.8
Water	11.5	10.6
Superplasticizer	0.52	0.53
Air release agent	0.02	0.02
Bentonite	0.30	0.32

[1] Limestone/aggregate ratio expressed in specific surfaces.

Recipes for the four grout materials used in the laboratory investigations presented in ***Paper II*** and ***Paper III***, are shown in *Table 6.* Fine content of aggregates was 25.0 % (L/A ratio = 1.4) and 27.5 % (L/A ratio = 1.7) in the 4 mm grout material and 26.5 % (L/A ratio = 1.4) and 29.0 % (L/A ratio = 1.7) in the 2 mm grout material. Water content was 12 %. The grout material used in the laboratory investigation presented in ***Paper III*** was both grout materials with an L/A ratio = 1.7 but only with 0.53 weight-% of superplasticizer added, i.e., the high-consistency grout material.

Table 6. Grout materials used in ***Paper II****. All amounts in weight-%.*

D_{max}	4 mm	4 mm[3]	2 mm	2 mm[3]
L/A ratio[1]	1.4	1.7	1.4	1.7
0/4 mm gravel	40.7	38.1		
0/4 mm (D_{max} 2 mm)[2]			40.7	38.1
0/2 mm sand B	15.9	15.1	15.9	15.1
Limestone filler	31.9	35.4	31.9	35.4
Water	10.6	10.6	10.6	10.6
Superplasticizer	0.48 or 0.53	0.48 or 0.53[3]	0.48 or 0.53	0.48 or 0.53[3]
Air release agent	0.02	0.02	0.02	0.02
Bentonite	0.33	0.33	0.33	0.33

[1] Limestone/aggregate ratio expressed in specific surfaces. [2]0/4 mm gravel sieved through a 2 mm sieve. [3]Grout material used in the hydraulic evaluation presented in ***Paper III***.

Recipe for the grout material used in the laboratory investigation presented in ***Paper IV***, where remedial injection grouting was performed at the abutment of a large-scale test embankment dam is shown in *Table 7.* Fine content of aggregates was 36.5 % and water content 12 %. L/A ratio was only 1.2 since the fine-grained magnetite was regarded as an aggregate and not a filler material.

Table 7. Grout material used in ***Paper IV****. All amounts in weight-%.*

D_{max}	4 mm
L/A ratio[1]	1.2
0/4 mm gravel	33.7
Magnetite powder	17.7
Limestone filler	37.2
Water[2]	10.6
Superplasticizer[3]	0.48
Air release agent[3]	0.02
Bentonite[3]	0.33

[1] Limestone/aggregate ratio expressed in specific surfaces.

Particle size distribution for the grout materials presented in *Table 5 – Table 7* is shown in *Figure 21.*

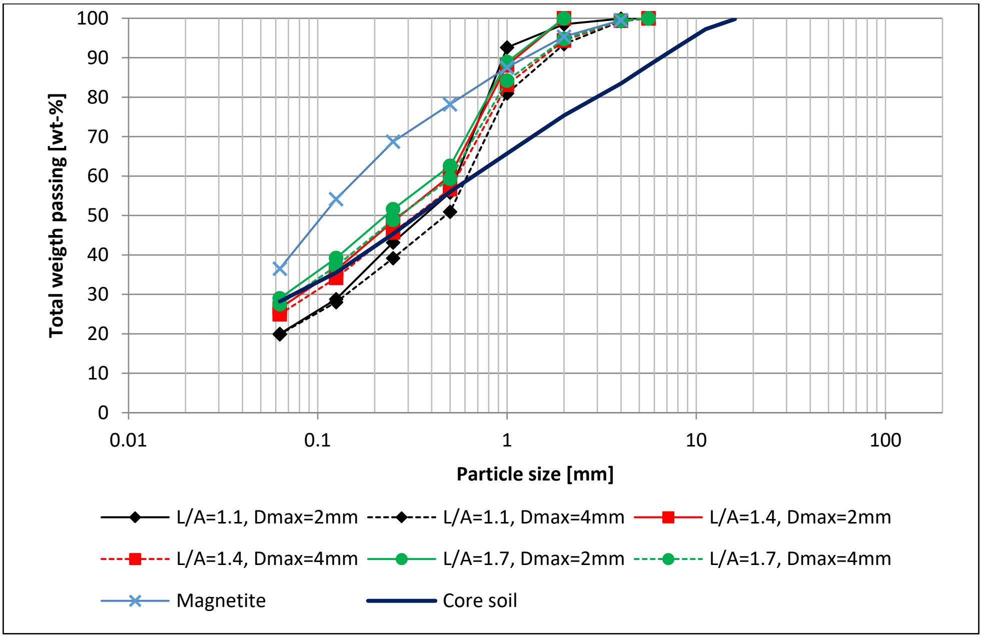

*Figure 21. L/A ratio = 1.1 grout materials presented in **Paper I**. L/A ratio = 1.4 and 1.7 grout materials presented in **Paper II** and **Paper III**. Magnetite grout material presented in **Paper IV**. Core soil from an embankment dam used in **Paper IV** as reference.*

4.2 Fresh properties

The influence of homogenization time of the grout material was investigated and presented in ***Paper I***. Homogenization time is important since the commonly used cementitious grout materials must always be continuously homogenized to delay their hardening. However, the grout material tested here does not contain cementitious materials. Its behaviour during and after homogenization is not well known.

Both grout materials presented in *Table 5* were tested. The two grout materials were either continuously homogenized for 125 minutes or homogenized for only 15 minutes and then left unattended for another 110 minutes. Bulk density, water and air content was measured after the initial 15 minutes of homogenization and after another 110 min of homogenization. The results from these measurements are shown in *Table 8.*

Table 8. Results from bulk density, water and air content in the two grout materials after 15 and 125 min of either ceased or continuous homogenization.

Grout material		D_{max} = 2 mm			D_{max} = 4 mm		
	Time [min]	ρ_{grout} [kg/m^3]	w [%]	n_a [%]	ρ_{tot} [kg/m^3]	w [%]	n_a [%]
Ceased	15	2130	13.2	4.1	2170	12.4	3.2
homogenization	125	2140	13.2	3.7	2170	11.9	3.7
Continuous	15	2150	13.4	3.0	2190	12.2	2.5
homogenization	125	1920	10.2	16.5	2180	9.1	6.4

During the *ceased homogenization*, bulk density, water and air content remained unchanged for both grout materials. During *continuous homogenization*, bulk density and water content was lower. Air content increased by a factor of 4.5 for the D_{max} = 2 mm grout material. For the D_{max} = 4 mm grout material, bulk density remained unchanged, water content was lower and air content increased by a factor of ~1.6. Overall, the D_{max} = 2 mm grout material was much more affected by the continuous homogenization than the D_{max} = 4 mm grout material.

Undrained shear strength of the fresh grout material was measured with a fall cone test after the initial 15 minutes of homogenization and thereafter every 10 minutes until a total time of 125 minutes. For testing during *continuous homogenization*, the Hobart mixer was briefly stopped to allow measurements. After the testing, the Hobart mixer was restarted. For testing during *ceased homogenization*, the grout material was first homogenized for 15 minutes and thereafter placed in cups and covered so water could not evaporate. After the initial 15 minutes of homogenization, the grout material in the cups were left until tested. Three drops were made during each testing with the fall cone. The following cones were used within each test series (weight of cone in grams and cone angle in degrees)

- D_{max} = 2 mm, *ceased homogenization*: (10 g and 60°) between 15–125 min.
- D_{max} = 2 mm, *continuous homogenization*: (10 g and 60°) between 15–65 min; (60 g and 60°) between 75–105 min; (100 g and 30°) between 115–125 min.
- D_{max} = 4 mm, *ceased homogenization*: (10 g and 60°) between 15–45 min; (60 g and 60°) between 55–85 min; (100 g and 30°) between 95–125 min.
- D_{max} = 4 mm, *continuous homogenization*: (10 g and 60°) between 15–125 min.

Results (mean value of three drops) from the measurements are shown in *Figure 22.*

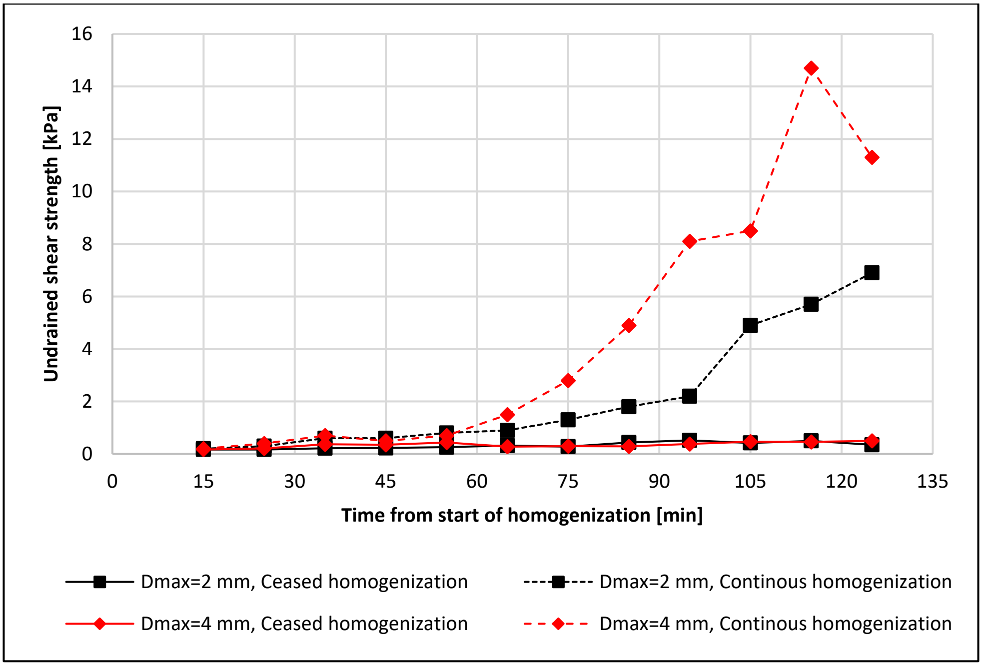

Figure 22. Development of undrained shear strength in the two grout materials tested during either ceased or continuous homogenization.

The undrained shear strength of the grout materials increased during the *continuous homogenization* and particularly in the D_{max} =4 mm grout material. Both grout materials however became very "lumpy" with time during the continuous homogenization. During *ceased homogenization*, undrained shear strength of the grout materials remained low during the whole testing procedure.

4.3 Hardened properties

The influence of storage time on the hardening of the grout materials was investigated in ***Paper I***. The intention was to investigate how the effect of the superplasticizer wore off with time. Both grout materials were made and put in 170 mm heigh, 50 mm diameter fibre glass tubes and stored at a temperature of 8°C. The fibre glass tubes had an impermeable rubber cap at the top and a filter stone in the bottom, allowing the samples to drain during storage. Directly after the grout material had been produced and after 2, 4, 7, 15 and 34 days of storage, bulk density, water and air content, and settlements were measured. Results from these measurements are shown in *Figure 23* and *Table 9.*

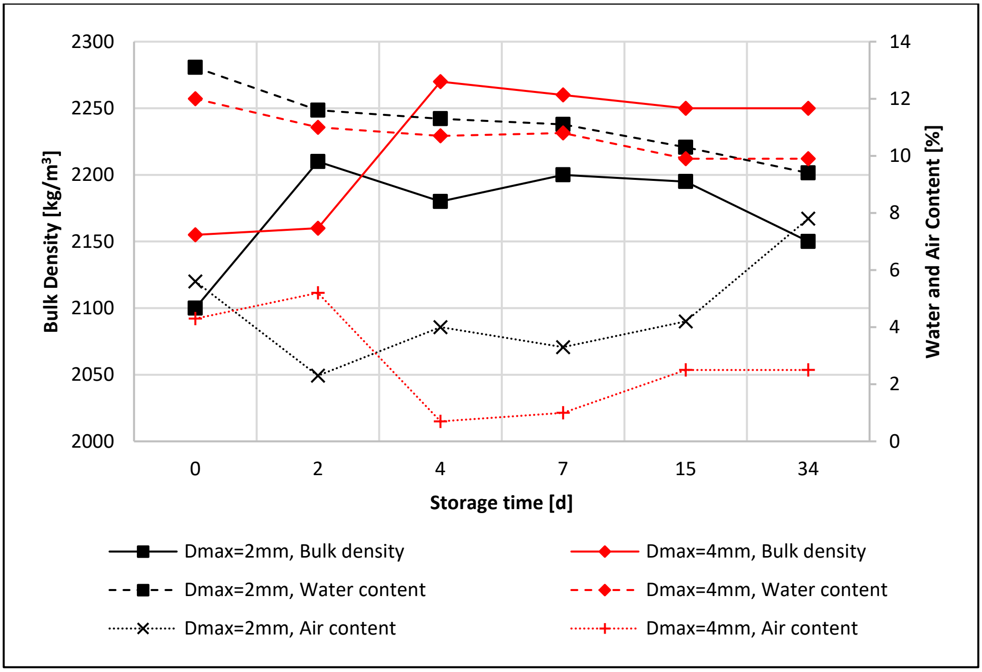

Figure 23. Bulk density, water content, and air content in stored grout material.

Table 9. Vertical settlements in samples used for fall cone test. Original height of sample was 170 mm.

	Storage time [d]	2	4	7	15	34
D_{max} = 2 mm	Settlements [%]	5.3	4.7	4.1	4.1	5.9
D_{max} = 4 mm	Settlements [%]	2.9	3.5	2.4	4.1	2.4

The bulk density increased during storage with 2.4 and 4.4 % in the D_{max} = 2 and 4 mm respectively. Water content continuously lowered with 28 and 18 % respectively and air content was increased by 39 % in the D_{max} =2 mm grout material while lowered with 42 % in the D_{max} = 4 mm grout material. Settlements of the grout material during storage did not increase with time.

Undrained shear strength of the stored samples was measured with the fall cone test after 2, 4, 7, 15 and 34 days of storage and measured with UCS testing after 7, 15 and 34 days of storage. For each testing day, three drops were used on each sample tested with fall cone and three samples were used for the UCS testing. Results from measurements of undrained shear strength is shown in *Figure 24*.

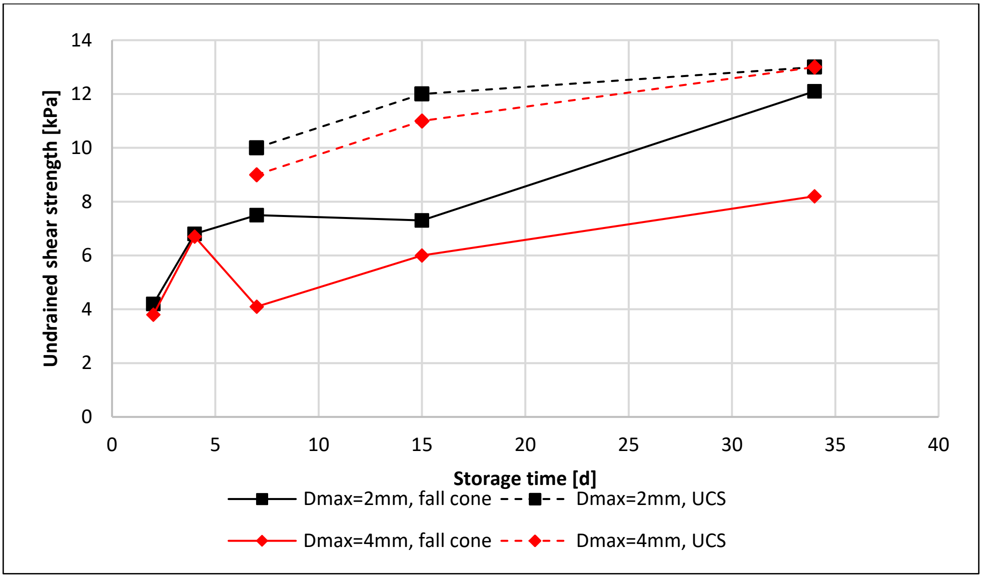

Figure 24. Development of undrained shear strength of stored samples measured using fall cone and UCS test.

The development of undrained shear strength measured with UCS was similar in the two grout materials between 7 and 34 days of storage. After 34 days, the undrained shear strength was 13 kPa in both grout materials. Undrained shear strength measured with a fall cone gave consistently lower results in comparison and a larger difference between the two grout materials. For both testing types, undrained shear strength was higher in the D_{max} = 2 mm grout material. Single spare samples were tested after 56 days (D_{max} = 2 mm) and 70 days (D_{max} = 4 mm) of storage. Undrained shear strength (UCS testing only) was measured to 19 kPa and 23 kPa, respectively.

The standard deviations for the fall cone tests were always higher than the maximum allowed 0.5 mm according to the standard (SS-EN ISO 17892-6:2017). In addition, the difference in undrained shear strength obtained by the fall cone testing were observed to be consistently lower than that of the UCS tests. However, the development of measured undrained shear strength was similar.

4.4 Permeation tests

In the laboratory investigation presented in ***Paper II*** and ***Paper III***, the grout materials shown in *Table 6* were injected into three different types of coarse-grained materials, i.e., a core soil damaged by suffusion. In ***Paper II***, grout material properties affecting how well a grout material can permeate a coarse-grained soil was investigate while the grout materials resistance to flow was evaluated in ***Paper III***. The particle size distribution of the three coarse-grained materials used for the permeation grouting is shown in *Figure 25* and its appearance is shown in *Figure 26*. Characterization is given in *Table 10*.

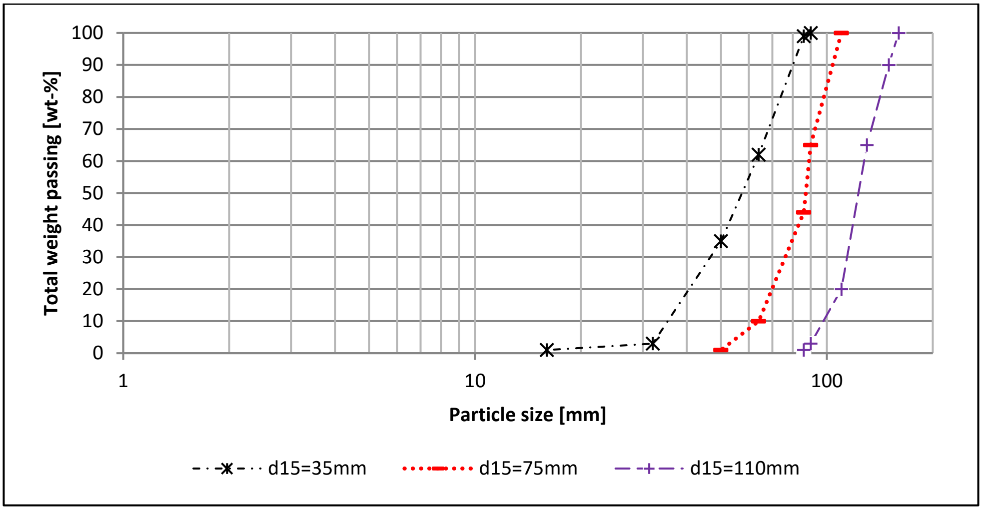

Figure 25. Particle size distribution of the three coarse-grained soils

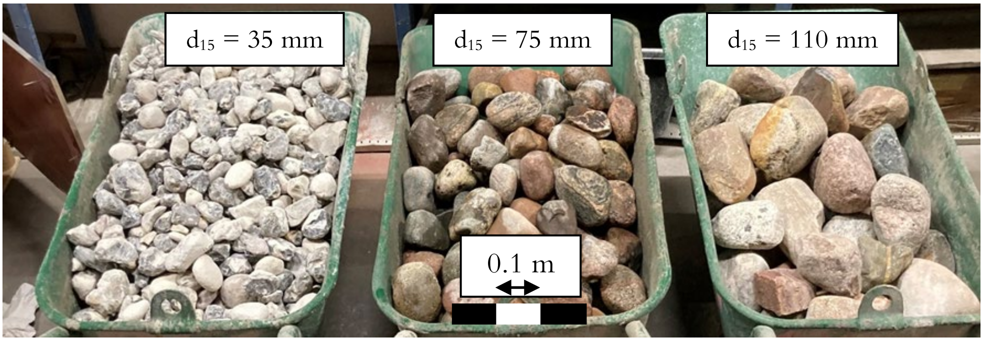

Figure 26. Used coarse-grained materials.

Table 10. Characterization of the three coarse-grained materials.

d_{15} [mm]	35	75	110
d_{max} [mm]	90	110	160
d_{min} [mm]	16	50	86
Porosity [-]	0.45	0.46	0.48
Bulk density [kg/m^3]	1460	1403	1350
Permeability [m^2]	n.a.	1.5x10^{-7}	2.0x10^{-7}

4.4.1 Grout material uptake

Grout material uptake, i.e., how much of the grout material available in each permeation test that permeated the coarse-grained materials, was measured in all tests. The results were presented in ***Paper*** **II**. Test matrix for all 48 permeation tests is presented in *subchapter 3.3.2, Table 3.*

Tested properties for grout materials were (1) L/A ratio, (2) D_{max}, (3) consistency and (4) injection method. Consistency values of ~100 or ~150 mm indicated either a stiff or easy-flowing grout material. For the coarse-grained material, three different d_{15} values were tested. Results for grout uptake from the first test series out of 8 is shown in *Table 11.* During test No. 1, 0.6 litres of the grout material was injected into the coarse-grained material during the first stage of the slow injection (the own weight of the grout material drove the injection). After a total of 280 kPa of compressed air had been added, 1.3 litres of the grout material had been injected. In test No. 6, 23.4 litres of the grout material were injected during the first phase. After an additional 40 kPa of compressed air, 24.6 litres were injected (full batch). Results from all permeation tests are shown in *Appendix A, Table A 1.*

Table 11. Results from the first series of permeation tests.

L/A ratio = 1.4, D_{max} = 4 mm, Slow injection				
Test No.	d_{15} soil [mm]	Consistency [mm]	Grout uptake own weight [litres]	Grout uptake 280 kPa extra pressure [litres]
1	35	102	0.6	1.3
2	75	100	3.5	4.7
3	110	103	16.2	20.8
4	35	149	1.2	2.1
5	75	150	4.7	7.7
6	110	150	23.4	24.6[1]

[1]Only 40 kPa extra pressure required.

Grout material uptake after the fast injection was measured after the grout material had come to a full stop. Description of slow and fast injection can be found in *subchapter 3.3.2.* Total batch size was ~25 litres, hence, results of grout uptake ~25 litres = all grout material was successfully injected.

The following observations could be made from the permeation test results:

1) A higher L/A ratio increased the grout material uptake.
2) A higher D_{max} increased the grout material uptake.
3) A higher consistency increased the grout material uptake, especially during slow injection.
4) Fast injection increased the grout material uptake even if the total amount of applied grout pressure was higher during slow injection.
5) A higher d_{15} of the coarse-grained material increased the grout material uptake.

4.4.2 Primary data of grout material flow rates from permeation tests

Time required for all permeation tests presented in ***Paper II*** is presented in Lagerlund (2023). Only results from grout material with an L/A ratio = 1.7, a consistency of 150 mm, d_{15} = 75 and 110 mm was used in ***Paper III***. The reason was that the grout material in these tests were the most easy flowing, i.e., possible to observe and measure an evenly distributed grout material surface inside the Plexiglass box. This would enable the use of a hydraulic characterization.

To facilitate the hydraulic characterization, grout material uptake is not presented in litres but as the height of the grout material surface inside the Plexiglass box, h_2. Each 5 kg of grout uptake was equal to ~2.5 cm of grout material inside the Plexiglas box. Results from the tests are therefore plotted as grout material flow rates vs. height of the grout material surface. Primary results from the permeation tests are shown in *Figure 27* (slow injection) and *Figure 28* (fast injection).

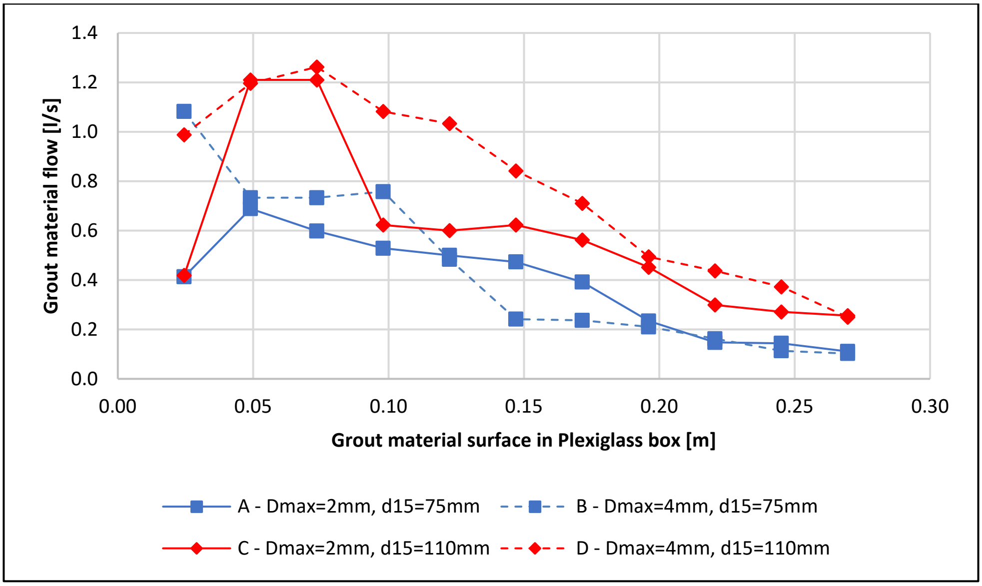

Figure 27. Primary results from permeation test with slow injection. A – test 41, B – test 29, C – test 42 and D – test 30.

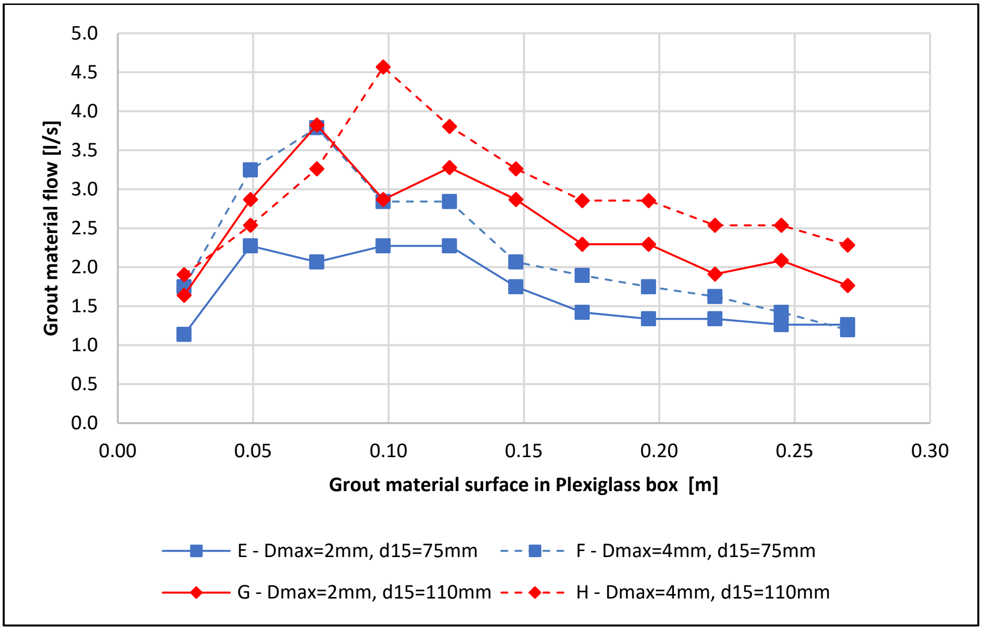

Figure 28. Primary results from permeation test with fast injection. E – test 47, F – test 35, G – test 48 and H – test 36.

Grout material flow rates was higher during fast injection, where 80 kPa was added at the start of each test. Grout material flow rates increased in the beginning of each test during the opening of the valve and filling of the initially empty pipeline. At a grout material height in the Plexiglass box between 0.05 – 0.1 m, a steady decrease of the grout material flow was initiated. This meant the pipeline had been filled. Decrease of grout material flow rate was steeper during slow injection compared to fast injection. The reason for this was that the final pressure in slow injection was zero while being 80 kPa for fast injection. Grout material flow rates were higher when D_{max} =4 mm grout material was injected. A higher d_{15} value of the coarse-grained material furthermore increased the grout material flow rates. Given the results presented in *Figure 27* and *Figure 28*, evaluations of the resistance to flow and hydraulic conductivities from all permeation tests was determined to be done at an h_2 between 0.075 or 0.1 – 0.27 m for all tests. Between these two h_2 measurements, the pipeline was always filled.

4.4.3 Resistance to flow

4.4.3.1 Friction losses

Viscosity of the grout materials used in ***Paper III*** was evaluated both from the permeation tests and with a blank test, i.e., a permeation test but without any coarse-grained material in the Plexiglass box, with Eq. 10. Mean values of all calculated viscosities from the permeation and blank tests are shown in *Table 12* and *Table 13*.

Table 12. Calculated fictitious viscosity from the permeation tests.

	d_{15} = 75 mm		d_{15} = 110 mm	
	Slow injection [Pas]	Fast injection [Pas]	Slow injection [Pas]	Fast injection [Pas]
μ D_{max}=2 mm	37.4	30.6	18.5	18.4
μ mean	**34.0**		**18.4**	
μ D_{max}=4 mm	28.6	18.5	17.8	15.2
μ mean	**23.6**		**16.5**	

Table 13. Evaluated viscosity from the blank tests presented in Figure 29.

	Slow injection [Pas]	Fast injection [Pas]
μ D_{max}=2 mm	12.1	13.1
μ mean	**12.6**	
μ D_{max}=4 mm	11.4	12.2
μ mean	**11.8**	

As expected, fictitious viscosities calculated from the permeation tests were higher than viscosities calculated from the blank tests and higher for the D_{max} = 2 mm grout material than the D_{max} = 4 mm grout material. Calculated fictitious viscosities were also higher in permeation tests when the d_{15} =75 mm coarse-grained material was permeated compared to the d_{15} =110 mm coarse-grained material. This latter finding indicated the presence of a h_{perm} or a different outflow situation during the permeation tests with the coarse-grained materials.

From the permeation tests and the blank tests, h_{fl}/m was plotted against pipeline velocity. These values, presented in *Figure 29*, were extracted from the actual measured h_1, h_2 and V_1 when the pipeline became full. Results from both grout materials, i.e., D_{max} =2 or 4 mm, are presented separately.

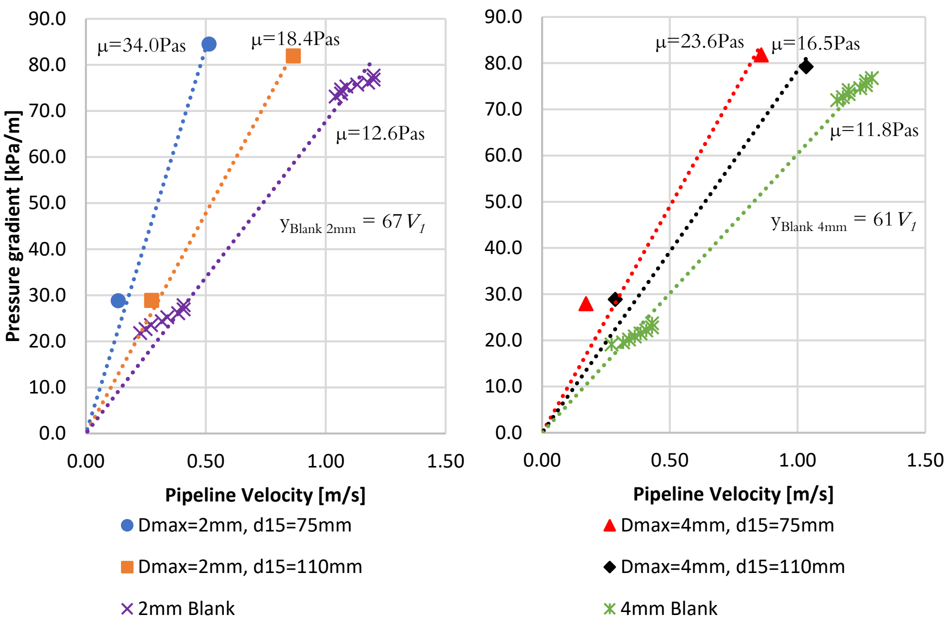

Figure 29. Measured pressure gradient vs. pipeline velocity of grout material with D_{max} = 2 and 4 mm respectively. h_{fl} measured. Trendlines set to go through origo (Newtonian behaviour). Viscosities, μ, taken from Table 12 and Table 13.

From the results presented in *Figure 29*, resistance to flow is higher when the D_{max} = 2 mm grout material is injected compared to the D_{max} = 4 mm grout material. It can also be seen that the h_{perm} is significantly affecting the obtained results at h_2 =

0.1 m, except in the blank tests. The influence of the outflow situation, affecting h_l and consequently the pipeline velocity, can't be distinguished from the results.

Viscosity and yield strength was also measured on the grout material with an L/A ratio = 1.7 at both consistencies of either 100 or 150 mm. Results from these measurements are shown in *Table 14.*

Table 14. Measurement of viscosity and yield strength for both L/A ratio = 1.7 grout materials with a Contec BML viscometer.

	Viscosity		Yield strength	
Consistency [mm]	D_{max} =2 mm [Pas]	D_{max} =4 mm [Pas]	D_{max} =2 mm [Pa]	D_{max} =4 mm [Pa]
100	**23.3**	**14.3**	491	256
150	**14.4**	**9,4**	73	106

Grout material with a lower consistency had both higher viscosity and yield strength compared to the high consistency grout material. Viscosity and yield strength was higher in the D_{max} = 2 mm grout material apart from the high consistency grout material. Here, the difference between the D_{max} = 2 and 4 mm grout material was minor. Mean viscosities for D_{max} = 2 and 4 mm grout material calculated from the tests with Eq.10 were expected to be lower than the viscometrical values shown in *Table 14.* This was however not the case. The viscosities were similar.

A hydraulic characterization was performed, and the results were presented in ***Paper III***. With the hydraulic characterization, frictional losses within the grouting system were evaluated. This was done for the permeation tests where an even grout material surface could be observed and measured through the side wall of the Plexiglass box.

The following information, required for the hydraulic characterization, was obtained during direct measurement in each of the 8 selected permeation test A – H:

- h_1 – height of the grout material surface in the grout container.
- h_2 – height of the grout material surface in the Plexiglass box.
- V_1 – pipeline velocity.

The following calculations could then be made to evaluate the frictional losses:

- $h_{available}$ – available pressure height, calculated with Eq. 8. or Eq. 9. for slow or fast injection respectively.
- h_{fl} – sum of frictional losses in the pipeline and at the pipeline exit plotted for the blank tests in *Figure 29*. To estimate h_{fl} in the permeation tests when D_{max} = 2 mm grout material was used, measured pipeline velocity was multiplied with 67 (see *Figure 29 left*) and the length of the pipeline. For the D_{max} = 4 mm grout material, pipeline velocity was multiplied with 61 (see *Figure 29 right*) and the length of the pipeline.
- h_{perm} – frictional losses due to the permeation of the coarse-grained material calculated with Eq. 11.

Results from the hydraulic characterization of test A and E is shown in *Table 15*. Results for all tests are presented in *Appendix B, Table B 1* and *Table B 2*.

Table 15. Evaluated data from tests with D_{max} = 2 mm grout material with slow injection (Test A) and fast injection (Test E). h_{fl} measured and h_{perm} calculated.

Test A[1], D_{max} = 2 mm, d_{15} = 75 mm									
V_1 [m/s]	0.14	0.12	0.11	0.09	0.05	0.03	0.03	0.03	0.01
$h_{available}$ [m]	1.74	1.69	1.64	1.58	1.53	1.47	1.42	1.37	1.31
h_{fl}^3 [m]	0.54	0.48	0.43	0.35	0.21	0.13	0.13	0.10	0.05
h_{perm} [m]	1.20	1.21	1.21	1.23	1.32	1.34	1.29	1.27	1.26
Test E[2], D_{max} = 2 mm, d_{15} = 75 mm									
V_1 [m/s]	0.51	0.51	0.40	0.32	0.30	0.30	0.29	0.29	
$h_{available}$ [m]	5.09	5.04	5.05	5.05	5.00	4.95	4.91	4.86	
h_{fl}^3 [m]	2.06	2.06	1.58	1.29	1.21	1.21	1.14	1.14	
h_{perm} [m]	3.03	2.98	3.47	3.76	3.79	3.74	3.77	3.71	

[1]Pipeline filled at h_2 = ~0.075 m. [2]Pipeline filled at h_2 = ~0.1 m. [3]$y_{2mm,\ Blank} = 67\,V_1$ used for h_{fl}.

During each permeation test procedure, V_1 lowered and consequently, h_{fl} lowered. Resistance to flow within the coarse-grained material, h_{perm}, was balanced during each permeation test with slow injection but increasing when fast injection was used. This occurred since $h_{available}$ at the end of a permeation test with slow injection was 0 while being ~3.6 m (80 kPa) with fast injection. Higher resistance to flow occurred in the d_{15} = 75 mm coarse-grained material compared to the d_{15} = 110 mm coarse-grained material as well as when the D_{max} = 2 mm grout material was used compared to the D_{max} = 4 mm grout material.

4.4.3.2 Hydraulic conductivity

Calculations of the hydraulic conductivity of the grout material permeating the coarse-grained material was presented in ***Paper III***. Hydraulic conductivity was calculated for all tests (A – H) and for each 5 kg grout material uptake. Calculations of the hydraulic conductivity from the tests was done with Eq. 12. Hydraulic conductivity was furthermore calculated assuming two different main grout material flow paths, ΔL, see *Figure 18*, resulting in either a maximum or minimum hydraulic conductivity, K_{max} or K_{min}. With the h_{perm} from the hydraulic characterization, see *Appendix B, Table B 1* and *Table B 2,* hydraulic conductivities could be calculated. The calculated hydraulic conductivity was compared with expected hydraulic conductivity calculated with Eq. 13. Results are shown in *Table 16.*

Table 16. Mean values of calculated hydraulic conductivities for the two coarse grained materials when permeated with either of the two grout materials.

	D_{max} =2 mm		D_{max} =4 mm		Expected[1]	
	K_{max} [m/s]	K_{min} [m/s]	K_{max} [m/s]	K_{min} [m/s]	$K_{Dmax\ 2mm}$ [m/s]	$K_{Dmax\ 4mm}$ [m/s]
d_{15}=75 mm	1.0×10^{-3}	1.7×10^{-4}	1.5×10^{-3}	1.4×10^{-4}	2.5×10^{-4}	3.4×10^{-4}
d_{15}=110 mm	2.4×10^{-3}	2.1×10^{-4}	3.8×10^{-3}	3.3×10^{-4}	2.7×10^{-4}	3.7×10^{-4}

[1]*Eq. 13.*

K_{min} was in better agreement with expected hydraulic conductivities compared to K_{max}. Mean values of K_{min} were close to expected values, indicating that the grout material flow path followed ΔL_{min} as shown in *Figure 18.* All calculated hydraulic conductivities are also shown in a grout material flow rate vs. hydraulic conductivity plot. Results from these plots are shown in *Appendix C, Figure C 1 - Figure C 4.* The results show a small tendency of the hydraulic conductivity to lower as the grout material flow rate lowers. Mean grout material pore velocities varied between 2.3×10^{-2} – 6.0×10^{-4} m/s in all permeation tests.

4.5 Large-scale grouting test

Remedial injection grouting of an abutment in a large-scale test embankment dam was performed with the grout material presented in *Table 7.* Results from this test are presented in ***Paper IV***. A 3.6 m long, 88 mm internal diameter steel casing was installed via rotary percussion drilling. After the casing had been installed, the core soil inside it was removed with a solid stem auger. Core soil from 1, 2 and 3 m depth was tested for its water content. Results from these measurements are shown in *Table 17.*

Table 17. Drilling and sampling at the left abutment. Water content from the time of dam construction (Oct – Nov 2019) compared to the water content during the time of drilling (15 Nov 2022).

Depth [m]	Water content when built [%]	Water content [%]	Increase [%]
1	8.3	15.2	83
2	9.5	14.8	56
3	9.9	14.3	44

At ~0.9 m depth a 10 cm thick zone of 4/8 mm gravel was found. The core soil had been significantly wetter with time but the increase in water content decreased slightly with increased depth. Seepage from the dam was continuously logged during the test. Results from these measurements are shown in *Figure 30*.

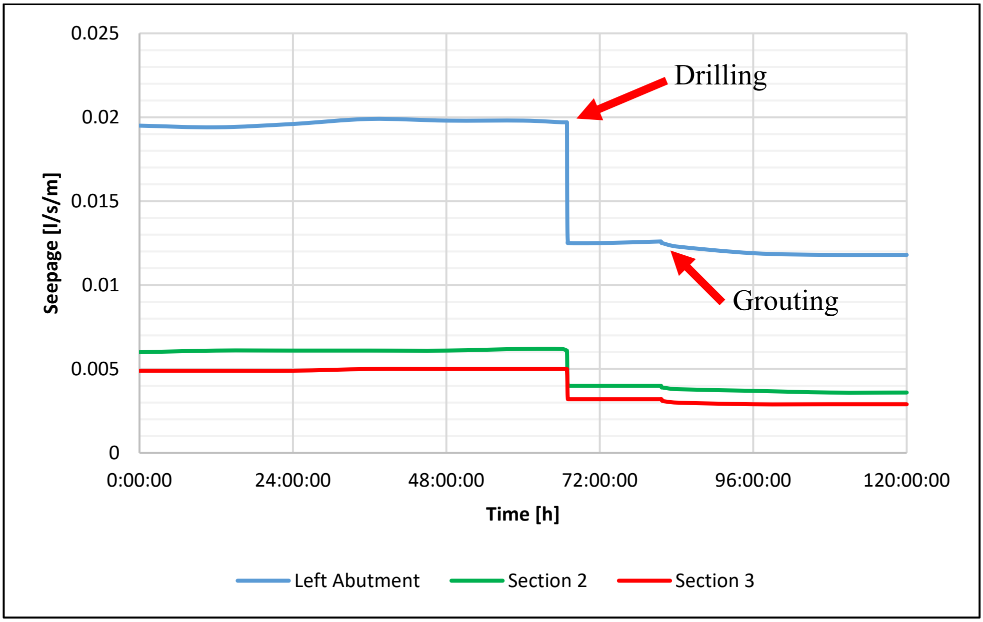

Figure 30. Seepage measurements expressed as l/s for each meter at the downstream side of the left abutment and the two closest sections next to it (section 2 and 3).

Seepage was mainly reduced during drilling and to a lesser extent during the grouting. Seepage reduction was largest in the zone closest to the abutment but also lowered in the two zones next to it. The seepage reduction in all measured sections occurred at the same time. Total seepage reduction was ca 40 % directly after the grouting operation (November 2022). In December 2023, seepage reduction was ca 70 % (not shown in *Figure 30*).

5 DISCUSSION

5.1 Proportioning of the grout material

The intention of the grout material proportioning was to develop a grout material with similar geotechnical properties as a fine-grained moraine. Pumping of the grout material was made possible by replacing the fines with a limestone filler plus the addition of a superplasticizer. This lowered the viscosity and yield strength of the grout material without affecting any other properties. The proportioning process was presented in ***Paper I***.

The proportioning of the grout material was determined via an iterative pre-testing process. The intention was to develop two grout materials with different D_{max} of 2 and 4 mm. D_{max} of the aggregates is an important property when predicting how well a grout material can permeate a coarser soil material (Lindvall, 2012). D_{max} of 2 and 4 mm were chosen since a D_{max} ≥4 mm would require too coarse-grained soil material, not likely to be found in a dam, to be permeated in the laboratory. Before the start of the pre-testing procedure, the following properties were determined:

- The aggregates used for the D_{max} = 2 mm grout material were two different 0/2 mm natural sands labelled sand A (C_u = 3.6) and sand B (C_u = 1.5). Aggregates used for the D_{max} = 4 mm grout material was the 0/2 mm natural sand (sand B) and a 0/4 mm natural gravel (C_u = 6.4), see *Figure 20*. All aggregate particles were rounded with a grain density of 2650 kg/m^3. The limestone filler was a crushed material, 0/0.5 mm with a grain density of 2710 kg/m^3.
- Amount of fines = 20 weight-% so the grout material would have a low permeability.
- Water content had to have a starting value of 12 % since 10 % gave a grout material that became very sticky (too high viscosity).

With the particle size distribution of aggregates and water content decided beforehand, the necessary amounts of superplasticizer, air release agent and bentonite powder were investigated. The amount of superplasticizer had a starting value of 3 weight-% of the amount of water in the grout material. The goal was to find the amount needed to obtain a consistency measurement of 100 mm as measured with a mini-slump flow test (Tan et al., 2017). In the mini-slump flow test, a conical steel ring with a height of 40 mm and a bottom and top diameter of 85 and 75 mm respectively is filled with grout material. The ring is removed upwards, allowing the sides of the grout material to move horizontally outwards, see *Figure 31*. Because of the outward movement, the bottom diameter of the grout material increases, and the grout material settles. Yield strength is related to the resulting diameter of the grout material and viscosity is related to the time it takes to settle.

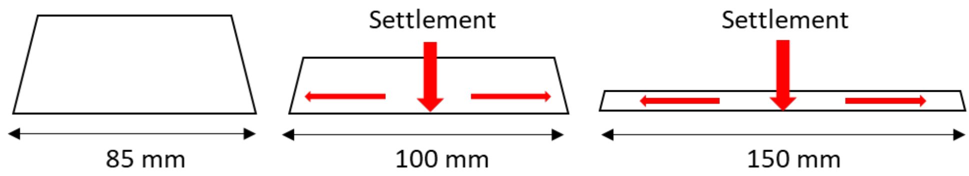

Figure 31. Mini-slump flow test. Bottom diameter of the grout material is measured. Consistency in figure is 100 or 150 mm.

When the right amount of superplasticizer was found, the amount of air release agent was investigated. Starting value was 0.5 weight-% of the amount of water used. Finally, the amount of bentonite powder was investigated, starting with 3 weight-% of the amount of water used. All pre-test batches were either approved or improved by comparing measured bulk density, bleeding, settlement and consistency to the pre-determined limit values presented in *subchapter 3.3.1*.

Without the superplasticizer, the grout material behaved like a moist, lumpy fine-grained sand. With the superplasticizer, the grout material was transformed into a pumpable paste-like material. The water content in the D_{max} = 2 mm grout material had to be slightly increased compared to the D_{max} = 4 mm grout material since the former became very sticky, i.e., the viscosity was too high. This behaviour could only be adjusted by adding more water.

5.2 Fresh properties

The influence of homogenization method of the grout material was investigated and presented in ***Paper I***. In the pre-tests, the dry aggregates were homogenized for 5 minutes before water and additives were added and then homogenized for another 10 minutes. In extreme cases, air contents increased up to 20 %. The influence of homogenization time was therefore tested. Both grout materials presented in *Table 5* experienced an increase of air content and loss of water content when continuously homogenized for 125 minutes, see *Table 8*. In the D_{max} = 2 mm grout material, the increase in air content was particularly high. After 125 minutes of continuous homogenization, both grout materials became lumpy. The results indicate the tendency of these types of grout materials to absorb air when homogenized for a longer period, a behaviour also observed by Lu et al. (2019).

The undrained shear strength was tested with fall cone test after 15 and 125 minutes of either ceased or continuous homogenization, see *Table 18*.

Table 18. Undrained shear strength measured with fall cone after 15 minutes (first test) and 125 minutes (last test) of "ceased homogenization" or "continuous homogenization".

Grout material		D_{max} = 2 mm		D_{max} = 4 mm	
	Time [min]	τ_{fu} [kPa]	Increase [%]	τ_{fu} [kPa]	Increase [%]
Ceased homogenization	15	0.18		0.18	
	125	0.35	~100	0.50	~180
Continuous homogenization	15	0.18		0.18	
	125	6.9	~3700	11.3	~6200

Grout material continuously homogenized for a longer time will have an increased undrained shear strength. This is most likely caused by absorption of air into the grout material during the homogenization. Moisture evaporates and consequently, the effect of the superplasticizer is diminished. For both types of grout material with ceased homogenization, the changes in undrained shear strength were minimal compared to grout material with continuous homogenization. Homogenization time of this type of grout material should therefore be kept short (<15 minutes) since a stiff, low density grout material that will be difficult to pump.

5.3 Hardened properties

The strength development of the grout material after storage was investigated and presented in ***Paper I***. Since the grout material contained no cementitious material, its shear strength after grouting was not expected to be very high. Undrained shear strength of grout material was therefore tested on samples stored up to 34 days under drained conditions in a fridge at +8°C. Undrained shear strength was investigated with either fall cone or UCS testing.

The undrained shear strength development was slow and the difference between the two grout materials was minor. After 34 days of storage, the undrained shear strength of the grout materials was ~13 kPa according to the UCS testing. Values from the fall cone testing was lower but the variations in these results were higher than accepted by the standard (SS-EN ISO 17892-6:2017). Results from fall cone testing had the same trends as the USC testing. According to Gribulis et al. (2019), undrained shear strength for natural moraine is between 30 – 220 kPa. The compacted core soil in the large-scale test embankment dam presented in ***Paper IV*** had an undrained shear strength of ~34 kPa, (Bernstone et al., 2021). From this point of view, the undrained shear strength results of the grout materials were low.

However, the grout material was not compacted when the samples were made. Single spare samples were also tested after 56 days (D_{max} = 2 mm) and 70 days (D_{max} = 4 mm) of storage. Measured undrained shear strength was 19 kPa and 23 kPa, respectively. Water content and bulk density of stored samples were similar to the core soil in the large-scale test embankment dam presented in ***Paper IV***. Water content of the moraine core soil was 8 – 10 % and bulk density 2200 – 2250 kg/m^3 (Bernstone et al., 2021).

Settlements of the grout material during storage was higher than found during the pre-testing and exceeded the pre-determined level of 1 % after 24 h of storage. However, the grout material was not allowed to be drained during the pre-testing. Settlements occurred after 2 days of storage and did not increase with time. Minimizing settlements in grout materials that were used in ***Paper II*** and ***Paper III***, was done by adding more fine material to the grout material, increasing its L/A ratio.

5.4 Permeation tests

5.4.1 Grout material uptake

Influence of *L/A ratio*, D_{max}, *consistency* of the grout material and *injection method* on how well the grout material permeated three types of coarse-grained soils was investigated in ***Paper II***. All results are available in *Appendix A*, *Table A 1.*

5.4.1.1 Influence of L/A ratio on grout material uptake

A comparison of grout material uptake due to different L/A ratios was done by comparing results from all permeation tests with slow injection, see *Table 19*. For all tests with an L/A ratio = 1.7, the uptake of grout material was significantly improved. Discussion is supported by *Figure 32*.

Table 19. Influence of L/A ratio on grout material uptake. Slow injection.

		Consistency =100 mm		Consistency =150 mm	
D_{max} [mm]	d_{15} [mm]	L/A = 1.4 [litres]	L/A = 1.7 [litres]	L/A = 1.4 [litres]	L/A = 1.7 [litres]
2	35	0.2	2.3	0.0	3.7
2	75	1.7	6.9	2.0	25.0[1]
2	110	2.4	19.0	3.2	25.4[1]
4	35	0.6	5.9	1.2	6.7
4	75	3.5	21.4	4.7	25.0[1]
4	110	16.2	25.1[1]	23.4	25.6[1]

[1]No grout material left in the grout container.

L/A ratio = 1.4 L/A ratio =1.7

Figure 32. Influence of L/A ratio on grout material uptake (coarse-grained material, d_{15} = 75 mm). D_{max} = 4 mm, consistency = 150 mm, slow injection.

During primary testing of the grouting equipment, the grout materials tested in ***Paper I***, see *Table 5*, were used. Injection with these grout materials, where the L/A ratio was 1.1, was impossible since grout material stuck inside the pipeline. No grout material uptake was therefore ever observed at this L/A ratio. A grout material should ideally flow under hydrodynamic interactions but can also flow by friction between its particles (Yammine et al., 2008 and Browne and Bamforth, 1977). Injection pressure will decrease linearly from end to end in a straight pipeline during hydrodynamic flow but exponentially during friction governed flow (Feys et al., 2022). As highlighted by Thorsén (2017) and Betonghandboken (2017), the amount of paste-to-aggregate in concrete to improve its pumping capability is very important. It can therefore be assumed that at lower L/A ratios, the flow of grout material became more governed by friction, resulting in no to little grout uptake. No higher L/A ratios than 1.7 was tested.

5.4.1.2 Influence of D_{max} on grout material uptake

A comparison of grout material uptake due to different D_{max} was done by comparing results from all permeation tests done with slow injection, see *Table 20*. Discussion is supported by *Figure 33*.

Table 20. Influence of D_{max} on grout material uptake. Slow injection.

		L/A ratio = 1.4		L/A ratio = 1.7	
Consistency [mm]	d_{15} [mm]	D_{max} = 2 mm [litres]	D_{max} = 4 mm [litres]	D_{max} = 2 mm [litres]	D_{max} = 4 mm [litres]
100	35	0.2	0.6	2.3	5.9
100	75	1.7	3.5	6.9	21.4
100	110	2.4	16.2	19.0	25.1[1]
150	35	0.0	1.2	3.7	6.7
150	75	2.0	4.7	25.0[1]	25.0[1]
150	110	3.2	23.4	25.4[1]	25.6[1]

[1]No grout material left in the grout container.

D_{max} = 2 mm D_{max} =4 mm

Figure 33. Influence of D_{max} on grout material uptake (coarse-grained material, d_{15} = 75 mm). L/A ratio = 1.7, consistency = 150 mm, slow injection.

Grout material uptake was always higher when D_{max} = 4 mm grout material was used. The penetrability of a grout material is explained either by its filtration tendency (Eklund and Stille, 2008) or its yield strength (Eriksson, 2002 and Hässler, 1991). Filtration tendency describes the ability of the aggregates in a grout material to form a plug, hindering further penetration of the grout material. Filtration tendency may be estimated from the ratio between D_{max} of the grout material and the aperture, i.e., crack width, to be grouted. According to Bergman et al. (1970), plug formation of the grout material will likely occur if the aperture is $<3D_{max}$. Grouting a coarse-grained material is however different from grouting an aperture.

There are no examples in the literature of similar grouting tests as performed within this thesis but experiences from two-stage concrete may be used. Two-stage concrete is a type of concrete where the coarser aggregates are pre-placed and compacted in a formwork and injected with a cementitious paste. There is no consensus regarding the ratio between aggregate and paste particle sizes to achieve permeation. The following ratios are however proposed in the literature:

- $d_{15}/D_{max} \geq 14$ (Betonghandboken, 1997).
- $d_{min}/D_{max} \geq 8 - 10$ (Lindvall, 2012).
- $d_{min}/D_{max} \geq 10$ (Awal, 1984).
- "The minimum size of coarse aggregate determines the void dimensions through which the grout material must pass" (ACI 1991).
- Rheology of the grout material, e.g., lower yield strength gives better permeation (Abdelgader, 1996).

The least favourable test setup from a filtration tendency point of view, was when grout material (D_{max} = 4 mm) was injected into the coarse-grained material d_{min} = 16 mm (d_{min}/D_{max} = 4) or d_{15} = 35 mm (d_{15}/D_{max} = 8.75). At these ratios, injection was successful but only with fast injection. The D_{max} in the grout materials did therefore not seem to cause any plug formation during the performed permeation tests.

Since filtration tendency did not seem to affect the grout material uptake, the difference in results must be explained by the consistency of the grout materials. When the D_{max} = 2 mm grout material was made, the same gravel was used as for the D_{max} = 4 mm grout material. However, removing grains >2 mm meant that the D_{max} = 2 mm grout material got a higher proportion of smaller aggregates. This would slightly lower the L/A ratio for the D_{max} = 2 mm grout material. A lower L/A ratio will diminish the grout uptake, see *Table 19*.

5.4.1.3 Influence of consistency on grout material uptake

A comparison in grout material uptake due to different consistency was done by comparing results from all permeation tests done with slow injection, see Table 21. Discussion is supported by *Figure 34*.

Table 21. Influence of consistency on grout material uptake. Slow injection.

		L/A ratio = 1.4		L/A ratio = 1.7	
D_{max} [mm]	d_{15} [mm]	100 mm [litres]	150 mm [litres]	100 mm [litres]	150 mm [litres]
2	35	0.2	0.0	2.3	3.7
2	75	1.7	2.0	6.9	25.0[1]
2	110	2.4	3.2	19.0	25.4[1]
4	35	0.6	1.2	5.9	6.7
4	75	3.5	4.7	21.4	25.0[1]
4	110	16.2	23.4	25.1[1]	25.6[1]

[1]No grout material left in the grout container.

Grout material uptake was higher when the consistency was 150 mm compared to 100 mm. Grout materials with a consistency of ~100 mm had a higher yield strength compared to grout materials with a consistency of ~150 mm. Time between the removal of the steel ring and final settlement during the mini-slump flow test was never measured. It was however noticed that the time of the test differed between the different grout materials. Even though the consistency was 100 or 150 mm for all D_{max} = 2 and 4 mm grout materials, it took longer time for the grout material with D_{max} = 2 mm to settle. This indicated not only a lower yield strength in the grout materials with higher consistency, but also a lower viscosity. Grout material with a consistency of 100 mm permeated the coarse-grained material in a more upward direction. In *Figure 34 left*, 21.4 litres of grout material with a consistency of 100 mm permeated the coarse-grained material while in *Figure 34 right*, 25.0 litres of grout material with a consistency of 150 mm had permeated the coarse-grained material.

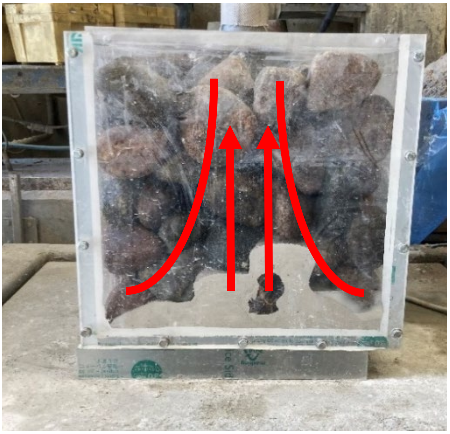

Consistency = 100 mm

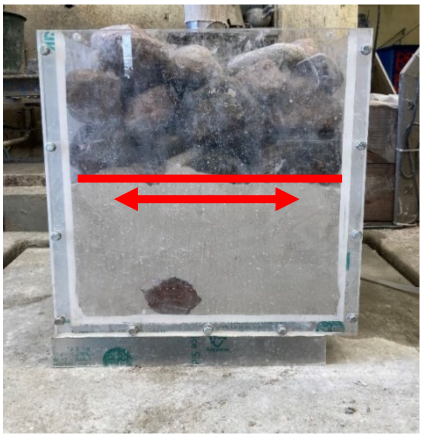

Consistency = 150 mm

Figure 34. Influence of consistency on grout material uptake (coarse-grained material, d_{15} = 75 mm). L/A ratio = 1.7, D_{max} = 4 mm, slow injection.

When observing *Figure 34*, the difference in grout uptake between the two photos seems higher. However, when removing the coarse-grained material after the test, it was found that most of the grout material with a consistency of 100 mm was concentrated along the pipeline. This could not be visually observed from the outside. This implies that when grouting a horizontally orientated damaged zone in an embankment dam, the grout material should have a higher consistency value.

5.4.2 Influence of injection method on grout material penetrability

A comparison in grout material uptake due to different injection method was done by comparing results from all permeation tests with 100 mm grout material consistency, see *Table 22*. Discussion is supported by *Figure 35*.

Table 22. Influence of injection method on grout material uptake. Consistency = 100 mm of the grout material.

		L/A ratio = 1.4		L/A ratio = 1.7	
D_{max} [mm]	d_{15} [mm]	Slow injection [litres]	Fast injection [litres]	Slow injection [litres]	Fast injection [litres]
2	35	0.2	2.9	2.3	25.0[1]
2	75	1.7	13.4	6.9	24.3[2]
2	110	2.4	25.1[1]	19.0	25.1[1]
4	35	0.6	3.3	5.9	25.5[1]
4	75	3.5	20.0	21.4	25.0[1]
4	110	16.2	24.5[1]	25.1[1]	25.3[1]

[1] No grout material left in the grout container. [2] Some grout material stuck on the inside wall of the grout container.

Using fast injection greatly improved the grout material uptake. Grout material uptake was particularly improved when grout material with a consistency of 100 mm was injected. Slow injection was quite ineffective for the grout material with a consistency of 100 mm, see *Figure 35*.

The consensus from all tests with slow injection was that when the grout material came to a stop, it was very difficult to restart the flow of grout material by stepwise increasing the pressure. For grout material with an L/A ratio = 1.4 it could never be restarted but for grout material with an L/A ratio = 1.7 it was possible. Maximal final pressure during slow injection was 317 kPa (~244 kPa/m pipeline). At this pressure, neither heave nor bulging of the walls of the Plexiglass box was observed. The scale however registered a load corresponding to the applied pressure, suggesting that the pressure direction in the grout material was focused downwards. This was in particular evident when grout material with a consistency of 100 mm and an L/A ratio = 1.4 was tested. This observation suggest that the risk of heave will lower when grout materials with lower consistencies are injected.

Slow injection Fast injection

Figure 35. Influence of injection method on grout material uptake (grouted material, d_{15} = 75 mm). L/A ratio = 1.7, D_{max} = 4 mm, consistency = 100 mm.

5.4.2.1 Influence of d_{15} of the permeated coarse-grained material

As expected, it was easier to permeate the larger coarse-grained materials compared to the smaller. With increased particle sizes, both voids and constrictions become larger, enabling easier permeation. Additionally, the amount of contact points between the grains are reduced as the coarse-grained material becomes larger. At each contact point, the width between the grains is zero, i.e., no grout material can pass it. A less coarse-grained material will furthermore have a higher specific surface area. If grout material permeates a coarse-grained material with a higher specific area, the resistance to flow will be higher compared to a coarse-grained material with a lower specific area.

Finally, the grout material had a higher tendency to permeate the coarse-grained material upward along the outside of the pipeline as the particle size of the coarse-grained material was smaller, see *Figure 36*.

Figure 36. Difference in grout material distribution after a permeation test as seen during dismantling. To the left, d_{15} =35 mm and to the right d_{15} =75 mm.

In *Figure 36*, two different coarse-grained materials, i.e., d_{15} = 35 and 75 mm, have been permeated with a grout material with an L/A ratio = 1.7, D_{max} = 4 mm and a consistency of 100 mm with fast injection. When the d_{15} = 35 mm coarse-grained material was permeated, the grout material "climbed" the full height of the Plexiglass box around the pipeline. When the d_{15} = 75 mm coarse-grained material was permeated, the grout material reached a height of ~2/3 of the height of the Plexiglass box. The grout material in the latter example had permeated the coarse-grained material in a more horizontal direction. In both permeation test shown in *Figure 36*, all grout material available for the permeation test was injected, i.e., ~25 litres.

5.4.3 Resistance to flow

The grout materials resistance to flow in the pipeline, at the pipeline exit and through the pores of the coarse-grained material was investigated and presented in ***Paper III***. The basis for the evaluations were 8 permeation tests presented in ***Paper II***, where an evenly distributed grout material surface inside the Plexiglass box could be observed and measured. The permeation tests that fulfilled this requirement were tests where a grout material with an L/A ratio = 1.7, consistency = 150 mm and D_{max} = 2 or 4 mm was injected into the coarse-grained material with a d_{15} = 75 or 110 mm with both slow and fast injection. The grout material used for hydraulic characterization in ***Paper III*** was thus the most easy-flowing grout materials injected into the most coarse-grained materials as tested in ***Paper II***.

5.4.3.1 Frictional losses

From the test results, obtained at a h_2 = 0.075 or 0.1 - 0.27 m (pipeline always filled), ***pipeline (h_f), local (h_l),*** and ***permeation losses (h_{perm})*** were evaluated.

Pipeline loss, h_f

Since h_f and h_l could not be distinguished from the tests, they are discussed as one product, i.e., h_{fl}. This product represents the total frictional head loss in the grout material before it permeates the coarse-grained material in the plexiglass box. Measured h_{fl}/m during all 8 tests were between 67 kPa/m (1.03 m/s) and 0.9 kPa/m (0.01 m/s). Mean value of h_{fl}/m and mean pipeline velocities for all tests are presented in *Table 23*.

Table 23. Mean friction losses in kPa/m and mean pipeline velocities, measured during all permeation tests.

Test	kPa/m	Mean V_1 [m/s]
A	4.5	0.07
B	4.0	0.07
C	7.6	0.11
D	10.1	0.16
E	24.2	0.37
F	30.2	0.49
G	38.6	0.58
H	43.2	0.70

Frictional loss on similar material injected vertically is difficult to find in the literature. Feys et al. (2013) reports measured frictional losses on self-compacting concrete with similar viscosity as tested here, pumped through a horizontal 106 mm diameter pipeline at 0.6 and 1.04 m/s to 7.6 and 11.6 kPa/m. In their later research, Feys et al. (2016) states that if the diameter of the pipeline is reduced by 20 %, the frictional losses are doubled. If this is applied to the results from Feys et al. (2013), corresponding frictional losses are 22.8 and 34.8 kPa/m, slightly lower than the measured frictional losses as shown in *Table 23*. However, in this thesis, frictional losses per m pipeline includes the local loss, h_l, which was not the case in Feys et al. (2013). Therefore, measured frictional losses here will be higher.

Local loss, h_l

Only h_{fl} could be measured, neither h_f nor h_l could be distinguished separately. Eq. 7., for the calculation of h_l could however be used to understand the complexity of the outflow situation at the pipeline exit. The use of Eq. 7. is valid for liquids, but here it was used for a grout material. No better approximation could be found in the literature. According to Feys et al. (2022), the local loss, h_l, is mentioned in the literature as a complex problem and the parameters that controls it is unknown. The problem is most likely the separation of larger aggregates from the grout material as well as the damping characteristics of the paste, i.e., viscosity and yield strength. Another mentioned problem is that the coarser aggregates may be pushed ahead of the grout material during downward pumping followed by a horizontal or upward flow (Kaplan et al., 2005). Due to the complexity, it seems that criterion similar to Eq. 7. is not in use compared to the concept of equivalent length. A common assumption is that a 90° bend corresponds to an equivalence of 2 m pipeline. With grout materials velocities of 0.5 and 1 m/s, the resistance to flow here would be 5 – 10 kPa/m, equal to a total extra local loss of 10 – 20 kPa.

Another uncertainty related to h_l is the influence of the coarse-grained material at the pipeline exit. For the coarse-grained materials with d_{15} = 75 or 110 mm it was possible to place the coarse-grained material around the pipeline exit in such way the grains did not directly interfere with the grout material outflow. For the coarse-grained material with d_{15} = 35 mm, this was not possible, see *Figure 37*. How this affected the outflow situation at the pipeline exit remains unknown.

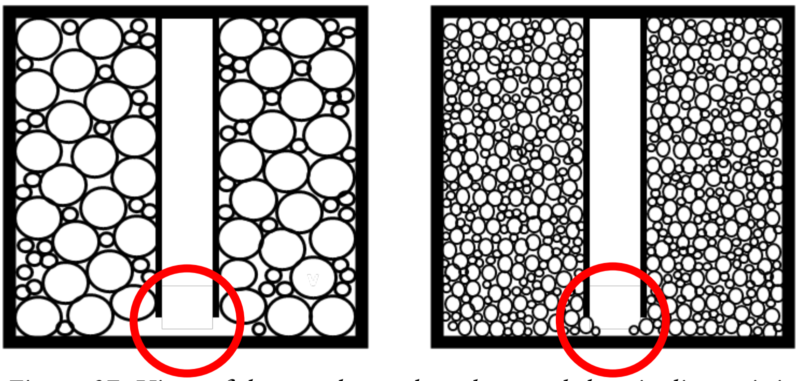

Figure 37. View of the area beneath and around the pipeline exit in the permeation tests where d_{15} was either 75 or 110 mm (left) and 35 mm (right).

Any estimation of h_l requires knowledge of the grout material direction after the pipeline exit, i.e., 90° horizontally - 180° vertically upward. According to Miller

(1990), the outflow direction of a fluid affects the pressure loss. The test setup represents relatively well an actual situation with permeation grouting. Grout material flow behaviour was therefore carefully observed both during the permeation and blank tests. During permeation tests, the grout material flow could be observed as directed upward along the pipeline before turning horizontally close to the grout material surface inside the Plexiglass box. This was particularly evident with the high consistency grout materials. During the blank tests, the grout material outflow initially occurred along the bottom of the Plexiglas box until it reached the side walls. When the grout material surface started to rise, the grout material flow was immediately shifted inwards, focusing the grout material flow around the pipeline, before turning horizontally outward in all directions (360°) close to the grout material surface. see *Figure* 38.

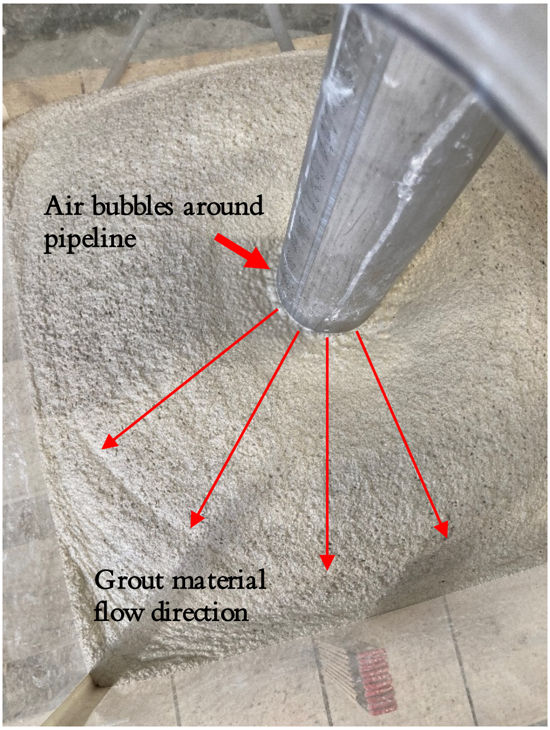

Figure 38. Grout material after a blank test with fast injection. Photo is taken from the top of the Plexiglass box, looking down the pipeline.

A shown in *Figure 38*, circular flow patterns marked with red arrows were formed on the grout material surface. The air bubbles seen around the pipeline emerged after all grout material had been injected, before the 80 kPa of air pressure had been switched off. From the observations made, the grout material flow behaviour was similar in both permeation and blank tests.

Influence of longer pipelines

The influence of h_l in longer pipelines is a minor issue in the field. Assume that the pipeline friction losses gradient h_f/L equals the local losses introduced in Eq. 4. and Eq. 7. Identification of Eq. 7 with Eq. 8., solving pipeline length, L, with Re_{ref} = 1000, K_l = *1* and pipeline diameter, D = 0.075 m, then Eq. 14 becomes.

$$L = \frac{1}{\left({Re_{ref}}/{64}\right) K_l D} \qquad \text{Eq. 14.}$$

Which equals 0.85 m grout material per m pipeline (~19 kPa/m). This means in the permeation tests that the estimated local losses, h_l, can be simulated with an additional active pipeline length of 1.3 × 0.85 = ~ 1.10 m (~25 kPa). $h_{available}$, in m grout material to overcome the friction losses in the 0.075m diameter pipeline with the local losses expressed by Eq. 14. can then be expressed as Eq. 15. The total friction head loss, h_{fl} over a length, L, can then be expressed as follows:

$$h_{fl} = \frac{64}{Re_{pipe}} \times \frac{V_1^2}{2g} \times \left[\left(\frac{L}{D}\right) + \left(\frac{Re_{ref}}{64} K_l\right)\right] \qquad \text{Eq. 15.}$$

Where the last term represents the local losses, here assumed with Re_{ref} = 1000. With L = 2 ,10, and 100 m, h_l stands for 59, 13 and 1 %, respectively of total losses h_{fl}.

Permeation loss, h_{perm}

Permeation loss, h_{perm}, will be discussed in the subsequent *subchapter 5.4.4.*

5.4.3.2 Rheology

The viscosity and yield strength of all grout materials with an *L/A* ratio = 1.7 was measured with a viscometer. Evaluations of the viscometrical results were done under the assumption the grout material was a Bingham fluid and the results were presented in ***Paper II***. The results hereof indicated that the flow of the most easy-flowing grout materials, used in ***Paper III***, could be considered as Newtonian (Wennberg, 2010). When h_{fl}/m was plotted vs. pipeline viscosity, *Figure 29,* there was a Newtonian behaviour and particularly during the blank tests.

When viscosity was extracted from the permeation tests, it couldn't be properly calculated. The reason for this was the presence of h_{perm}, causing an overestimation of the total frictional head loss h_{fl} and consequently the viscosity. When viscosity was extracted from the blank tests however, h_{perm} was not present. An evaluation of h_{fl} from the permeation tests where h_2 was between 0.05 to 0.1 m meant that losses related to the permeation of the coarse-grained material in the vicinity to the pipeline exit was included in the h_{fl}. Therefore, blank tests with both grout materials were carried out where the Plexiglass box was empty. An injection test into an empty Plexiglass box means that the resistance to flow in the Plexiglas box can be considered as negligible due to low grout material velocities over a large area. If the plexiglass box is approximated to a circular pipe with same area as the Plexiglass box, V_1 = 1 m/s, V_2 = 47 mm/s, μ =10 Pas and ρ_{grout} = 2200 kg/m^3, then pipeline loss according to Eq. 4. will be ~0.5 mm.

Viscosity from the blank tests (12.6 and 11.8 Pas) were expected to be lower than those obtained from the viscometrical results (14.4 and 9.4 Pas), but they were similar. The similar viscosities are most likely caused by the uncertainty in determining h_l in Eq. 10. in the evaluations. The grout material is similar to self-compacting concrete and as such, cannot be considered to flow in a pipeline during completely homogeneous conditions. A fine particle dominated lubrication layer may develop in the near pipeline wall region as reviewed by e.g., Feys et al. (2022). The inhomogeneity means that idealized assumptions of the ordinary rheological Bingham fluid model for pipeline friction losses are not fulfilled in the wall region. Consequently, the ordinary Bingham fluid model usually gives overestimated results of viscosity and yield strength. Kaplan et al. (2005) therefore formulated a Bingham rheological model for self-compacting concrete pipeline flow in terms of combined gliding and shearing parameters, which means reduced pipeline friction losses. Feys et al. (2022) also states that characterization of the near pipeline wall layer are related to laboratory testing devices with smooth cylinder rotating in a concentric cylinder without ribs or vane blades encouraging layer development at the wall. The viscometer used for the testing presented in ***Paper II*** had ribbed surfaces, i.e., no lubrication layer developed at the wall.

5.4.4 Hydraulic conductivity

To verify the measurements of h_{fl}/m, the hydraulic conductivity of the coarse-grained material when permeated by the two different grout materials were calculated from the remaining term h_{perm}. These calculations were presented in ***Paper III***. Hydraulic conductivity according to Darcy's law (Eq. 12.) is calculated for liquids at laminar flows in a saturated environment. Its use within the tests must therefore be discussed.

Firstly, from the discussion in *subchapter 5.4.1.2*, it was found that the grains in the grout materials did not seem to affect the permeation. Secondly, permeation of the coarse-grained material occurred bottom up so that air inside the pores were evacuated upwards. No air pockets within the coarse-grained material could be seen during dismantling of the Plexiglass box after any permeation test. Hence, the coarse-grained material that had been permeated was saturated. Thirdly, grout material velocities in the pores of the coarse-grained material were very low (ca $10^{-2} - 10^{-4}$ m/s), the grout material flow was laminar. To verify the calculated hydraulic conductivities, the permeability of the coarse-grained materials, grout material density and viscosity (from the blank test) were used in Eq. 13. Four expected hydraulic conductivities were calculated; two grout materials combined with two coarse-grained materials. These hydraulic conductivities were used as a reference.

The grout material flow, i.e., pore velocities, affected the hydraulic conductivity, see *Appendix C, Figure C 1 – Figure C 4*. The calculated hydraulic conductivity of each coarse-grained material decreased as the pipeline velocity in each test lowered. Hydraulic conductivities calculated with ΔL_{min}, i.e., K_{min}, gave results on par with expected values, see *Table 24*. This suggest that the main flow direction of the grout material during permeation was upward, close to the pipeline, i.e., shortest route to the grout material surface as observed during the tests, see *subchapter 5.4.3.1*.

Table 24. Calculated mean hydraulic conductivities compared to expected.

	D_{max} =2 mm		D_{max} =4 mm	
	K_{min} [10^{-4} m/s]	$K_{expected}$ [10^{-4} m/s]	K_{min} [10^{-4} m/s]	$K_{expected}$ [10^{-4} m/s]
d_{15}=75 mm	1.7	2.5	1.4	2.7
d_{15}=110 mm	2.1	3.4	3.3	3.7

Calculation of the hydraulic conductivity requires an estimation of the frictional losses h_{fl} as they are deducted from $h_{available}$ (Eq. 11). The remaining frictional loss, h_{perm}, is then used to calculate the hydraulic conductivity. Since the mean values from calculated hydraulic conductivities from the permeation tests were in agreement with expected hydraulic conductivities, h_{perm} seemed correctly estimated. However, there are uncertainties due to the transient injection procedure, e.g., grout material flow paths, ΔL, and grout material pore velocities, V_2. Further research is required. Hydraulic conductivity testing under steady-state, laminar flow conditions at different grout material velocities should therefore be performed.

5.5 Large-scale grouting test

Planning and performing a grouting operation was investigated and presented in ***Paper IV***. The remediation method, *identification – localization – characterization – remediation*, was tested on a large-scale embankment test dam at Vattenfall R&D the laboratory in Älvkarleby, Sweden.

A higher-than-normal seepage was *identified* at the left abutment of the embankment dam after two years of operation. Seepage rates were 20 times higher compared to the measurements at the middle of the embankment dam. From temperature measurements it was discovered that a high permeable zone was *located* at 1 m depth beneath the crest just at the left abutment. During drilling of the abutment down to a depth of 3.7 m, a ~0.1 m thick, zone of 4/8 mm gravel traversing the core soil horizontally was *localized* and *characterized* at a depth of 1 m. The whole depth of the core soil at the abutment had an increased water content compared to as built (~9 % → ~15 %). The increased water content in the core soil decreased with depth. This suggested the high permeable zone had wetted the core soil underneath it. The decision was made to *remediate* the abutment with a non-hardening, low consistency (100 mm) non-hardening grout material.

The used grout material contained 17.7 weight-% of magnetite powder. The intention of the magnetite powder was to enable geophysical measurements to find the position of the grout material after injection. These measurements were however not made within the test. The developed magnetite grout material was easy to pump and inject even though its *L/A* ratio became as low as 1.2. This shows that optimal *L/A* ratios will be different in different grout materials and no general values are applicable.

Injection pressures used were pre-calculated for the setup with the intension to have the grout material in the pipeline balanced. With an expected frictional loss, h_f, in the 3.5 m long pipeline of ~50 kPa, the same amount of pressure was applied in the grout container. The pressure of the grout material at the exit of the pipeline was thus equal the height of the grout material inside the pipeline (21.6 kPa/m pipeline). As the pipeline was removed upwards, the amount of pressure inside the grout container was lowered accordingly. The intention of the grouting was not to allow the grout material to turn 180° at the pipeline exit. Local loss, h_l, was not present.

The steel casing with the grout pipeline inserted into it, worked well and allowed air to be vented and drained during injection. Venting air could be heard during the first 20 – 30 s of the grouting. Water was never seen between the casing and the pipeline, see *Figure 39*.

Upward removal of pipeline Escape point for air

Figure 39. To the left: The grouting equipment (grout container, pipeline and casing) were simultaneously hoisted upwards while 50 kPa was applied in the grout container. To the right: Closeup of the bottom of the grout container, pipeline and casing. Red arrow marks the exit point of water and air.

Ca 10 cm above the exit of the pipeline, a rigid steel packer was installed. Its intension was to close off the possibility for grout material to move upward between the pipeline and casing while letting through water and air. The distance between the inner diameter of casing and inner diameter of steel packer was only 2 mm. The steel packer at the bottom of the pipeline worked quite well but grout material could be found ca 10 – 20 cm above it, see *Figure 40*. This was unexpected since the maximum slot between the packer and casing was only 2 mm and D_{max} of the grout material was 4 mm. The particle size distribution of the grout material found above the steel packer was similar to the original particle size distribution of the grout material. Particles with D_{max} = 4 mm had thus managed to pass an aperture of only 2 mm. The reason behind this could never be found.

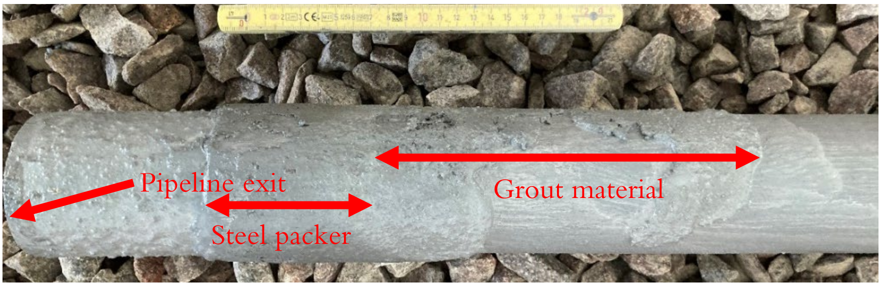

Figure 40. Magnetite grout material found above the steel packer.

The injection process took 19 minutes from start of injection to the moment when the pipeline was above the crest (11.6 m/h), which was longer than planned. The grouting equipment was quite rudimentary but worked well. Development of the grouting equipment is needed and how to withdraw the grouting equipment upward at an even pace and not in increments.

The seepage rates at the left abutment and how it was affected by the rotary percussion drilling and grouting can be seen in *Figure 30*. The damage traversing the core soil was seemingly cut off during the instalment of casing. This meant that the damage was probably smaller than the width of the casing (100 mm) or the wet core soil was densified by the rotary percussion drilling procedure. After the injection, the grout material seemed to have successfully closed the damage since the seepage did not increase after the removal of the casing and pipeline. Furthermore, the compaction of soil around the grouted section seems to have caused an additional decrease in seepage at the abutment. The seepage at the abutment section and the two sections next to it was reduced by ~40 %. One year after the test, seepage had been reduced by ~70 %.

6 CONCLUSIONS

The grout material tested in this thesis should only be used in non-acute situations. For acute remediation, it should be done with other type of grout materials or lowering of the reservoir level to stop the seepage. If a damage where a stream of water is present, the grout material as tested within this thesis is likely to disperse, resulting in little to no sealing effect.

If a core soil damaged by suffusion is grouted with a grout material as tested here, the grouted soil will be gap graded and susceptible to internal erosion. If a grout material can permeate a coarse-grained soil, it can also be eroded from it since the filter criteria is not fulfilled. Permeation grout materials normally contain cementitious materials and will harden after injection. With the permeation tests, the possibility of using a superplasticizer in a non-hardening low-mobility grout material for permeation grouting was proven. Further development of this type of grout material is however needed in terms resistance to internal erosion.

A grouting operation in an embankment dam should not be regarded as a last resort. Grouting with the type of grout material as tested here could be a part of a maintenance program for embankment dams. The grout material can be used in the most common types of damages in dams. Modification of the grout material can easily be done in the field by adding different amounts of superplasticizers to use it both for compaction grouting and permeation grouting. As seen from the large-scale grouting test, the grout material, and particularly the drilling, had a positive effect on the seepage reduction.

Grout material properties

The grout material attracts air when homogenized. If homogenized longer than 15 minutes, it becomes difficult to pump. However, the grout material does not harden, so continuous stirring is not necessary.

After 34 days of storage, the water content and the bulk density of the grout material samples were measured to be ~10 % and 2150 – 2250 kg/m^3, respectively, which are similar to that of the core soil. The undrained shear strength was only ~13 kPa, which was lower than expected from a core soil, although it slowly increased with time.

A higher amount of paste in the grout material greatly improves the permeation. If the ratio between limestone filler and aggregates, expressed in their respective total surface areas, is increased from 1.4 to 1.7, about 5 to 7 times more grout material can be injected.

The injection method is very important for permeation. Injecting with an extra 80 kPa at the start of a test improves the permeation. If the flow of the grout material is stopped during injection, it is difficult to restart even if the final injection pressure is as high as 280 kPa. Injection restart is particularly difficult at L/A ratio = 1.4.

A grout material with a consistency measurement of 150 mm, compared to 100 mm, improved the permeation. A higher D_{max} of the grout material (4 mm compared to 2 mm) improved the permeation. This difference might be caused by higher yield strength and viscosity of the D_{max} = 2 mm grout material. The lowest ratio between the minimum particle size of the coarse-grained material and maximum particle size of the grout material tested was 4, and the grouting was successful.

Resistance to flow

Frictional losses within the pipeline and local loss at the pipeline exit can be estimated by regarding the grout material flow as Newtonian laminar. This will facilitate estimations of how much of the grouting pressure at the pump is transferred into the core soil during a grouting operation. This knowledge should minimize the risk of unintentional hydraulic fracturing or heave during a grouting operation. Frictional pipeline and local loss at the end of the pipeline during the tests were measured to be 1 – 18 kPa/m (0.01–0.29 m/s) during slow injection and 19–67 kPa/m (0.29–1.03 m/s) during fast injection.

The viscosity of the grout materials can be calculated from the tests. However, it is necessary to do a blank test in which the full injection procedure is performed but without any permeation of the coarse-grained material. The viscosity was calculated to be 12.6 and 11.8 Pas for the grout materials with D_{max} of 2 mm and 4 mm, respectively. Using a viscometer, the viscosity was measured to be 14.4 and 9.4 Pas for both grout materials.

Frictional losses due to the permeation of the coarse-grained materials can be estimated using hydraulic conductivity. When the estimated pipeline and local losses are used to calculate hydraulic conductivity, the results are in good agreement with the expected values. The mean hydraulic conductivities in the d_{15} = 75 mm coarse-grained material, when permeated by the D_{max} = 2 mm and 4 mm grout materials, were measured to be 1.7×10^{-4} and 1.4×10^{-4} m/s, respectively; whereas in d_{15} = 110 mm, the values were 2.1×10^{-4} and 3.3×10^{-4} m/s. The expected hydraulic conductivities in the d_{15} = 75 mm coarse-grained material, when permeated by the D_{max} = 2 mm and 4 mm grout materials, were 2.5×10^{-4} and 2.7×10^{-4} m/s, respectively; whereas in d_{15} = 110 mm, the values were 3.5×10^{-4} and 3.7×10^{-4} m/s. Grout material pore velocities during permeation were low, i.e., 10^{-2}–10^{-4} m/s. At these low velocities, higher frictional losses than expected occur at lower grout material pore velocities. The possibility to extract hydraulic conductivities for a coarse-grained material when permeated by a grout material can be used when estimating the permeation depth of a grout material vis-à-vis used injection pressures.

Remedial injection grouting in the field

The grout material was used in a large-scale grouting test, where an abutment was remediated with a non-hardening grout material. The drilling method (rotary percussion) seemed to instantly lower the seepage rate at the abutment and it was reduced by 40 % immediately and by 70 % a year after the finalization of the test.

To conclude the thesis; a non-hardening low mobility grout material was modified so it could be used for both compaction and permeation grouting of damages commonly found in embankment dams. After injection, the grout material will slowly become a part of the original core soil. This will not only remediate the dam but restore it.

7 FUTURE WORK

The following issues should be investigated in the future to complement the results from this thesis and improve the knowledge of grouting in embankment dams in general:

Pressure distribution (X- and Y direction) in a grout material with respect to yield strength. It was found during the laboratory tests that grout material with low consistency tended to direct the applied grout material pressure in a straight down direction. This is important information since it may enable higher grout pressures to be used during grouting, i.e., better compaction without risking heave nor hydraulic fracturing.

Relationship between grout material viscosity, yield strength and frictional losses in pipelines with a diameter < 0.075 m. This is important in order to choose a pipeline with a diameter small enough to prevent free fall of grout material.

Vertical pressure of a grout material at the exit of a vertical pipeline with respect to the yield strength of the grout material and pipeline height and diameter when pipeline velocity is zero. This is important since the own weight of the grout material can cause high pressures of the grout material inside the embankment dam at the pipeline exit.

Required pressure needed to restart a grouting procedure inside a coarse-grained soil that has come to stop. This is important if the grouting equipment malfunctions and needs to be restarted. As seen in the permeation tests, restarting a grout material flow was difficult.

Grouting tests in a porous media with the aim of finding lowest possible d_{min}/D_{max} ratio. Lower d_{min}/D_{max} ratio should diminish the risk of internal erosion of the injected grout material.

Grouting tests in a porous media in a confined space. If air and water can't be safely evacuated during grouting, pore pressures in the surrounding soil will increase. As a consequence, the voids will not be completely grouted. If larger voids are present after injection, the grouting operation is less likely to remain durable.

Grouting tests in a porous media with seepage present. Will the grout keep together or be diluted? Critical seepage velocities? How is the pore water pressure affected when the seepage comes to a sudden stop?

Viscosity and yield strength modification with increased temperatures in the grout material. Viscosity of a fluid is dependent on the temperature. If temperature is increased, viscosity will decrease. Increasing the temperature of a grout material may thus reduce the need for superplasticizer.

Long-term shear strength development in a grout material exposed to more life-like storage conditions. How will percolation of the grout material during storage affect the efficiency of superplasticizer. If the superplasticizer is washed out, the shear strength of the grout material should increase.

Grout material frictional losses occurring at the exit of a vertical pipeline during injection with respect to viscosity, pipeline velocity and outflow behaviour. This is important since there are uncertainties regarding the local loss on the frictional losses in the grouting system.

Dynamic injection testing for improvement of penetrability of the grout material. Dynamic injection enables slight "vibrations" into the grout material from the pump, similar to vibrating conventional concrete during placement.

Development of grout material that may be detected and localized after injection. This is important since it is very difficult to tell where the grout material went after an injection procedure.

Development of grouting equipment so the grout material can be injected continuously without the need of pressurized grout containers of limited sizes.

Hydraulic conductivity testing with grout material at steady-state conditions. This is important since the hydraulic conductivity increased as the grout material flow increased in the transient permeation tests. It is not known if this behaviour was caused by the grout material or from uncertainties in estimating flow path lengths and grout material pore velocities.

REFERENCES

Abdelgader, H.S. (1997). Effect of sand on the compressive strength of two-stage concrete. *Magazine of Concrete Research, 48(177), 353 – 360.* http://dx.doi.org/10.1680/macr.1996.48.177.353

ACI (1991). Guide for the use of preplaced aggregate concrete for structural and mass concrete applications. ACI materials journal, *Committee Report no. 88-M67, 88(6) November-December 1991.* https://doi.org/10.14359/1186

Adiguzel, D. and Bascetin, A. (2019). The investigation of effect of particle size distribution on flow behavior of paste tailings. *Journal of Environmental Management 243, 393 – 401.* https://doi.org/10.1016/j.jenvman.2019.05.039

Awal, A.S.M.A. (1984). Manufacture and properties of prepacked aggregate concrete. Master thesis, Department of Civil Engineering, University of Melbourne, March, 1984. http://hdl.handle.net/11343/39522

Baltazar, L.G., Henrique, F.M.A. and Jorne, F. (2012). Optimization of flow behavior and stability of superplasticized fresh hydraulic lime grouts through design of experiments. *Construction and Building Materials 35, 838 – 845.* https://doi.org/10.1016/j.conbuildmat.2012.04.084

Benjeddou, O., Soussi, C., Jedidi, M. and Benali, M. (2017). Experimental and theoretical study of the effect of the particle size of limestone fillers on the rheology of self-compacting concrete. *Journal of Building Engineering 10, .32 – 41.* https://doi.org/10.1016/j.jobe.2017.02.003

Bernstone, C., Lagerlund, J., Toromanovic, J. and Juhlin, C. (2021). Deformationer och portryck i en experimentell fyllningsdamm [Deformations and Pore Pressures in an Experimental Embankment Dam]. Energiforsk Report 2021:772 (In Swedish).

Betonghandboken (1997). Betonghandboken Del 2 – Arbetsutförande [Concrete Handbook part 2 – Practical Work]. Svensk Byggtjänst. 2nd edition, ISBN 9789173327985 (In Swedish).

Betonghandboken (2017). Betonghandbok Material – Delmaterial samt färsk och hårdnande betong, Del 1 [Concrete Handbook Material – Constituents, Fresh and Hardened Concrete]. Svensk Byggtjänst. 3rd edition. ISBN 978-91-733-803-5 (In Swedish).

Bergman, S.G.A., Lindman, K. and Söderman, P. (1970). Injekteringsmedels inträngning i sand och tunna spalter [Penetrability of Grout Material in Sand and Narrow Slots]. BFR-rapport R45, 1970, Stockholm (In Swedish).

Bradley J., Bruce D., Ferguson K., Poulos S., Talbot, J. and Vrymoed (2007). Center Hill Dam Consensus Report. August 30, 2007.

Brantberger, M. (2000). Metodik för förinjektering i hårt berg [Method for Pre-Grouting in Hard Rock]. Licentiate thesis, Royal Institute of Technology, Department of Civil and Architectural Engineering, Division of Soil and Rock Mechanics, Stockholm (In Swedish).

Brown, D.R., and Warner, J. (1973). Compaction grouting. *Journal of the soil mechanics and foundation division 99(8), 589–601.* https://doi.org/10.1061/JSFEAQ.0001911

Browne, R and Bamforth, P (1977). Tests to establish concrete pumpability. *American Concrete Institute. 74(5), 193-203.* https://doi.org/10.14359/11001

Cernica, J. (1995). Geotechnical engineering – Soil mechanics. ISBN 0-471-30884-6.

Chen, Y.J. (1982). Grouting for sealing the cohesive fills of embankment dams. 14th ICOLD meeting in Rio de Janeiro 1982.

Chevalier, T., Chevalier, C, Clain, X., Dupla, J. C., Canou, J., Rodts, S. and Coussot, P. (2013). Darcy's law for yield stress fluid flowing through a porous medium. Journal of Non-Newtonian Fluid Mechanics 195, pp. 57-66. https://doi.org/10.1016/j.jnnfm.2012.12.005

Danzinger, W.M., Saitoh, K., Jost, P. and Maeder, U. (2003). New generation of admixture polymers and its role in concrete technology. In proceedings of the 11th International Congress on the Chemistry of Cement (ICCC), 11 – 16 May 2003, Durban, South Africa, 2271 – 2275, ISBN Number: 0-9584085-8-0.

Eklund, D. and Stille, H. (2008). Penetrability due to filtration tendency of cement-based grouts. *Tunneling and Underground Space Technology 23, 389 – 398.* https://doi.org/10.1016/j.tust.2007.06.011

Ekström, T. and Pusch, R. (2001). Bentonit i fyllningsdammar – Allmän beskrivning av bentonit, tidigare användning av bentonit i Sverige samt några synpunkter på blandningar av bentonit och jordar [Bentonite in Embankment Dams]. ELFORSK Report 01:15 (In Swedish).

Ekström, I., Nilsson, Å. and Wilén, P. (2016). Reparationsmetoder för fyllningsdammar – Sammanställning av erfarenheter med relevans för svenska förhållanden [Repair Methods for Embankment Dams]. Energiforsk Report 2016:333 (In Swedish).

El-Kelesh, A.M., Matsui, T. and Tokida, K. (2012). Field investigation into effectiveness of compaction grouting. *Journal of Geotechnical and Geoenvironmental Engineering 138(4), 451 – 460.* https://doi.org/10.1061/(ASCE)GT.1943-5606.0000540

Ericsson, J. and Jender, M. (1998). Dokumentation och undersökning av skador i Lövödammen [Documentation and Investigation of Damages in the Lövö Dam]. Master thesis, Luleå university of technology, Department of Civil, Mining and Environmental Engineering (In Swedish).

Eriksson, M. (2002). Prediction of grout spread and sealing effect, a probabilistic approach. Ph.D.-Thesis, Royal Institute of Technology, Stockholm, Sweden.

Fannin, J. (2008). Karl Terzaghi: From theory to practice in geotechnical filter design. *Journal of Geotechnical and Geoenvironmental Engineering 134(3), 267 – 276.* https://doi.org/10.1061/(ASCE)1090-0241(2008)134:3(267)

Fannin J. and Slangen P. (2014). On the distinct phenomena of suffusion and soffosion. *Géotechnique letters, 4, 289 – 294.* https://doi.org/10.1680/geolett.14.00051

Fell, R., Wan, C.F., Cyganiewicz, J. and Foster, M. (2003). Time for development of internal erosion and piping in embankment dams. *Journal of Geotechnical and Geoenvironmental Engineering, 129(4), 307-314.* https://doi.org/10.1061/(ASCE)1090-0241(2003)129:4(307)

Fell, R, Macgregor, P, Stapleton, P and Bell, G. (2005). Geotechnical engineering of dams. Taylor & Francis Ltd. https://doi.org/10.1201/NOE0415364409

Fell R., Foster M., Wan C. F. (2007). A framework for assessing the likelihood of internal erosion and piping of embankment dams and their foundations. Internal erosion of dams and their foundations, Taylor and Francis, May 2007, 65-70. https://doi.org/10.1201/9781482266146

Fell R., Foster M., Davidson R., Cyganiewicz J., Sills G. and Vroman N. (2008). A unified method for estimating probabilities of failure of embankment dams by internal erosion and piping. UNICIV Report R 446, The school of civil and environmental engineering, University of New South Wales, Sydney, Australia 2052. ISBN:85841 413 9.

Feys, D., De Schutter, G. and Verhoeven, R. (2013). Parameters influencing pressure during pumping of self-compacting concrete. *Materials and Structures 46, 533 – 555.* https://doi.org/10.1617/s11527-012-9912-4

Feys, D., Khayat, K.H. and Khatib, R. (2016). How do concrete rheology, tribology, flow rate and pipe radius influence pumping pressure? *Cement and Concrete Composites 66, 38 – 46.* http://dx.doi.org/10.1016/j.cemconcomp.2015.11.002

Feys, D., De Schutter, G., Fataei, S., Martys, N.S. and Mechtcherine, V. (2022). Pumping of concrete: Understanding a common placement method with lots of challenges. *Cement and Concrete Research. 154(4) 106720.* https://doi.org/10.1016/j.cemconres.2022.106720

Flatt, R., and Schober, I. (2012). Understanding the Rheology of Concrete, 7 - Superplasticizers and the rheology of concrete. *Woodhead Publishing Series in Civil and Structural Engineering, 144 – 208.* https://doi.org/10.1533/9780857095282.2.144

Foster, M, Fell, R and Spannagle, M (2000). The statistics of embankment dam failures and accidents. *Canadian Geotechnical Journal 37, 1000 – 1024.* https://doi.org/10.1139/t00-030

Fransson, Å., Funehag, J. and Thörn, J. (2016). Swedish grouting design; hydraulic testing and grout selection. *Ground Improvement 169(4), 275 – 285.* https://doi.org/10.1680/jgrim.15.00020.

Garner, S. (2006). Presentation at ICOLD Workshop in Stockholm, 11th September, 2006.

Garner, S.J. and Fannin, R.J. (2010). Understanding internal erosion: a decade of research following a sinkhole event. *International Journal on Hydropower and Dams, 17(3), 93-98.*

Granata, R., Vanni, D. and Mauro, M. (2012). New Experiences in Ground Treatment by Permeation Grouting, in Grouting and Deep Mixing 2012. ASCE, Reston, VA, USA, 2013 – 2023.

Gribulis, D., Žaržojus, G., Gadeikis, S., Gadeikyte, S. and Urbaitis, D. (2019). Research of undrained shear strength of fine till soils (moraine). 13th international conference on modern building materials, structures and techniques. 16 – 17 May 2019. https://doi.org/10.3846/mbmst.2019.040

Guidoux, C., Faure, Y-H., Beguin, R. and Ho, C-C. (2010). Contact erosion at the interface between granular coarse soil and various base soils under tangential flow condition. *Journal of Geotechnical and Geoenvironmental Engineering, 136(5), 741 – 750.* https://doi.org/10.1061/(ASCE)GT.1943-5606.0000268

Hansson, P. (1999). Teknikbevakning av injekteringsarbeten [Technical Review of Grouting Works]. ELFORSK Report 99:37 (In Swedish).

Hansson, P. (2005). Injektering av fyllningsdammar – Storskaliga modellförsök [Injection of Embankment Dams]. Vattenfall Research and Development (In Swedish).

Hässler, L. (1991). Grouting of Rock-Simulation and Classification. Ph.D.-Thesis, Department of Soil and Rock Mechanics, Royal Institute of Technology, Stockholm.

ICOLD (1993). Rock materials for rockfill dams - Bulletin 92.

ICOLD (2008). Weak rock and shales in dams - Bulletin 134.

ICOLD (2017). Internal erosion of existing dams, levees, and dikes, and their foundations - Bulletin 164.

ISO 17892-7:2017. Geotechnical investigation and testing -- Laboratory testing of soil -- Part 7: Unconfined compression test.

Johansson, F. and Edeskär, T. (2012). Reparationsinjektering av dammar och underground [Remedial Injection Grouting of Dams and Underground]. ELFORSK Report 12:65 (In Swedish).

Johansson S., Stork A., David A., Mondanos M., and Nygren C. (2020). Fibre-optic Distributed Acoustic Sensing for detection of seepage and internal erosion, Energiforsk Report 2020:682.

Johansson, S., Beaupretre, S., Boue, A. and Stork, A. (2021). Distributed Acoustic Sensing for Detection of Defects in the Test Dam at Älvkarleby. Energiforsk Report 2021:732.

Kaplan, D., De Larrard, F. and Sedran, T. (2005). Avoidance of blockages in concrete pumping process. *ACI Materials Journal, May 2005, 102(3), 183 – 191.* https://doi.org/10.14359/14446

Karol, R.H. (2003). Chemical grouting and soil stabilization. 3rd edition, revised and expanded. New York: Marcel Dekker Inc. ISBN 9780824740658

Kociánová, M., Cerný, V. and Drochyta, R. (2015). Development of grout for additional seal embankment dams. *Procedia Engineering 108, 632 – 638.* https://doi.org/10.1016/j.proeng.2015.06.191

Koenders, M.A. and Sellmeijer, J.B. (1992). Mathematical model for piping. *Journal of Geotechnical Engineering, ASCE,118(6), 943 – 946.* https://doi.org/10.1061/(ASCE)0733-9410(1992)118:6(943)

Krizek, R.J. and Madden, M. (1985). Performance of chemically grouted sands. Issues in dam grouting. A session of ASCE convention, Denver, Colorado, April 30.

Lagerblad B, Westerholm M, Fjällberg L, Gram H-E. (2008). Bergkrossmaterial som ballast i betong [Crushed Rock as Aggregate in Concrete]. CBI-rapport nr 1. CBI Betonginstitutet, Stockholm (In Swedish).

Lagerlund, J. (2007). Reparationsmetoder för dammkropp i relation till inre erosion – Kriterier för val av injekteringsmetod och injekteringsmaterial [Remedial Injection Grouting for Embankment Dams in Relation to Internal Erosion]. ELFORSK Report 07:53 (In Swedish).

Lagerlund, J. (2009). Remedial Injection grouting of embankment dams with non-hardening grouts. Licentiate thesis, Royal Institute of Technology, Department of Civil and Architectural Engineering, Division of Soil and Rock Mechanics, Stockholm.

Lagerlund, J., Thorsell, P-E. and Liljeby, E. (2014). Utveckling av kringgjutnigasbruk för 1BMA [Development of Grout Material for 1 BMA]. Vattenfall Research and Development, Civil engineering, Report U14-02. (In Swedish).

Lagerlund, J and Nilsson, Å. (2020). Anslutningar i fyllningsdammar [Abutments in Embankment Dams]. Energiforsk Report 2020:643 (In Swedish).

Lagerlund, J. and Holmberg, H. (2021). Silobruk – undersökning av bruk med bentonit [Grout Material for the Silo – Investigation of Grout Material Containing Bentonite]. Vattenfall Research & Development, Civil engineering, Report VRD-R12:2021 (In Swedish).

Lagerlund, J. (2022). Hydraulisk konduktivitet i grovkorniga jordar [Hydraulic conductivity in coarse-grained soils]. Energiforsk Report 2022:849.

Lagerlund, J., Bernstone, C., Viklander, P. and Nordström, E. (2022). Embankment Test Dam of Älvkarleby - Description of installed defects and their position. Mendeley Data, V3, doi: 10.17632/k7zrrbxxnb.3

Lagerlund, J. (2023). Grouting tests of coarse-grained soils with a non-hardening grout material developed for embankment dams. Mendeley Dataset. DOI: 10.13140/RG.2.2.13459.76326

Lange, A. and Plank, J. (2012). Study on the foaming behavior of allyl ether-based polycarboxylate superplasticizers. *Cement and Concrete Research 42(2), 484 – 489.* https://doi.org/10.1016/j.cemconres.2011.11.017

Li, L. and Deng, Y. (2023). Fracture analysis-based mode-I stress intensity factors of crack under fracture grouting in elastic-plastic soils. *Scientific Reports 13, 1389.* https://doi.org/10.1038/s41598-023-28649-2

Lim, H.D., Lee, K.H., Lee, J.Y. and Oh, B.H. (2004). Leakage investigation, remedial works and its effects on seepage control of Unmun dam. In: Proceedings of the ICOLD 72nd Annual Meeting, Workshop on Dam Safety Problems and Solutions – Sharing Experience. KNCOLD, 225 – 243.

Lindvall, A. (2012). Injekteringsbetong – Mekaniska och beständighetsegenskaper [Injection Concrete – Mechanical and Durability Aspects]. SBUF Report, ID: 12550 (In Swedish).

Littlejohn, S. (2003). The Development of Practice in Permeation and Compensation Grouting: A Historical Review (1802–2002): Part 1 Permeation Grouting, Grouting and Ground Treatment. ASCE, Reston, VA, USA, pp. 50 – 99.

Lu, B., Weng, Y., Li, M., Qian, Y., Leong, K.F., Tan, M.J., and Qian, S. (2019). A systematical review of 3D printable cementitious materials. *Construction and Building materials 207, 477 – 490.* https://doi.org/10.1016/j.conbuildmat.2019.02.144

Miller D.S. (1990). Internal flow systems. 2nd Edition. ISBN: 0947711775.

Mitchell, J. and Soga, K. (2006). Fundamentals of soil bahavior – Third edition. ISBN-13: 978-0-471-46302-7.

Nilsson, Å. (1993). Åldersförändringar i fyllningsdammar [Age induced Changes in Embankment Dams]. VASO dammkommittés rapport nr 16. ISSN 1400-7827 (In Swedish).

Nilsson, Å., Ekström, I. and Söder, C-O. (1999). Inre erosion i svenska dammar - Beskrivning och utvärdering av sjunkgropar [Internal Erosion in Swedish Dams]. ELFORSK Report 99:34 (In Swedish).

Nooroz, R., Olsson, P-I, Dahlin, T., Günther, T. and Bernstone, C. (2021). A geoelectrical pre-study of Älvkarleby test embankment dam: 3D forward modelling and effects of structural constraints on the 3D inversion model of zoned embankment dams. *Journal of Applied Geophysics 191, 104355.* https://doi.org/10.1016/j.jappgeo.2021.104355

Pan, D., Zhang, Y., Bu, Z. and Xu, Z. (2023). Numerical investigation of slurry property effect on grouting and blocking of flowing water in rock fractures. *International Journal for Numerical and Analytical Methods in Geomechanics, 47(9), 1681 – 1698.* https://doi.org/10.1002/nag.3534

Park, D., Oh, J. (2018). Permeation grouting for remediation of dam cores. *Engineering Geology 233, 63 – 75.* https://doi.org/10.1016/j.enggeo.2017.12.011

Partheniades, E. (1965). Erosion and deposition of cohesive soils. *Journal of the Hydraulics Division, 91(1), 105 – 139.* https://doi.org/10.1061/JYCEAJ.0001165

Peng, Y. and Jacobsen, S. (2013). Influence of water/cement ratio, admixtures and filler on sedimentation and bleeding of cement paste. *Cement and Concrete Research. 54, 133–142.* https://doi.org/10.1016/j.cemconres.2013.09.003

Rice J. D. and Duncan M. (2010). Findings of case histories on the long-term performance of seepage barriers in dams. *Journal of Geotechnical and Geoenvironmental Engineering, 136 (1), 2 – 15.* https://doi.org/10.1061/(ASCE)GT.1943-5606.0000175

RIDAS (2020). Energiföretagens riktlinjer för dammsäkerhet. Tillämpningsvägledning, kapitel 9. Date: August 2020 [The Energy Companies Guidlines for Dam Safety, Chapter 9] (In Swedish).

Rönnqvist H. (2015). On the assessment of internal erosion of dam cores of glacial till. Doctoral thesis, Luleå University of Technology, Department of Civil, Environmental and Natural Resources Engineering, Division of Mining and Geotechnical Engineering. ISSN 1402-1544.

Rönnqvist, H. (2020). Fyllningsdammars tätkärna och filter [The Core and Filters of Embankment Dams]. Energiforsk Report 2019:630 (In Swedish).

Salas Romero, S., Juhlin, C. and Bernstone, C. (2020). The potential of detecting flaws in an experimental dam at Älvkarleby, Sweden, using P-wave traveltime tomography. EGU General Assembly 2020, Online event, 4–8 May 2020, Vienna, Austria.

Sherard, J.L. (1953). Influence of soil properties and construction methods on the performance of homogeneous earth dams. Ph.D.-thesis, Harvard University, technical memorandum 645, Bureau of Reclamation, Denver, CO.

Sherard J.L., Woodward R. and Clevenger S. (1963). Earth and earth-rock dams – engineering problems of design and construction. ISBN – 10: 9780471785477

Sherard J.L. (1986). Hydraulic fracturing in embankment dams. *Journal of Geotechnical Engineering, 1986, 112 (10), 905 – 927.* https://doi.org/10.1061/(ASCE)0733-9410(1986)112:10(905)

Shrivastava, N. and Zen, K. (2018). An experimental study of compaction grouting on its densification and confining effects. *Geotechnical and Geological Engineering, 36(2), 983-993.* https://doi.org/10.1007/s10706-017-0369-7

Shuttle, D. and Jefferies, M. (2000). Prediction and validation of compaction grout effectiveness. ASCE conference Geo-Denver 2000, August 5 – 8, Denver, Colorado.

Sjöström, Ö. (1999). Reparation av jorddammar genom injektering [Reparation of Embankment dams With Injection Grouting]. ELFORSK Report 99:48 (In Swedish).

SS-EN ISO 17892-1:2014. Geotechnical investigation and testing - Laboratory testing of soil - Part 1: Determination of water content - Amendment 1 (ISO 17892-1:2014/Amd 1:2022)

SS-EN ISO 17892-2:2014. Geotechnical investigation and testing - Laboratory testing of soil - Part 2: Determination of bulk density (ISO 17892-2:2014).

SS-EN ISO 17892-6:2017. Geotechnical investigation and testing - Laboratory testing of soil - Part 6: Fall cone test (ISO 17892-6:2017)

SS-EN 480-4:2005. Admixtures for concrete, mortar and grout - Test methods - Part 4: Determination of bleeding of concrete.

Tan, Z., Bernal, S.A. and Provis, J.L. (2017). Reproducible mini-slump test procedure for measuring the yield stress of cementitious pastes. *Materials and Structures 50, article number 235*. https://doi.org/10.1617/s11527-017-1103-x

Terzaghi K., Peck R. and Gholamreza M. (1996). Soil mechanics in engineering practice – third edition. ISBN 0-471-08658-4.

Thorsén, Å. (2017). Omelettmetoden – en proportioneringsmetod för sprutbetong [The Omelett Method – A Proportioning Method for Shotcrete]. Presentation at the VUC day for producers of factory concrete 2017 (In Swedish).

Toromanovic, J., Lagerlund, J., Viklander, P. and Laue, J. (2020). Geotechnical instrumentation of an experimental embankment dam. ECPMG 2020, 4th European conference on physical modelling in geotechnics, 171 – 176.

USBR (2012). Design standards No. 13. Chapter 12: Foundation and earth materials investigation.

Van Beek, V.M., Bezuijen, A., Sellmeijer, J.B. and Barends, F.B.J. (2014). Initiation of backward erosion piping in uniform sands. *Géotechnique 64(12), 927 – 941*. https://doi.org/10.1680/geot.13.P.210

Vattenfall. (1988). Jord- och stenfyllningsdammar [Earth and Rockfill Dams]. Stockholm, Sweden: Happy Printing AB (In Swedish).

Viklander, P. (1997). Compaction and thaw deformation of frozen soil. Ph.D.-thesis, Luleå University of technology, Luleå, Sweden.

Viklander, P., Lagerlund, J., Riaz, S. and Nordström, E. (2023). Non-destructive test methods for detecting defects in an experimental embankment dam. *Hydropower & Dams 30(3), 74-79*.

Vogt, C. (2010). Ultrafine particles in concrete – Influence of ultrafine particles on concrete properties and applications to concrete mix design. Doctoral thesis, School of Architecture and the Built Environment, Division of Concrete Structures, Royal Institute of Technology, Stockholm, Sweden. ISSN 1103-4270.

Vuola, P., Konrad, J-M. and Bartsch, M. (2007). Effects of frost and thaw on dams. Assessment of the risk of internal erosion of water retaining structures, Intermediate Report of the European working group of internal erosion, Freising, Germany, 2007.

Wallevik, O.H. and Wallevik, J.E. (2011). Rheology as a tool in concrete science: the use of rheographs and workability boxes. *Cement and Concrete Research 41, 1279 – 1288.* https://doi.org/10.1016/j.cemconres.2011.01.009

Warner, J., Jefferies, M.G. and Garner, S.J., (2003). Compaction grouting for sinkhole repair at WAC Bennet dam. ASCE 3rd International conference on grouting and ground treatment, February 10 – 13, New Orleans.

Warner, J. (2004). Practical Handbook of Grouting. Soil, Rock and Structures. New Jersey: John Wiley. ISBN: 978-0-471-46303-0

Wennberg, T. (2010). Transporting highly concentrated slurries with centrifugal pumps – The thickened minerals tailings example. Licentiate thesis, Luleå University of Technology, Department of chemical Engineering and Geosciences, Mineral processing, Luleå, Sweden. ISBN: 978-91-7439-169-5.

Widing, S. (1987). Några allmänna synpunkter på Damminjektering [Some General Thoughts on Embankment Dam Grouting]. Seminar about dams. 20-21 of November 1986, Royal Institute of Technology Stockholm. (In Swedish).

Windelhed, K. (2001). Jetinjektering. En intressant reparationsmetod för jorddammar [Jet Grouting. An Interessant Remedial Method for Embankment Dams]. ELFORSK Report 99:48 (In Swedish).

Yammine, J., Chaouche, M., Guerinet, M., Moranville, M. and Roussel, N. (2008). From ordinary rheology concrete to self-compacting concrete: A transition between frictional and hydrodynamic interactions. *Cement and Concrete Research. 38(7), 890-896.* https://doi.org/10.1016/j.cemconres.2008.03.011

Yea, G.G., Kim, T.H., Kim, J.H., Kim, H.Y. (2013). Rehabilitation of the core zone of an earth-fill dam. *Journal of Performance of Constructed Facilities 27(4), 485-495.* https://doi.org/10.1061/(ASCE)CF.1943-5509.0000335

Yerro A., Rohe A., Soga K. (2017). Modelling internal erosion with the material point method. *Procedia Engineering 175, 365 – 372.* https://doi.org/10.1016/j.proeng.2017.01.048

Yongmin, Y., Zheng, C., Wanhui, F., Yumei, N., Minhui, Y. and Yunchao, T. (2021). Shrinkage compensation design and mechanism of geopolymer pastes. *Construction and Building Materials 299, 123916.* https://doi.org/10.1016/j.conbuildmat.2021.123916

Zerbino, R., Barragán, B., Garcia, T., Agulló, L. and Gettu, R. (2009). Workability tests and rheological parameters in self-compacting concrete. *Materials and Strutures 42, 947–960 (2009).* https://doi.org/10.1617/s11527-008-9434-2

APPENDIX

A – Grout material uptake

Complete results from grout material uptake from all permeation tests presented in ***Paper II*** is shown in *Table A 1*. When slow injection was used, the first value is the measured grout uptake after the own weight driven injection and the second value is after a total of 280 kPa had been added. Values for fast injection was after the grout material had come to a full stop or no more grout material was available. Total batch size was ~25 litres. Results of grout uptake ~25 litres = all grout material was injected.

Table A 1. Grout material uptake measured after the tests.

L/A ratio = 1.4, D_{max} = 4 mm, Slow injection				
Test No.	d_{15} soil [mm]	Consistency [mm]	Grout uptake own weight [litres]	Grout uptake 280 kPa extra pressure [litres]
1	35	102	0.6	1.3
2	75	100	3.5	4.7
3	110	103	16.2	16.2
4	35	149	1.2	2.1
5	75	150	4.7	7.7
6	110	150	23.4	24.6[1]
L/A ratio = 1.4, D_{max} = 4 mm, Fast injection				
Test No.	d_{15} soil [mm]	Consistency [mm]	Grout uptake [litres]	
7	35	102	3.3	
8	75	104	20.0	
9	110	101	24.5	
10	35	147	4.6	
11	75	150	15.3	
12	110	149	24.7	
L/A ratio = 1.4, D_{max} = 2 mm, Slow injection				
Test No.	d_{15} soil [mm]	Consistency [mm]	Grout uptake own weight [litres]	Grout uptake 280 kPa extra pressure [litres]
13	35	101	0.2	0.6
14	75	100	1.7	6.1
15	110	101	2.4	6.0
16	35	152	0.0	0.0
17	75	147	2.0	4.8
18	110	151	3.2	5.1

[1]Only 40 kPa extra pressure required.

L/A ratio = 1.4, D_{max} = 2 mm, Fast injection				
Test No.	d_{15} soil [mm]	Consistency [mm]	Grout uptake [litres]	
19	35	102	2.9	
20	75	102	13.4	
21	110	104	25.1	
22	35	150	4.1	
23	75	146	2.8	
24	110	151	24.9	
L/A ratio = 1.7, D_{max} = 4 mm, Slow injection				
Test No.	d_{15} soil [mm]	Consistency [mm]	Grout uptake own weight [litres]	Grout uptake 280 kPa extra pressure [litres]
25	35	104	5.9	7.8
26	75	103	21.4	25.4[1]
27	110	101	25.1	
28	35	151	6.7	9.1
29	75	151	25.0	
30	110	151	25.6	
L/A ratio = 1.7, D_{max} = 4 mm, Fast injection				
Test No.	d_{15} soil [mm]	Consistency [mm]	Grout uptake [litres]	
31	35	104	25.5	
32	75	103	25.0	
33	110	102	25.3	
34	35	150	25.0	
35	75	146	24.4	
36	110	149	25.0	
L/A ratio = 1.7, D_{max} = 2 mm, Slow injection				
Test No.	d_{15} soil [mm]	Consistency [mm]	Grout uptake own weight [litres]	Grout uptake 280 kPa extra pressure [litres]
37	35	102	2.3	3.7
38	75	102	6.9	8.2
39	110	102	19.0	24.1[1]
40	35	149	3.7	5.5
41	75	151	25.0	25.0
42	110	149	25.4	25.4

[1]Only 40 kPa extra pressure required.

L/A ratio = 1.7, D_{max} = 2 mm, Fast injection			
Test No.	d_{15} soil [mm]	Consistency [mm]	Grout uptake [litres]
43	35	104	25
44	75	104	24.3
45	110	101	25.1
46	35	150	25.1
47	75	146	24.4
48	110	146	24.9

B – Hydraulic evaluation primary data

Presentation of measured V_1, h_{fl} and calculated $h_{available}$, and h_{perm} during permeation tests performed with slow injection used in ***Paper III*** is shown in *Table B 1.* All grout material had an L/A ratio = 1.7, D_{max} of either 2 or 4 mm and a consistency of 150 mm.

Table B 1. Measured and evaluated data from tests A – D, slow injection.

Test A[1], D_{max} = 2 mm, d_{15} = 75 mm									
V_1 [m/s]	0.14	0.12	0.11	0.09	0.05	0.03	0.03	0.03	
$h_{available}$ [m]	1.74	1.69	1.64	1.58	1.53	1.47	1.42	1.37	
h_{fl}[3] [m]	0.54	0.48	0.43	0.35	0.21	0.13	0.13	0.10	
h_{perm} [m]	1.20	1.21	1.21	1.23	1.32	1.34	1.29	1.27	
Test B[1], D_{max} = 4 mm, d_{15} = 75 mm									
V_1 [m/s]	0.17	0.11	0.05	0.05	0.05	0.04	0.03	0.02	
$h_{available}$ [m]	1.69	1.64	1.58	1.53	1.47	1.42	1.37	1.32	
h_{fl}[4] [m]	0.64	0.41	0.20	0.20	0.18	0.14	0.10	0.09	
h_{perm} [m]	1.05	1.23	1.38	1.33	1.30	1.28	1.27	1.23	
Test C[2], D_{max} = 2 mm, d_{15} = 110 mm									
V_1 [m/s]	0.27	0.14	0.14	0.13	0.10	0.07	0.06	0.06	0.06
$h_{available}$ [m]	1.75	1.69	1.64	1.59	1.54	1.48	1.43	1.38	1.33
h_{fl}[3] [m]	1.10	0.56	0.56	0.51	0.41	0.27	0.25	0.23	0.23
h_{perm} [m]	0.66	1.13	1.08	1.08	1.13	1.21	1.19	1.15	1.10
Test D[2], D_{max} = 4 mm, d_{15} = 110 mm									
V_1 [m/s]	0.29	0.24	0.23	0.19	0.16	0.11	0.10	0.08	0.06
$h_{available}$ [m]	1.75	1.70	1.65	1.60	1.54	1.49	1.43	1.38	1.33
h_{fl}[4] [m]	1.07	0.91	0.87	0.71	0.60	0.42	0.37	0.31	0.21
h_{perm} [m]	0.69	0.79	0.78	0.88	0.94	1.07	1.07	1.07	1.12

[1]Pipeline full at h_2 = ~0.075 m. [2] Pipeline full at h_2 = ~0.01 m. [3]$y_{2mm,\ Blank} = 67\,V_1$ used for h_{fl}. [4]$y_{4mm,\ Blank} = 61\,V_1$ used for h_{fl}.

Presentation of measured V_1, h_{fl} and calculated $h_{available}$, and h_{perm} during permeation tests performed with fast injection used in ***Paper III*** is shown in *Table B 2.* All grout material had an L/A ratio = 1.7, D_{max} of either 2 or 4 mm and a consistency of 150 mm.

Table B 2 Measured and evaluated data from tests E – H, fast injection.

	Test E[1], D_{max} = 2 mm, d_{15} = 75 mm								
V_1 [m/s]	0.51	0.51	0.40	0.32	0.30	0.30	0.29	0.29	
$h_{available}$ [m]	5.09	5.04	5.05	5.05	5.00	4.95	4.91	4.86	
h_{fl}[3] [m]	2.06	2.06	1.58	1.29	1.21	1.21	1.14	1.14	
h_{perm} [m]	3.03	2.98	3.47	3.76	3.79	3.74	3.77	3.71	
	Test F[2], D_{max} = 4 mm, d_{15} = 75 mm								
V_1 [m/s]	0.86	0.64	0.64	0.47	0.43	0.40	0.37	0.32	0.27
$h_{available}$ [m]	4.93	5.00	4.95	5.00	4.97	4.94	4.90	4.88	4.86
h_{fl}[4] [m]	3.20	2.40	2.40	1.75	1.60	1.48	1.37	1.20	1.01
h_{perm} [m]	1.72	2.60	2.55	3.26	3.37	3.46	3.53	3.68	3.85
	Test G[2], D_{max} = 2 mm, d_{15} = 110 mm								
V_1 [m/s]	0.87	0.65	0.74	0.65	0.52	0.52	0.43	0.47	0.40
$h_{available}$ [m]	4.93	5.01	4.90	4.91	4.93	4.88	4.88	4.81	4.80
h_{fl}[3] [m]	3.46	2.60	2.97	2.60	2.08	2.08	1.73	1.89	1.60
h_{perm} [m]	1.47	2.42	1.94	2.31	2.86	2.81	3.15	2.92	3.20
	Test H[1], D_{max} = 4 mm, d_{15} = 110 mm								
V_1 [m/s]	1.03	0.86	0.74	0.65	0.65	0.57	0.57	0.52	
$h_{available}$ [m]	4.77	4.82	4.85	4.85	4.80	4.79	4.74	4.72	
h_{fl}[4] [m]	3.86	3.22	2.76	2.41	2.41	2.14	2.14	1.93	
h_{perm} [m]	0.91	1.61	2.09	2.44	2.39	2.65	2.59	2.79	

[1]Pipeline full at h_2 = ~0.075 m. [2] Pipeline full at h_2 = ~0.01 m. [3]$y_{2mm, Blank} = 67\,V_1$ used for h_{fl}. [4]$y_{4mm, Blank} = 61\,V_1$ used for h_{fl}.

C – Hydraulic conductivity

Hydraulic conductivity vs. grout material flow is shown in *Figure C 1 – Figure C 4*. Only minimum hydraulic conductivity, K_{min}, plotted.

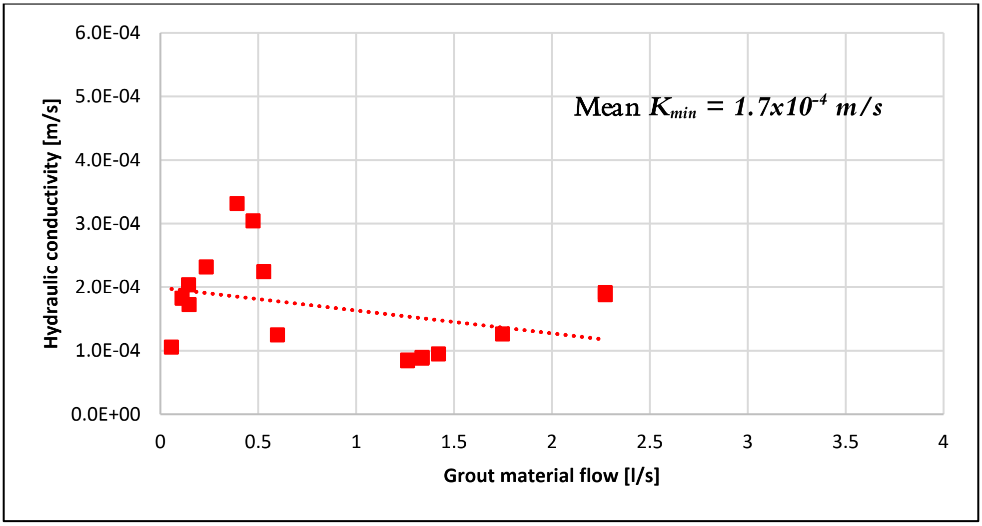

Figure C 1. Hydraulic conductivity calculated for each injected 5 kg of grout material. D_{max} = 2 mm, d_{15} = 75 mm.

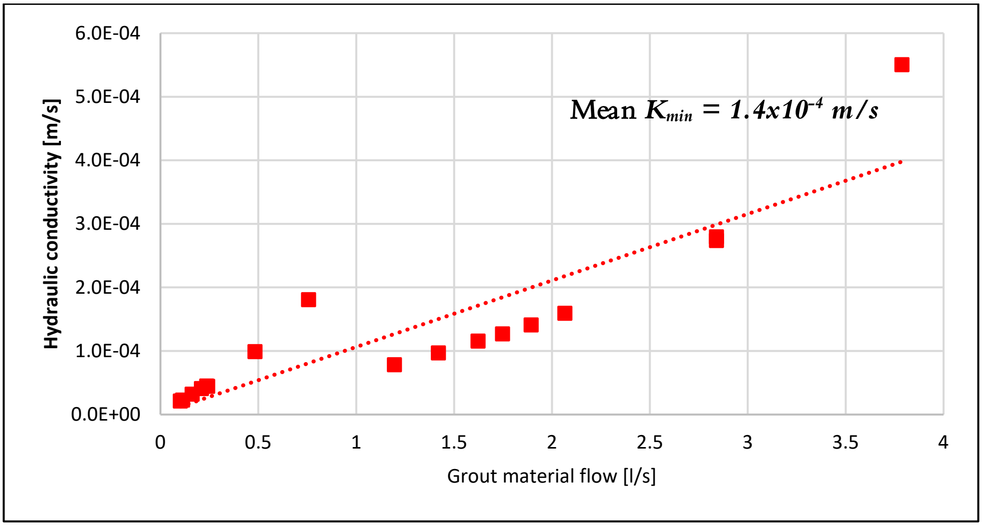

Figure C 2. Hydraulic conductivity calculated for each injected 5 kg of grout material. D_{max} = 4 mm, d_{15} = 75 mm.

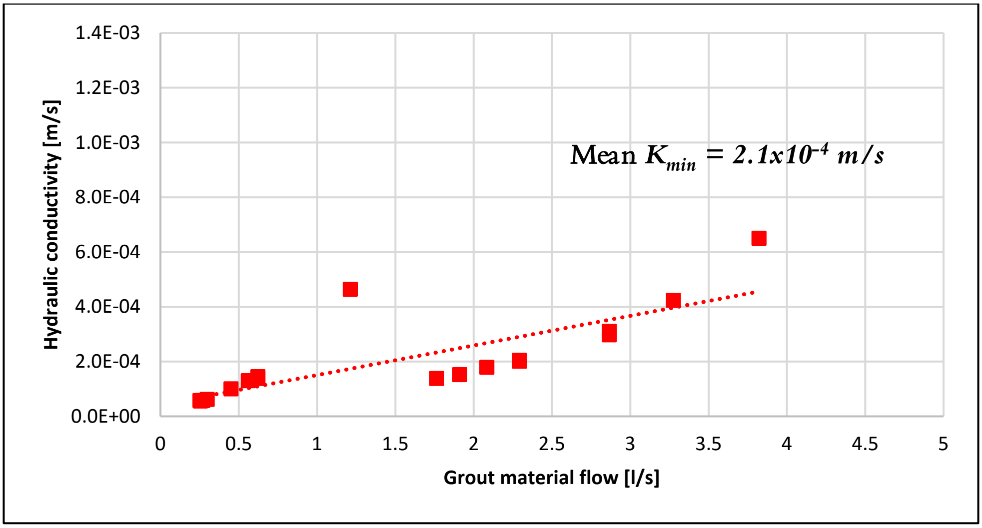

Figure C 3. Hydraulic conductivity calculated for each injected 5 kg of grout material. D_{max} = 2 mm d_{15} = 110 mm.

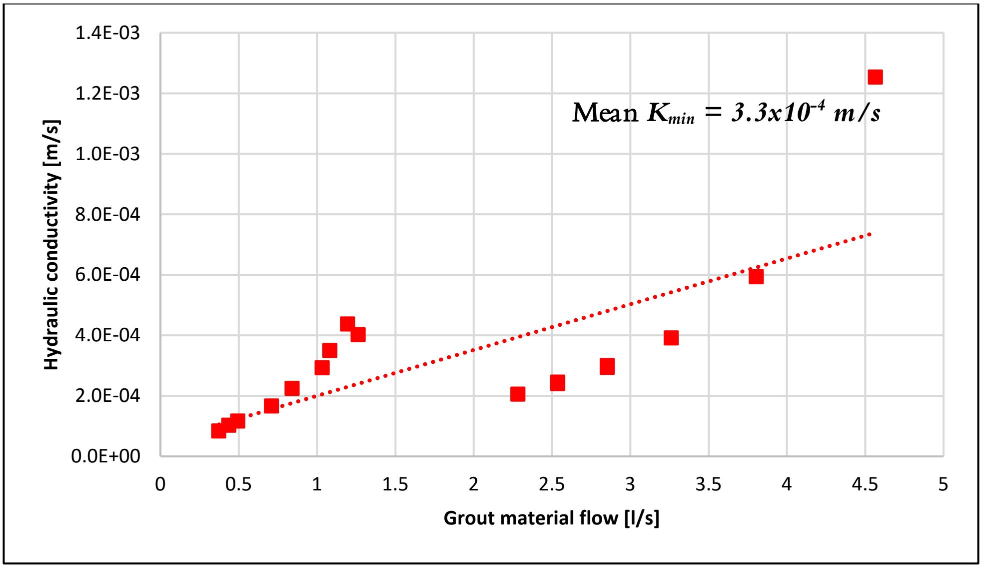

Figure C 4. Hydraulic conductivity calculated for each injected 5 kg of grout material. D_{max} = 4 mm, d15 = 110 mm.

Department of Civil, Environmental and Natural Resources Engineering
Division of Mining and Geotechnical Engineering

ISSN 1402-1544
ISBN 978-91-8048-476-3 (print)
ISBN 978-91-8048-477-0 (pdf)

Luleå University of Technology 2024